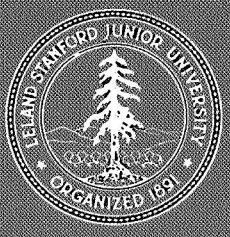

STANFORD UNIVERSITY
ENGINEERING IN MEDICINE AND BIOLOGY

THEORETICAL MODEL STUDIES OF WAVE PROPAGATION IN THE SEMICIRCULAR CANALS

PH. D. DISSERTATION

BY

MERLIN DORFMAN

BIOMECHANICS LABORATORY

DEPARTMENT OF AERONAUTICS AND ASTRONAUTICS

JANUARY 1969

This work was supported in part by the Office of Naval Research under contract number N000-14-67-A-0112-0007, and by the Graduate Study Program of Lockheed Missiles and Space Company. Ames Research Center, NASA, provided office and laboratory space, computation facilities, and photographic services, under a collaborative research arrangement with Stanford University (NASA Grant NGR-05-020-223).

SUDAAR NO. 367

Department of Aeronautics and Astronautics
Stanford University
Stanford, California

THEORETICAL MODEL STUDIES OF WAVE TRANSMISSION IN THE SEMICIRCULAR CANALS

by

Merlin Dorfman

SUDAAR No. 367
January 1969

This work was supported in part by the Office of Naval Research under contract number N000-14-67-A-0112-0007, and by the Graduate Study Program of Lockheed Missiles and Space Company. Ames Research Center, NASA, provided office and laboratory space, computation facilities, and photographic services, under a collaborative research arrangement with Stanford University (NASA Grant NGR-05-020-223).

ACKNOWLEDGEMENTS

The author wishes to express his gratitude to his adviser, Professor Max Anliker, for suggesting the thesis topic and for providing advice and guidance during the course of the research. Thanks are also due Professors I. D. Chang, C. C. Chao, and Holt Ashley for reviewing the preliminary manuscript, and the members of the Biomechanics Group for many valuable ideas and discussions.

Ames Research Center, NASA, provided office and laboratory space, computation facilities, and photographic services, under a collaborative research arrangement with Stanford University (NASA Grant NGR-05-020-223). The author is particularly indebted to Dr. John Billingham, Acting Chief of the Biotechnology Division, and Dr. Jorge Huertas, formerly Chief of the Neurobiology Branch, for their assistance.

Mrs. Jane Fajardo typed the final manuscript, and Mrs. Madeline Anderson drew the illustrations and wrote in the equations.

The work was supported in part by the U.S. Navy, Office of Naval Research, under Contract Number N00014-67-A-0112-0007, and by the Graduate Study Program of the Lockheed Missiles and Space Company.

ABSTRACT

In order to study the propagation of pressure waves in the semicircular canals, a single canal is modeled as an elastic toroid located inside a rigid toroidal channel. The elastic toroid is filled with incompressible, inviscid fluid, and similar fluid fills the space between the elastic toroid and the rigid channel.

First, the system is studied using the potential flow equations to describe the motion of the fluids, and the membrane equation to describe the behavior of the elastic toroid. It is found that the equations of motion can be solved only by a great volume of numerical computation, an effort probably unwarranted since there is as yet no confirmation of the assumptions incorporated in the equations.

Therefore it has been decided to formulate the problem in a more approximate manner, so that solutions could be obtained with less numerical effort. The classical Moens-Korteweg equation for pressure wave propagation in a straight circular cylinder is extended to the fluid-filled and immersed elastic toroid inside a rigid toroidal channel. The solutions (wave speeds and mode shapes as a function of frequency) are easily obtained. There is a nondispersive mode, corresponding to the breathing motion in a straight cylinder, and a linearly dispersive mode, involving mainly flexure of the tube axis in its own plane. Experiments show, however, that these results are inadequate, and more accurate equations of motion are required.

The Moens-Korteweg equations are improved by considering the effects of the mass of the elastic shell and by retaining the shear behavior in the equations of motion. With these refinements, a third mode appears, and the other two modes are significantly changed. The flexural mode is still normally dispersive, but is no longer linearly so. The breathing mode is anomalously dispersive at low frequencies but remains nondispersive at higher frequencies. The third mode, which is at the highest speed, consists mainly of extensional deformations of the elastic shell. It is nondispersive above low frequencies.

Mode shapes are worked out as functions of the geometric parameters of the toroids. It is found that in-plane motion of the tube axis dominates the

flexural modes, changes in the cross-sectional diameter of the tube and motion of the fluid dominate the breathing mode, and axial displacement of the tube wall dominates the extensional mode.

Experimental data is available for wave speeds in a fluid-filled toroidal shell without the exterior fluid or rigid channel. Comparison with the present theory for the same configuration confirms the general shape of all three modes, and agrees with the numerical values to 20%, often to better than 10%.

Some of the findings of this study are expected to be useful in a theoretical analysis of the wave transmission properties of the aortic arch and of its effects on the shape of the natural pulse wave generated by the heart.

TABLE OF CONTENTS

TABLE OF CONTENTS (Continued)

I. INTRODUCTION

Engineering analyses of the human physiology are important for at least two reasons. First, the foreign environment of space flight subjects the human organism to conditions unprecedented and in many cases impossible to simulate on the surface of the earth. The prediction of man's response would be aided by a deeper, quantitative understanding of the fundamental principles of operation of the various organs than is provided by clinical and other qualitative approaches. Second, and perhaps more important, is the necessity for developing accurate mathematical models of organ functions, not only for diagnosis and treatment but also for the design of artificial organs.

This investigation is concerned with some aspects of the mechanical behavior of the semicircular canals, the portions of the vestibular apparatus, in the inner ear of higher vertebrates, which are the end organs responsible for the sensation of angular accelerations. By way of introduction, the anatomy and physiology of the human semicircular canals will be very briefly outlined, previous studies of their dynamics will be mentioned, and the goals and objectives of this study will be set forth.

A. Anatomy and Physiology

The inner ear contains the cochlea, a hearing receptor, and the vestibular apparatus, a sensor for linear and angular accelerations (Figs. 1-1 to 1-6). It is known that the vestibular apparatus is sensitive to low-frequency motions while the cochlea responds to high frequency signals. However, it has not yet been established whether this behavior is due to the mechanical and physical properties of the end organs or to the characteristics of the sensory nerves and the central nervous system.

There are three semicircular canals in each ear, lying approximately in mutually orthogonal planes. Each is actually more nearly three-quarters of a circle. The remaining quarter circle includes the ampulla and a portion of the utricle. The ampulla has a larger cross section than the canal itself and contains the sensory nerve cells. The utricle connects through a very small duct with the saccule, which in turn joins the cochlea through another small channel. All these structures are made of a membranous material and are filled with a fluid called endolymph.

The entire membranous structure is suspended inside a similarly-shaped fluid-filled channel in the temporal bone of the skull. The fluid between the membrane and the bone is referred to as perilymph.

Each of the canals and its ampulla constitutes an angular acceleration sensor. The canals are made up of membranous and bony canals, perilymph, and endolymph. The ampulla contains a gelatinous protrusion called the cupula, which is attached at its base to the crista containing the sensory hairs. These hairs emerge from nerve cells which discharge at a rate depending on the deflection of the hair cells from their undisturbed position.

Qualitatively, the operation of the canals is easily explained. An angular acceleration of the head forces the membranous canal, which is attached to the bone by thread-like fibers, to accelerate in similar fashion. If the angular acceleration vector has a component perpendicular to the plane of any particular canal, the fluid's inertia will cause its motion to lag behind that of the membranous and bony material. This relative motion of the fluid with respect to the head deflects the cupula and its hair cells and changes the rate of firing of the nerve cells, which is interpreted as angular acceleration. Since there are three canals in mutually near-perpendicular planes any angular acceleration vector direction in space can be detected.

It should be mentioned that, with current techniques, direct measurement of the fluid motions or nerve firing rates in humans is impossible. Experimenters must use indirect methods, such as asking the subject whether he feels any angular acceleration, or measuring nystagmus, the involuntary eye motions associated with sensed angular velocity. Thus the canal response is filtered through the central nervous system and perhaps some output nerves and muscles (Fig. 1-7) before it can be measured.

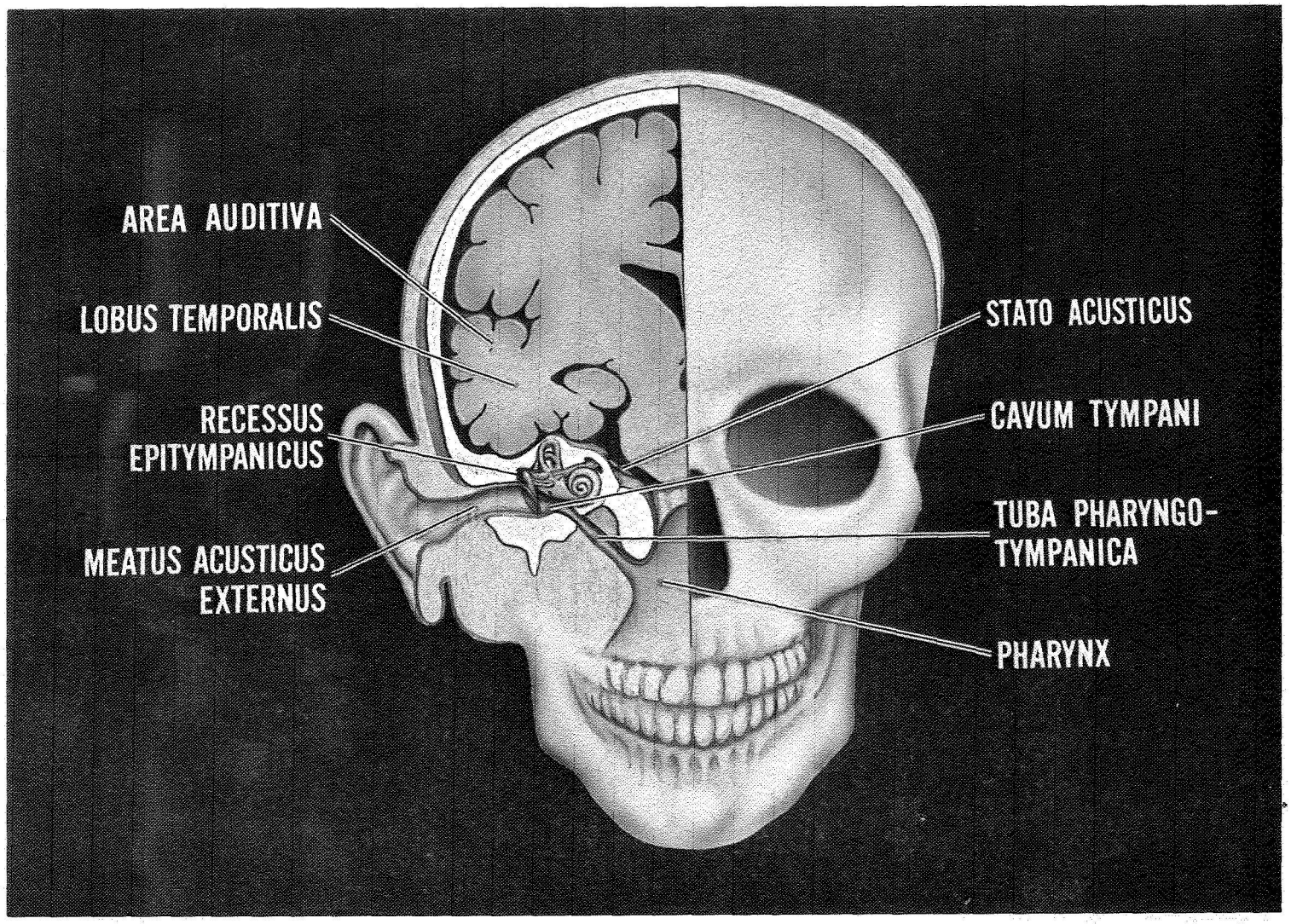

Fig. 1-1. Cross-section of Human Skull Showing the Inner Ear

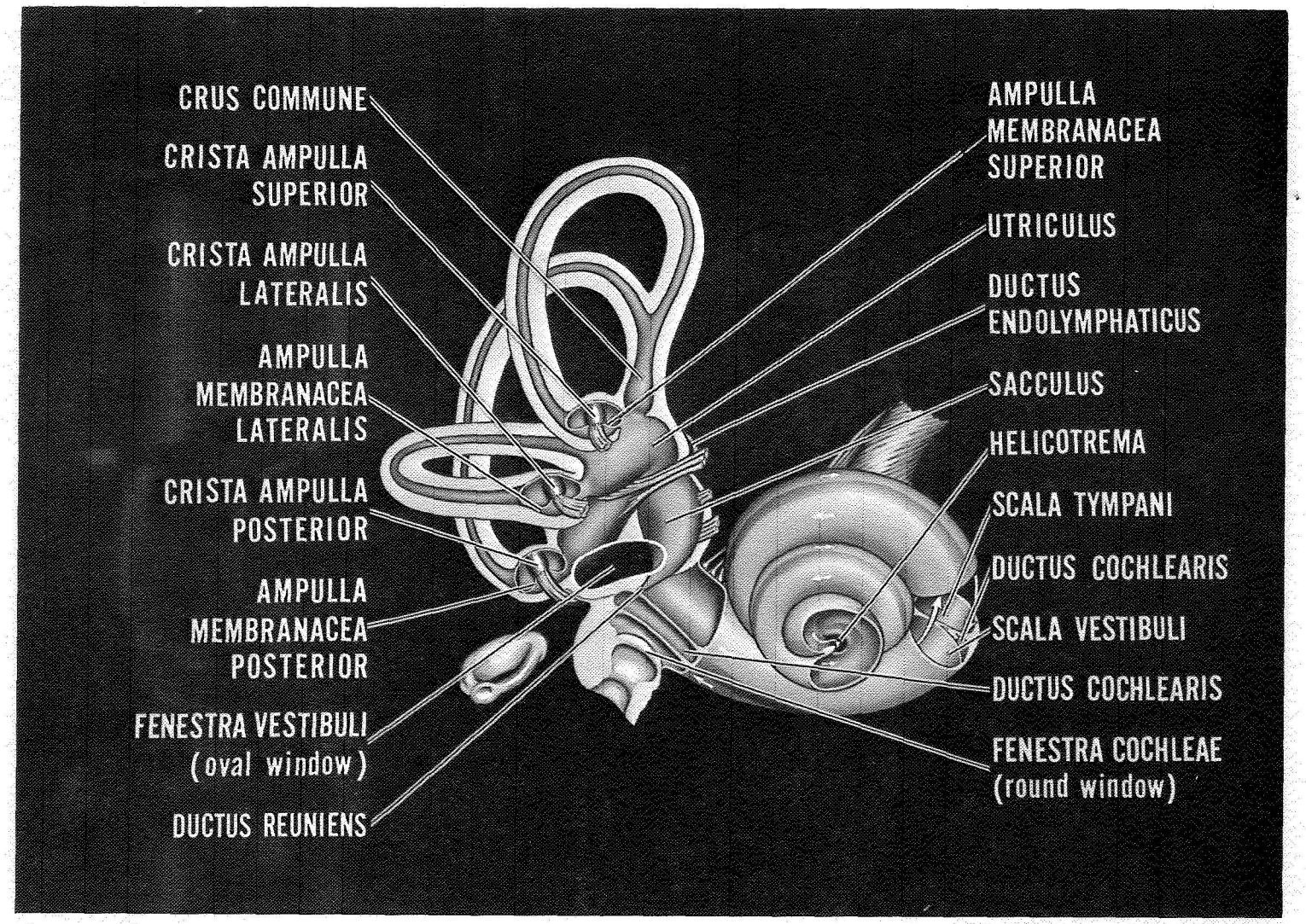

Fig. 1-2. Partial Cross-section of the Inner Ear

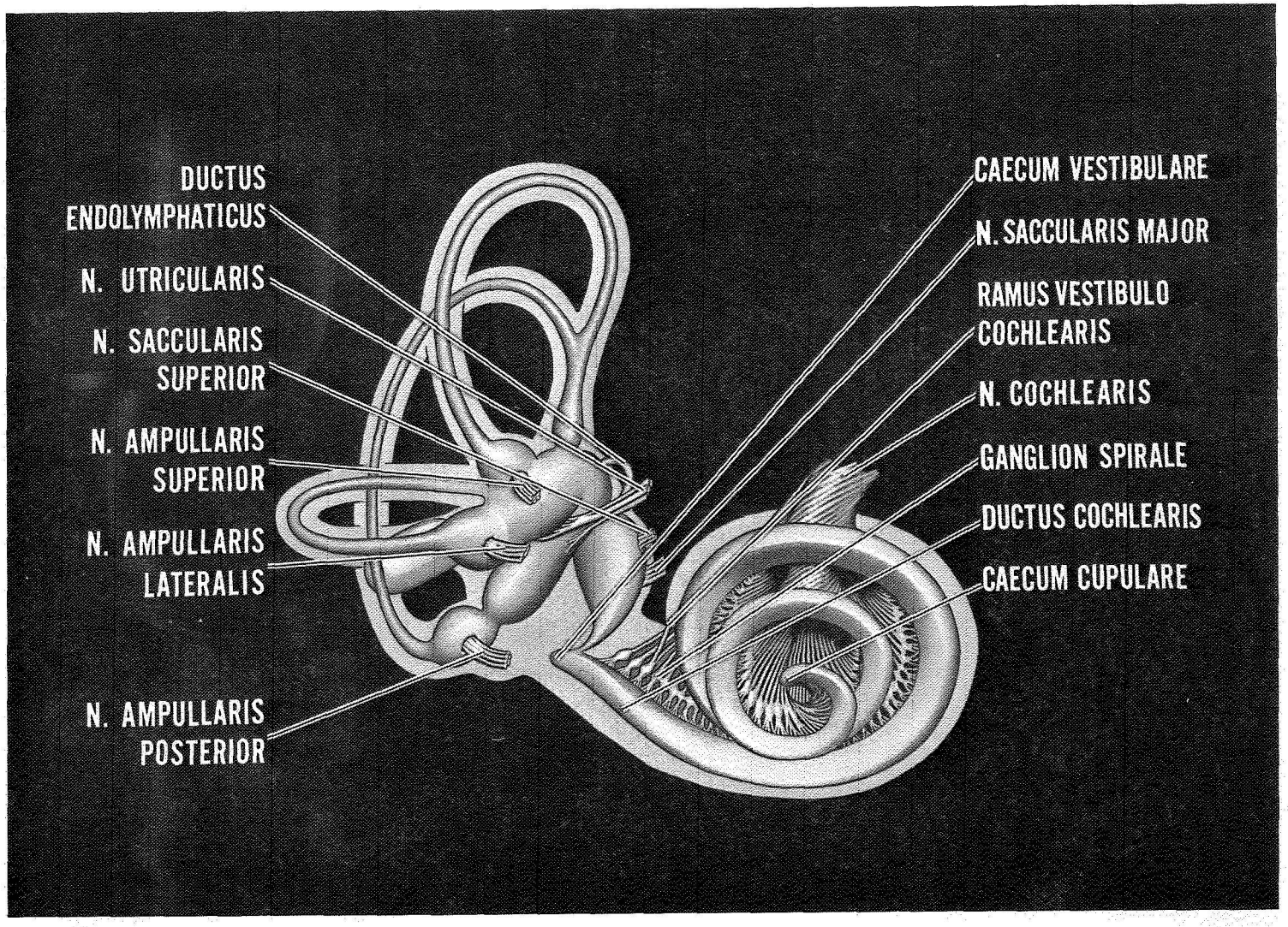

Fig. 1-3. Nerve Endings of the Inner Ear

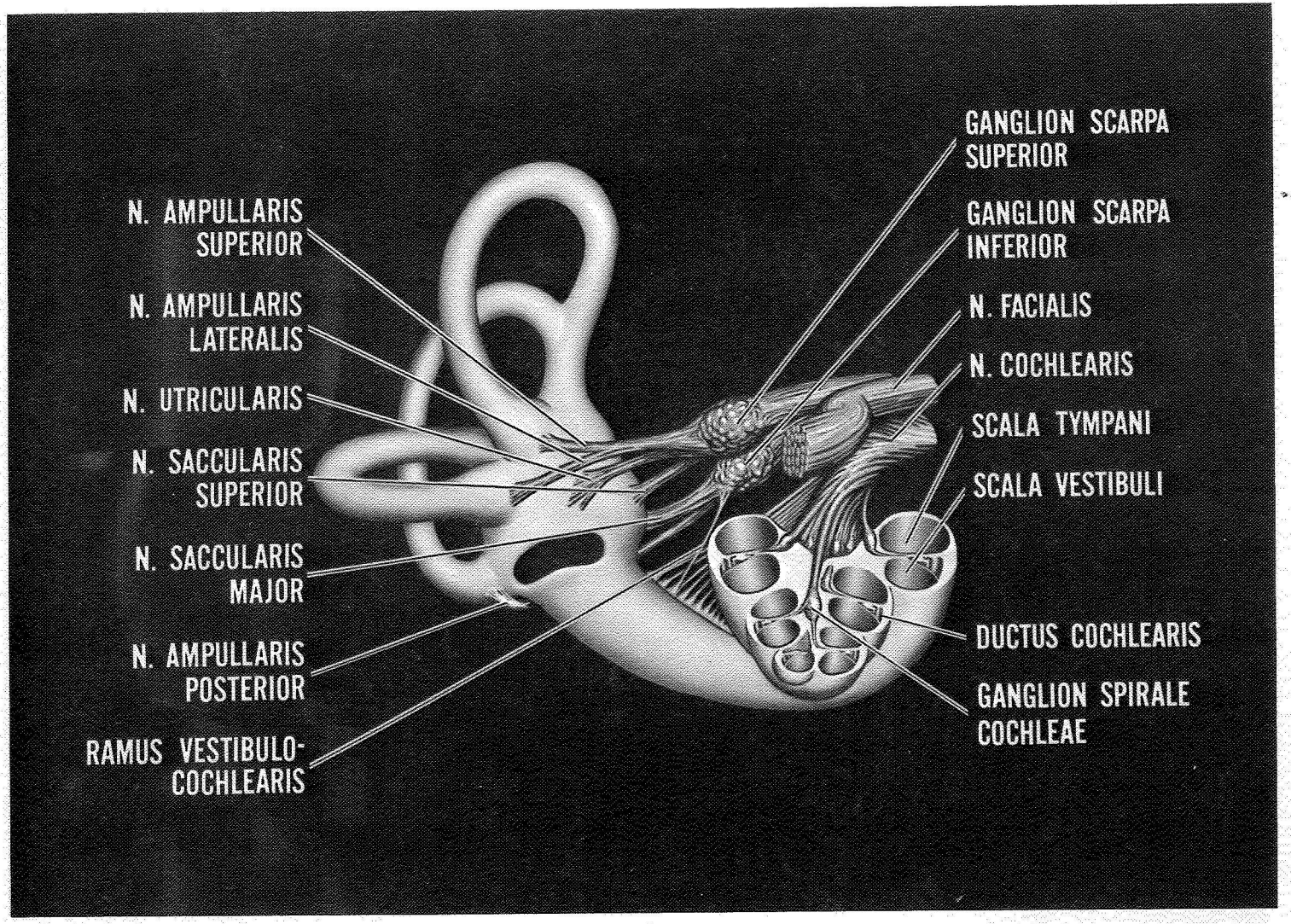

Fig. 1-4. Afferent Nerves of the Inner Ear

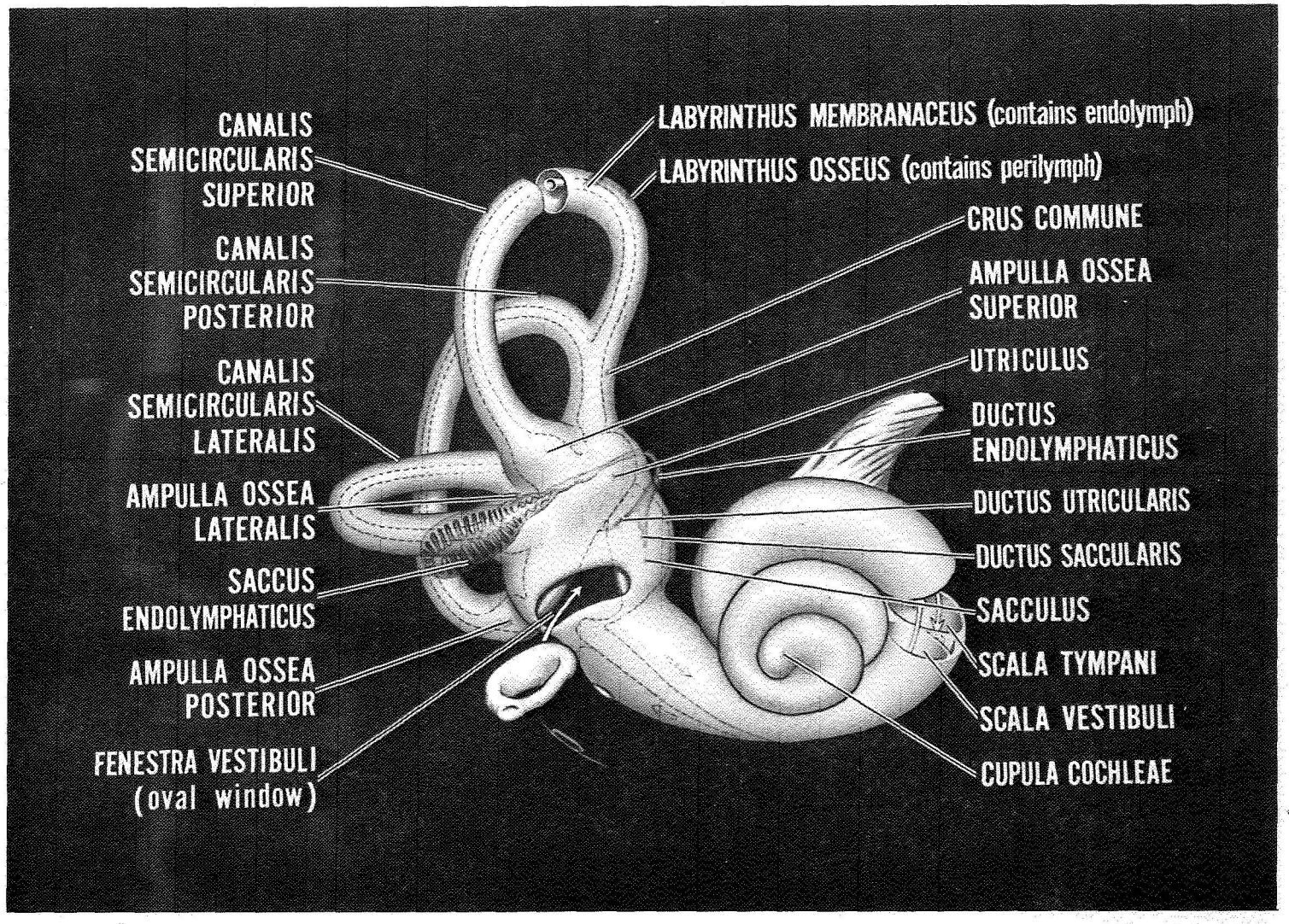

Fig. 1-5. The Bony Inner Ear

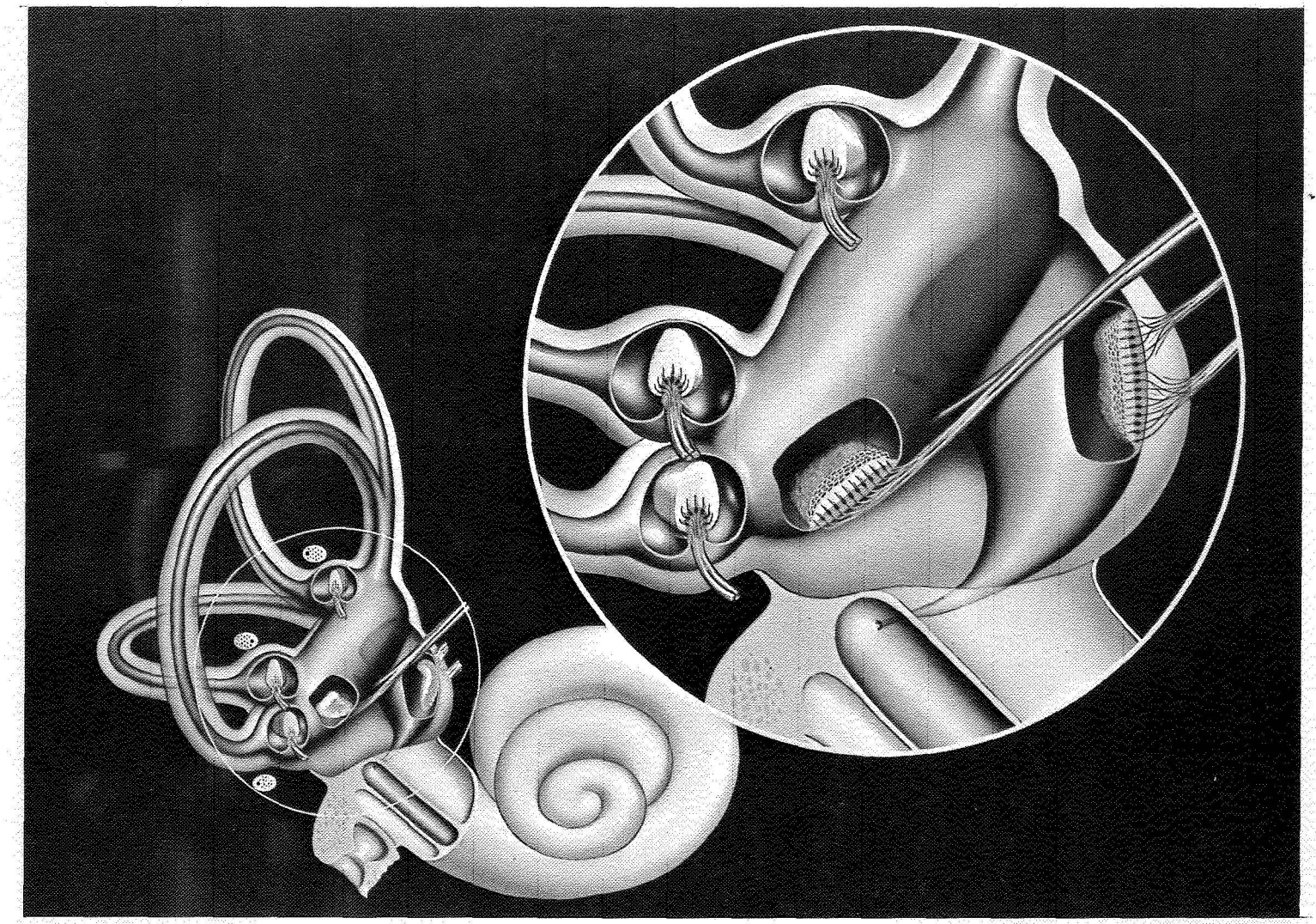

Fig. 1-6. The Vestibular Apparatus of Man

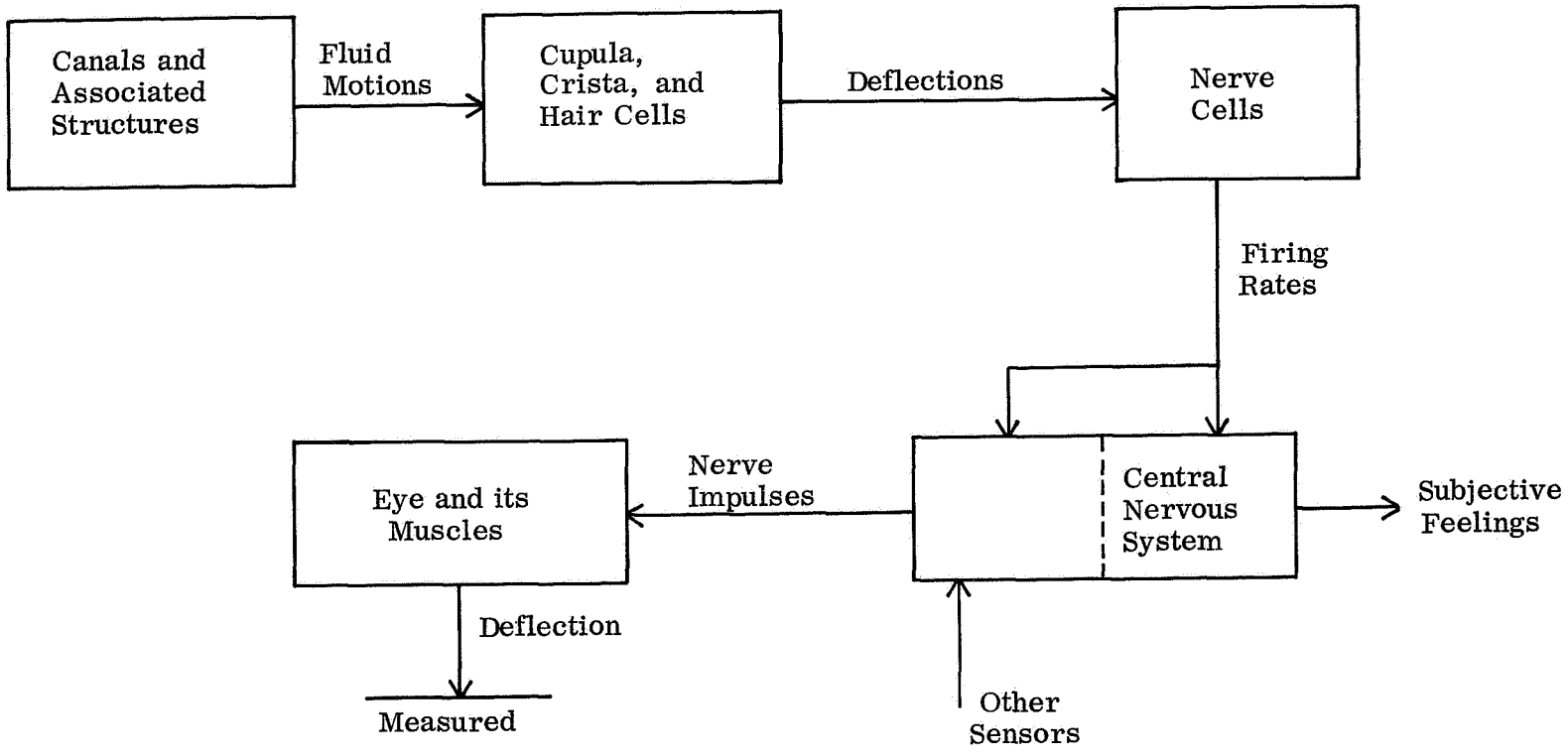

Fig. 1-7. Schematic Diagram of Sensory Mechanism for Angular Accelerations and Their Manifestations

B. Previous Work

Studies of the dynamics of the semicircular canals date from about 1930[10]. Early work, and until recently all work, assumed that the canals responded like overdamped torsion pendula to angular accelerations. That is, the canals' response to an angular acceleration step was the sum of two damped exponentials, with initial amplitudes such as to match the initial conditions of the problem. Empirical determination of coefficients produced a good fit to the general behavior of nystagmus or subjective sensation of angular acceleration, but there are obvious drawbacks to this approach. The model represents the entire system, consisting of the canals, cupula, sensory neurons, neural paths, central nervous system, and muscles of the eye. It is obviously oversimplified and somewhat empirical, and therefore can hardly be expected to give insight into the basic physical processes taking place in the end organ.

Recently Steer[8] has performed an engineering analysis of the mechanical behavior of the semicircular canals. He solved the Navier-Stokes equations for the flow of the endolymph assuming that the membranous canals behave like perfect rigid toroids. He also approximated the effects of the ampulla on the dynamic response of the canals. The results of Steer's approximate analysis also suggest that the cupula-endolymph system behaves like a damped torsion pendulum.

C. Goals and Objectives

The present investigation is a part of a continuing effort to achieve an understanding of the mechanical behavior of the semicircular canals, represented by the first block in Figure 1-7. Our analysis is based on a mathematical model which takes into account the elasticity of the membranous canals but neglects the effects of the viscosity of the labyrinthine fluids. As such it is the first attempt to analyze the interaction of endolymph, perilymph, and an elastic membranous canal wall.

For a number of different theoretical models, the free vibrations and wave transmission characteristics of the semicircular canals are studied by deriving and solving the corresponding linearized equations of motion.

First, the basic solutions to the potential flow equations in terms of toroidal coordinates are reviewed. In order to satisfy the boundary conditions, it is found that for each eigenvibration the mode shapes must be expressed as an

infinite series of the basic potential flow solutions. The determination of natural frequencies and mode shapes in this situation requires a massive numerical effort which is not warranted at present in view of the uncertainties about the validity of the basic assumptions.

Next, the classical Moens-Korteweg equation for the propagation of distension waves in straight elastic cylinders is adapted to toroids. The equations are derived and solved, but on the basis of simple experiments the results were found to be inaccurate.

Finally, the Moens-Korteweg approach is replaced by a more refined engineering analysis, whose results are in reasonably good agreement with experimental data obtained from laboratory models.

Yet to be considered are the effects produced by fluid viscosity, the presence of the ampulla, the nature of the suspension of the membranous canal in the bony canal, and by the interaction among the three canals and the utricle.

II. POTENTIAL FLOW ANALYSIS

One semicircular canal, not including the ampulla or any portion of the utricle, is approximated as a toroidal elastic membrane inside a rigid toroidal wall (for the moment we ignore the question of whether one toroid is centered inside the other). The fluid inside the membrane (endolymph) is referred to as the inner fluid; that between the membrane and the wall (perilymph) is the outer fluid. The two fluids are assumed to be incompressible and inviscid, but may have different densities.

The attempted method of solution is analogous to the linearized theory used in Ref. 1. For irrotational flow the motions of the fluids are governed by the Laplace equation for the velocity potentials of the fluids. The motions also must be compatible with the kinematic boundary conditions requiring the fluid velocity to match the membrane or wall velocity at the interfaces. The dynamic boundary condition to be satisfied is simply the equation of motion of the membrane. By linearizing the Euler equation the fluid pressure can be written as a function of the velocity potential.

Next the known solutions to the Laplace equations in the appropriate coordinates are given and some of the free parameters of the solutions are determined by satisfying the kinematic boundary conditions. Presumably there are an infinity of such solutions, which are the velocity potentials corresponding to the possible modes of fluid motion. These solutions define a class of membrane motions and pressure variations which, in general, are only compatible with the dynamic boundary conditions for certain frequencies at a given wavelength.

A. Equations of Motion

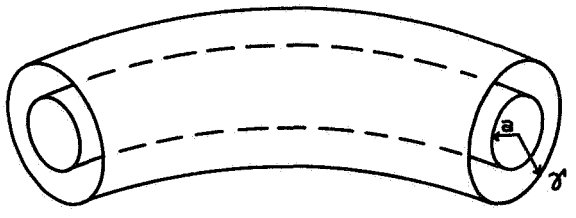

Fig. 2-1. Toroidal Membrane Inside Rigid Toroidal Channel

The tube radii of the elastic toroidal membrane and the rigid channel are a and γ respectively. p_i and p_e represent the pressures of the inner and outer fluids; ρ_i and ρ_e are their densities. ρ_w is the density of the membrane material and h its thickness. w is the displacement of the membrane normal to its equilibrium surface (positive outward). Φ and Ψ are the velocity potentials of the interior and exterior fluids.

The two equations of fluid motion are simply the continuity equations for the two fluids, $div\ \vec{V} = 0$. With $\vec{V} = \nabla\Phi$ for the inner fluid and $\nabla\Psi$ for the outer fluid, the continuity equations assume the classical form

$$\nabla^2 \Phi = 0 \tag{2-1}$$

$$\nabla^2 \Psi = 0 \tag{2-2}$$

The kinematic boundary condition at the rigid wall is

$$\nabla\Psi \cdot \vec{u}_n\Big|_\gamma = 0 \tag{2-3}$$

where $\vec{u}_n$ is the outward normal to the surface. At the membrane,

$$\nabla\Psi \cdot \vec{u}_n\Big|_a = \frac{\partial w}{\partial t} \tag{2-4}$$

$$\nabla\Phi \cdot \vec{u}_n\Big|_a = \frac{\partial w}{\partial t} \tag{2-5}$$

Here, as part of the linearization process, the boundary condition is enforced at the undeformed surface, r = a, instead of at r = a + w; the normal direction is also assumed to vary insignificantly as w changes.

The dynamic boundary condition is the membrane equation:

$$\Delta p = \frac{T_1}{R_1} + \frac{T_2}{R_2} + \rho_w h \frac{\partial^2 w}{\partial t^2} \tag{2-6}$$

Here R_1 and R_2 are the principal radii of curvature at any point on the membrane; T_1 and T_2 are the tensions (stress × thickness) at that point in the R_1 and R_2 directions. Δp is the pressure difference $p_i - p_e$ at that point. The pressures are evaluated from the linearized Euler equations

$$p_i = p_{io} - \rho_i \frac{\partial \Phi}{\partial t} \tag{2-7}$$

$$p_e = p_{eo} - \rho_e \frac{\partial \Psi}{\partial t} \tag{2-8}$$

p_{io} and p_{eo} are the equilibrium inside and outside pressures.

B. Coordinate Systems

We must now specify exactly how the elastic and rigid toroids are located with respect to each other. Two different systems are considered.

In concentric coordinates, the toroid of radius a is centered within the toroid of radius γ ; this system is convenient for differential geometry. In non-concentric coordinates the smaller toroid is not centered within the larger one; the Laplace equation has a known solution in this system.

1. Concentric Coordinates

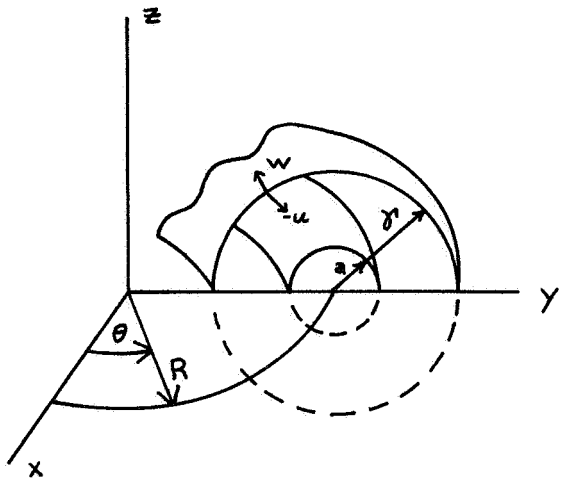

Fig. 2-2. Concentric Coordinate System

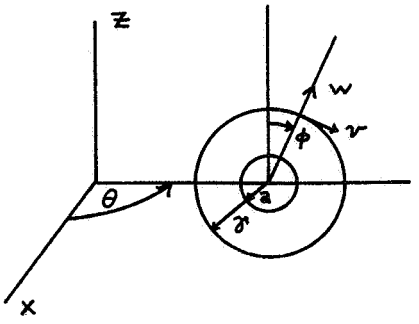

Fig. 2-3. Cross-section of Toroid

The curvilinear axis on which the cross-sections are centered is a circle in the xy plane with its center at the origin and with radius R (R is referred to as the ring radius). The cross-sections of the toroids are independent of θ and have radii a and γ (these are referred to as the tube radii). (See Fig. 2-2.) The angles ϕ and θ are defined in Fig. 2-3. Displacement components of a point on the surface of the toroid are u (in the θ direction), v (in the ϕ direction), and w (radially outward from the center of the cross-section). These displacements are functions of θ and ϕ .

The coordinates of any point on the shell, when $u = v = w = 0$, are

$$x = R\cos\theta + a\sin\phi\cos\theta$$
$$y = R\sin\theta + a\sin\phi\sin\theta$$
$$z = a\cos\phi$$

for the inner shell. Replace a with γ for the outer shell.

When displacements are permitted,

$$x = R\cos\theta + a\sin\phi\cos\theta + w\sin\phi\cos\theta + v\cos\phi\cos\theta - u\sin\theta$$

$$y = R\sin\theta + a\sin\phi\sin\theta + w\sin\phi\sin\theta + v\cos\phi\sin\theta + u\cos\theta$$

$$z = a\cos\phi + w\cos\phi - v\sin\phi$$

2. Nonconcentric Coordinates

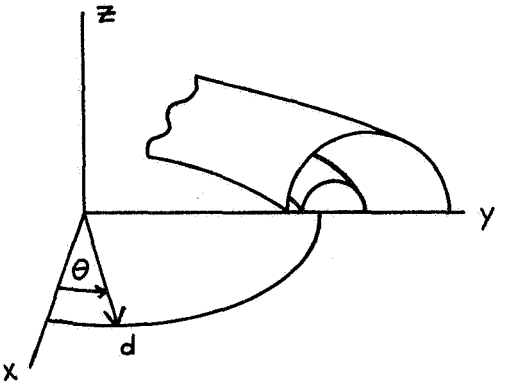

Fig. 2-4.
Nonconcentric Coordinate System

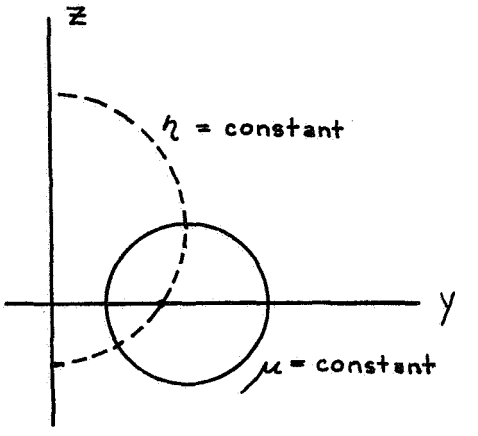

Fig. 2-5.
Cross-section of Torus

A toroidal surface is defined by μ = constant in the equations

$$x = \frac{d\sinh\mu\cos\theta}{\cosh\mu - \cos\eta} \qquad y = \frac{d\sinh\mu\sin\theta}{\cosh\mu - \cos\eta} \qquad z = \frac{d\sin\eta}{\cosh\mu - \cos\eta}$$

With θ = const, the surfaces μ = const are circles in the plane determined by the Z axis and θ = const. As $\mu \longrightarrow \infty$, the circles become smaller and finally vanish at a point a distance d from the Z axis. As $\mu \longrightarrow 0$, the circles grow without limit and their centers move infinitely far away from the Z axis. In general, each circle is centered at a distance $d\coth\mu$ and has radius $d\,\mathrm{csch}\,\mu$.

The surfaces η = const are spheres centered on the Z axis. They intersect each of the μ = const surfaces at right angles, and so must pass through the point representing $\mu \longrightarrow \infty$. Projected onto a θ = const plane, μ = const and η = const form families of mutually orthogonal circles. In these coordinates, the previously defined displacement components u, v, and w are in the directions of increasing θ, increasing η, and decreasing μ respectively (Fig. 2-6).

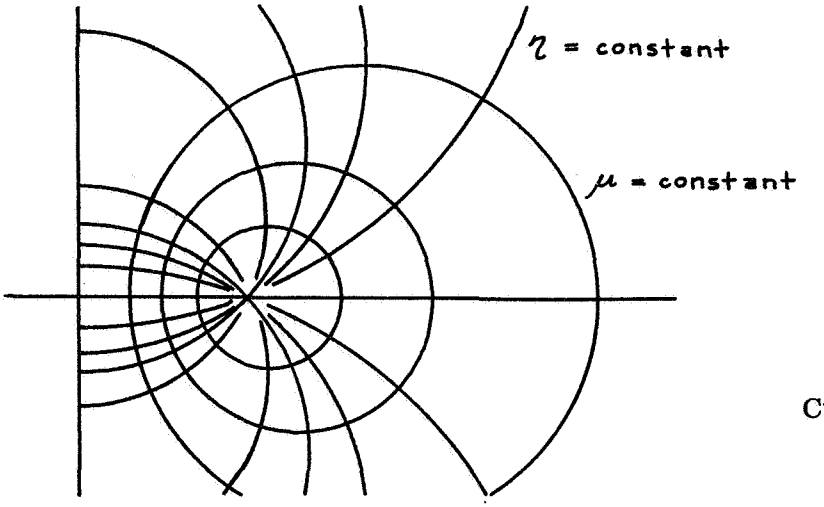

Fig. 2-6.
Curves of Constant Parameters

C. Differential Geometry of Deformed Torus

The membrane equation (Eq. 2-1) involves R_1 and R_2, the principal radii of curvature of the membrane. This section investigates the determination of these quantities for a toroidal surface in concentric coordinates.

1. General Equations (Ref. 4)

Let the equation of a point on the surface be

$$\vec{x} = f_1(u_1, u_2, u_3)\vec{u}_x + f_2(u_1, u_2, u_3)\vec{u}_y + f_3(u_1, u_2, u_3)\vec{u}_z$$

where u_1 and u_2 are the two coordinate quantities on the surface and $\vec{u}_x$, $\vec{u}_y$, and $\vec{u}_z$ are unit vectors in the cartesian x, y, and z directions. For example, for the toroid in its equilibrium state:

$$f_1 = R\cos\theta + a\sin\phi\cos\theta$$
$$f_2 = R\sin\theta + a\sin\phi\sin\theta$$
$$f_3 = a\cos\phi$$
$$u_1 = \phi\,, \quad u_2 = \theta$$

Letting the curvatures K_n be the reciprocals of the radii R_n $(n = 1, 2)$, the principal curvatures at any point on the surface are the roots of

$$K_n^2 - 2HK_n + K = 0 \qquad (2\text{-}9)$$

The quantities K and H are called the Gaussian and mean curvatures and are

$$K = \frac{b_{11}\,b_{22} - (b_{12})^2}{g_{11}\,g_{22} - (g_{12})^2}$$

$$H = \frac{1}{2}\left(\frac{b_{11}}{g_{11}} + 2\,\frac{b_{12}}{g_{12}} + \frac{b_{22}}{g_{22}}\right)$$

The b_{ij} and g_{ij} are defined from $\vec{x}$ and its derivatives, using the unit normal vector $\vec{n}$

$$\vec{n} = \frac{\frac{\partial \vec{x}}{\partial u_1} \times \frac{\partial \vec{x}}{\partial u_2}}{\left| \frac{\partial \vec{x}}{\partial u_1} \times \frac{\partial \vec{x}}{\partial u_2} \right|}$$

$$b_{ij} = \frac{\partial^2 \vec{x}}{\partial u_i \, \partial u_j} \cdot \vec{n} \qquad g_{ij} = \frac{\partial \vec{x}}{\partial u_i} \cdot \frac{\partial \vec{x}}{\partial u_j} \qquad i = 1,2$$

Clearly $b_{ij} = b_{ji}$ and $g_{ij} = g_{ji}$

If and only if $b_{12} = g_{12} = 0$, the coordinate curves in the surface (u_1 = const and u_2 = const) are lines of principal curvature. In this case, the roots of Eq. (2-9) are

$$K_1 = \frac{b_{11}}{g_{11}} \quad ; \quad K_2 = \frac{b_{22}}{g_{22}}$$

2. Toroid in Equilibrium Condition

Let us determine the radii of curvature of a toroid in concentric coordinates with $u = v = w = 0$

$$\vec{x} = (R\cos\theta + a\sin\phi\cos\theta)\,\vec{u}_x + (R\sin\theta + a\sin\phi\sin\theta)\,\vec{u}_y + a\cos\phi\,\vec{u}_z$$

$$\frac{\partial \vec{x}}{\partial \theta} = (-R\sin\theta - a\sin\phi\sin\theta)\,\vec{u}_x + (R\cos\theta + a\sin\phi\cos\theta)\,\vec{u}_y$$

$$\frac{\partial \vec{x}}{\partial \phi} = (a\cos\phi\cos\theta)\,\vec{u}_x + (a\cos\phi\sin\theta)\,\vec{u}_y - a\sin\phi\,\vec{u}_z$$

$$\vec{n} = -\left[(Ra\sin\phi\cos\theta + a^2\sin^2\phi\cos\theta)\,\vec{u}_x + (Ra\sin\phi\sin\theta + a^2\sin^2\phi\sin\theta)\,\vec{u}_y + (Ra\cos\phi + a^2\sin\phi\cos\phi)\,\vec{u}_z\right] / \; a(R + a\sin\phi)$$

$$g_{11} = \left(\frac{\partial \vec{x}}{\partial \phi}\right)^2 = a^2$$

$$g_{12} = \frac{\partial \vec{x}}{\partial \theta} \cdot \frac{\partial \vec{x}}{\partial \phi} = 0$$

$$g_{22} = \left(\frac{\partial \vec{x}}{\partial \theta}\right)^2 = (R + a \sin\phi)^2$$

$$\frac{\partial^2 \vec{x}}{\partial \phi^2} = -(a \sin\phi \cos\theta)\,\vec{u}_x - (a \sin\phi \sin\theta)\,\vec{u}_y - (a \cos\phi)\,\vec{u}_z$$

$$\frac{\partial^2 \vec{x}}{\partial \theta \partial \phi} = -(a \cos\phi \sin\theta)\,\vec{u}_x + (a \cos\phi \cos\theta)\,\vec{u}_y$$

$$\frac{\partial^2 \vec{x}}{\partial \theta^2} = -(R + a \sin\phi)\cos\theta\,\vec{u}_x - (R + a \sin\phi)\sin\theta\,\vec{u}_y$$

$$b_{11} = \frac{-a(R + a \sin\phi)}{R + a \sin\phi} = -a$$

$$b_{12} = 0$$

$$b_{22} = \frac{-(R + a \sin\phi)^2 \sin\phi}{R + a \sin\phi} = -(R + a \sin\phi)\sin\phi$$

The coordinate directions are principal directions and

$$K_1 = \frac{-a}{a^2} = -\frac{1}{a}$$ in the ϕ direction

$$K_2 = \frac{-(R + a \sin\phi)\sin\phi}{(R + a \sin\phi)^2} = -\frac{\sin\phi}{R + a \sin\phi}$$ in the θ direction

3. Toroid with $u = v = 0$ and $w = w(\theta)$

This surface has circular cross-section at all points, with radius $a + w$ and with the circle centered on the original axis (in the $z = 0$ plane a distance R from the origin).

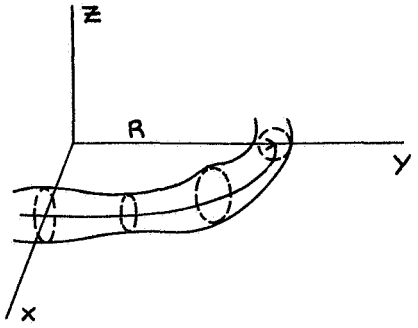

Fig. 2-8.
Sketch of $w = w(\theta)$

Using the notation $w' = dw/d\theta$, $w'' = d^2w/d\theta^2$ we can write

$$\frac{\partial \vec{x}}{\partial \phi} = (a\cos\phi + w\cos\phi)\cos\theta\,\vec{u}_x + (a\cos\phi + w\cos\phi)\sin\theta\,\vec{u}_y - (a\sin\phi + w\sin\phi)\,\vec{u}_z$$

$$\frac{\partial \vec{x}}{\partial \theta} = [-(R + a\sin\phi + w\sin\phi)\sin\theta + w'\sin\phi\cos\theta]\,\vec{u}_x + [(R + a\sin\phi + w\sin\phi)\cos\theta + w'\sin\phi\sin\theta]\,\vec{u}_y + w'\cos\phi\,\vec{u}_z$$

$$g_{11} = (a+w)^2\,; \qquad g_{12} = 0\,; \qquad g_{22} = (R + a\sin\phi + w\sin\phi)^2 + (w')^2$$

$$\vec{n} = \{[(a+w)^2\sin^2\phi\cos\theta + R(a+w)\sin\phi\cos\theta + w'(a+w)\sin\theta]\,\vec{u}_x + [(a+w)^2\sin^2\phi\sin\theta + R(a+w)\sin\phi\sin\theta - w'(a+w)\cos\theta]\,\vec{u}_y + [(a+w)^2\sin\phi\cos\phi + R(a+w)\cos\phi]\,\vec{u}_z\} \Big/ \{(a+w)[(R+(a+w)\sin\phi)^2 + (w')^2]^{1/2}\}$$

$$\frac{\partial^2 \vec{x}}{\partial \phi^2} = -(a\sin\phi + w\sin\phi)\cos\theta\,\vec{u}_x - (a\sin\phi + w\sin\phi)\sin\theta\,\vec{u}_y - (a\cos\phi + w\cos\phi)\,\vec{u}_z$$

$$\frac{\partial^2 \vec{x}}{\partial \phi \partial \theta} = [-(a\cos\phi + w\cos\phi)\sin\theta + w'\cos\phi\cos\theta]\,\vec{u}_x + [(a\cos\phi + w\cos\phi)\cos\theta + w'\cos\phi\sin\theta]\,\vec{u}_y - w'\sin\phi\,\vec{u}_z$$

$$\frac{\partial^2 \vec{x}}{\partial \theta^2} = [-(R + a\sin\phi + w\sin\phi)\cos\theta - 2w'\sin\phi\sin\theta + w''\sin\phi\cos\theta]\,\vec{u}_x$$
$$+ [-(R + a\sin\phi + w\sin\phi)\sin\theta + 2w'\sin\phi\cos\theta + w''\sin\phi\sin\theta]\,\vec{u}_y + w''\cos\phi\,\vec{u}_z$$

$$b_{11} = \frac{-(a+w)(a+w\sin\phi+R)}{[\{R+(a+w)\sin\phi\}^2 + (w')^2]^{1/2}} \cong -(a+w) \qquad \text{for} \quad |w''| << |R + a\sin\phi|$$

$$b_{12} = 0$$

$$b_{22} = \frac{\{[R+(a+w)\sin\phi]w'' - [R+(a+w)\sin\phi]^2\sin\phi - 2(w')^2\sin\phi\}}{[\{R+(a+w)\sin\phi\}^2 + (w')^2]^{1/2}}$$

Then $$K_1 = \frac{b_{11}}{g_{11}} = \frac{-(R + a\sin\phi + w\sin\phi)}{[\{R+(a+w)\sin\phi\}^2 + (w')^2]^{1/2}} \cong -\frac{1}{a+w}$$

$$K_2 = \frac{b_{22}}{g_{22}} = -\frac{\sin\phi}{R+(a+w)\sin\phi} + \frac{w''}{[R+(a+w)\sin\phi]^2} \cong \frac{-\sin\phi}{R+(a+w)\sin\phi}$$

These values can be rewritten in the nonconcentric toroidal coordinates by using the transformations given in section B:

$$K_1 = -\frac{1}{a+w}$$

$$K_2 = \frac{-\sin\eta\sqrt{\frac{4R^2}{a^2} - 1}}{\frac{2R^2}{a} - R\cos\eta + (a+w)\sin\eta\sqrt{\frac{4R^2}{a^2} - 1}} + \frac{w''\left[\frac{2R}{a} - \cos\eta\right]^2}{\left[\frac{2R^2}{a} - R\cos\eta + (a+w)\sin\eta\sqrt{\frac{4R^2}{a^2} - 1}\,\right]^2}$$

It would be possible to derive curvatures for other types of deformation, most importantly for w as a function of ϕ and θ ; but the algebra becomes extremely involved when the coordinate curves are no longer lines of principal curvature. Further, the membrane equation then becomes much more complicated and the solution of Laplace's equation more difficult.

D. The Membrane Equation

We next derive expressions for the principal tensions T_1 and T_2 for the two cases whose differential geometry has been discussed: $u = v = w = 0$ and $u = v = 0$, $w = w(\theta)$.

The membrane equation was given in section A as:

$$\Delta p = p_i - p_e = \frac{T_1}{R_1} + \frac{T_2}{R_2} + \rho_w h \frac{\partial^2 w}{\partial t^2}$$

where

p_i = internal pressure

p_e = external pressure

R_1, R_2 = principal radii of curvature

T_1, T_2 = tensions (stress × thickness) in these directions

ρ_w = membrane density

h = membrane thickness

w = membrane displacement (normal to surface)

1. Equilibrium Configuration

In the equilibrium configuration ($w = 0$) we have

$$p_i - p_e = \frac{T_1}{R_1} + \frac{T_2}{R_2} = T_1 K_1 + T_2 K_2 \qquad (2\text{-}10)$$

where the curvatures K are the reciprocals of the radii R.

From section C, K_1 (in the ϕ direction) is $-1/a$, and K_2 (in the θ direction) is $-\sin\phi / (R + a\sin\phi)$ and therefore

$$p_i - p_e = -\frac{T_1}{a} - \frac{T_2 \sin\phi}{R + a\sin\phi}$$

At $\phi = 0$ or π, we have $\sin\phi = 0$ and $T_1 = -a(p_i - p_e)$. It is now clear that the sign convention in the membrane equation is the reverse of the one used in the differential geometry derivation. We will therefore reverse the signs on K_1 and K_2 from section C:

$$p_i - p_e = \frac{T_1}{a} + \frac{T_2 \sin\phi}{R + a\sin\phi}; \qquad T_1(\phi = 0) = a(p_i - p_e) \qquad (2\text{-}11)$$

We need one more equation to be able to solve for T_1 and T_2. This is obtained by formulating the equilibrium in the ϕ direction of a small segment of shell.

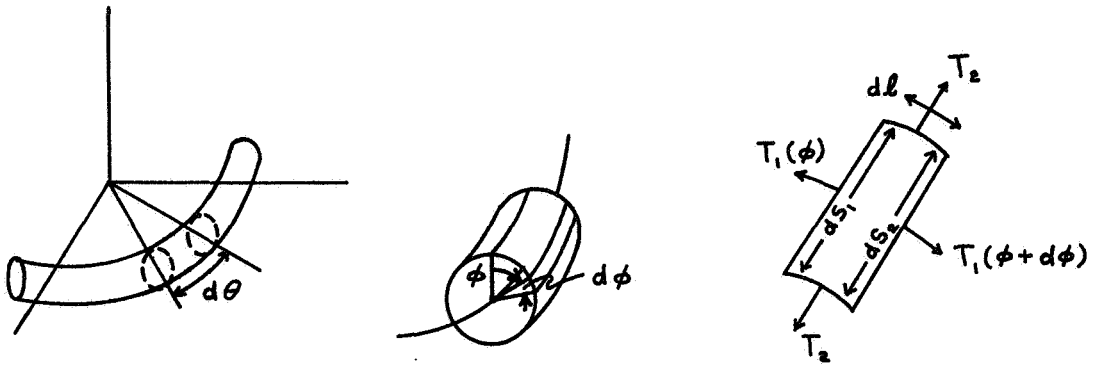

Fig. 2-9. Illustration of Shell Segment

First a portion of torus between θ_1 and θ_2 is removed. Then the segment of this portion between ϕ and $\phi + d\phi$ is isolated. T_1 and T_2 vary with ϕ ; neither varies with θ . Note that the two sides on which T_2 is acting are, in general, not parallel.

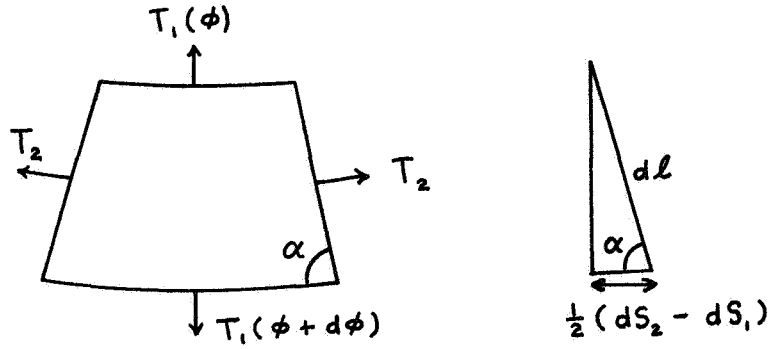

Fig. 2-10. Equilibrium of Shell Segment

Equilibrium in the ϕ direction requires

$$T_1(\phi)\, ds_1 - T_1(\phi + d\phi)\, ds_2 + 2\, T_2\, d\ell \cos\alpha = 0$$

with $d\ell = a\, d\phi$, $ds_1 = (R + a \sin\phi)\, d\theta$ (since the ds_1 line is a distance $R + a \sin\phi$ from the z axis), $ds_2 = [R + a \sin(\phi + d\phi)]\, d\theta$, and

$$\cos\alpha = \frac{\frac{1}{2}(ds_2 - ds_1)}{d\ell}$$

By using the relation

$$\sin(\phi + d\phi) \cong \sin\phi + \frac{d \sin\phi}{d\phi}\, d\phi = \sin\phi + \cos\phi\, d\phi$$

the equilibrium equation becomes, to first order,

$$\frac{dT_1}{d\phi} = \frac{(T_2 - T_1)\, a \cos\phi}{R + a\sin\phi} \tag{2-12}$$

We isolate T_2 from Eq. (2-11) as $T_2 = (\Delta p - \frac{T_1}{a})\ \frac{R + a\sin\phi}{\sin\phi}$, and substitute into (2-12) to obtain

$$\frac{dT_1}{d\phi} = \frac{a\Delta p}{\sin\phi}\cos\phi - \frac{T_1 a\cos\phi}{R + a\sin\phi}\left[\frac{R + a\sin\phi}{a\sin\phi} + 1\right] \tag{2-13}$$

which can be rewritten

$$dT_1 + \frac{a\cos\phi}{R + a\sin\phi}\left[\frac{R + a\sin\phi}{a\sin\phi} + 1\right] T_1\, d\phi = a\Delta p\ \frac{\cos\phi}{\sin\phi}\, d\phi \tag{2-14}$$

This equation has the form of the classical first-order linear non-homogeneous differential equation (Ref. 6)

$$dy + P(x)y\, dx = Q(x)\, dx$$

whose solution is

$$y\, e^{\int p(x)dx} = \int Q(x)\, e^{\int p(x)dx}\, dx + C$$

In the notation of Eq. (2-14),

$$\int p(x)dx \Rightarrow \int \frac{\cos\phi\, d\phi}{\sin\phi} + \int \frac{a\cos\phi\, d\phi}{R + a\sin\phi} = \log\sin\phi + \log(R + a\sin\phi)$$

$$e^{\int p(x)dx} \Longrightarrow \sin\phi(R + a\sin\phi)$$

The solution of Eq. (2-14) is then

$$T_1 \sin\phi(R + a\sin\phi) = \int a\Delta p\, \frac{\cos\phi}{\sin\phi}\, \sin\phi(R + a\sin\phi)\, d\phi + C$$

$$= \Delta p \int (R + a\sin\phi)\, d(R + a\sin\phi) + C = \frac{\Delta p}{2}(R + a\sin\phi)^2 + C$$

$$\text{or} \quad T_1 = \frac{\Delta p}{2}\ \frac{R + a\sin\phi}{\sin\phi} + \frac{C}{(R + a\sin\phi)\sin\phi}$$

The boundary condition, as before, is $T_1\ (\phi = 0) = a\Delta p$.

$$T_1 = \frac{1}{\sin\phi}\left[\frac{\Delta p}{2}(R + a\sin\phi) + \frac{C}{R + a\sin\phi}\right] \doteq \frac{1}{\sin\phi}\left[\frac{\Delta p}{2}R + \frac{C}{R}\right]$$

This cannot be finite unless the term in the brackets is zero. Let us see what happens in this case ($c = -\Delta p\, R^2/2$):

$$T_1 = \frac{\Delta p}{2}\frac{R + a\sin\phi}{\sin\phi} - \frac{\Delta p}{2}\frac{R^2}{\sin\phi\,(R + a\sin\phi)} = \frac{a\Delta p}{2}\frac{2R + a\sin\phi}{R + a\sin\phi}$$

Fortunately this meets the requirement that $T_1\ (\phi = 0) = a\Delta p$. We can now substitute T_1 back into Eq. (2-11) and solve for T_2, which turns out to be $a\Delta p/2$. Differentiation and substitution of these results verifies both forms of the differential equation, (2-12) and (2-13).

In summary, in the equilibrium configuration,

$$T_1 = \frac{a\Delta p}{2}\frac{2R + a\sin\phi}{R + a\sin\phi}$$

$$T_2 = \frac{a\Delta p}{2}$$

2. Deformed Toroid With $u = 0$, $v = 0$ and $w = w(\theta)$

Stress and strain equations will be derived, by two independent methods, for a toroidal membrane with a displacement w which is a function of θ only.

The first method simply involves substitution into the equations given in Ref. 7 for stress and strain in orthogonal curvilinear coordinates:

$$\epsilon_{ii} = \frac{\partial}{\partial\alpha_i}\left(\frac{u_i}{\sqrt{g_{ii}}}\right) + \frac{1}{2g_{ii}}\sum_{\kappa=1}^{3}\frac{\partial g_{ii}}{\partial\alpha_\kappa}\frac{u_\kappa}{\sqrt{g_{\kappa\kappa}}} \qquad i = 1,2,3$$

$$\epsilon_{ij} = \frac{1}{2\sqrt{g_{ii}\,g_{jj}}}\left[g_{ii}\frac{\partial}{\partial\alpha_j}\left(\frac{u_i}{\sqrt{g_{ii}}}\right) + g_{jj}\frac{\partial}{\partial\alpha_i}\left(\frac{u_j}{\sqrt{g_{jj}}}\right)\right] \qquad \begin{matrix} i = 1,2,3 \\ j = 1,2,3 \\ i \neq j \end{matrix}$$

where: ϵ_{ij} = strains

α_i are the three coordinates

u_i are the displacements in the α_i directions

$\sqrt{g_{ii}}$ are the metric coefficients

In this case

$$\alpha_1 = \phi\,,\quad \alpha_2 = \theta\,,\quad \alpha_3 = \rho$$

(Radial, in the direction of a and w from the tube axis)

$$u_1 = u_2 = 0\,,\quad u_3 = w(\theta)$$

$$\sqrt{g_{11}} = a + w = \rho\,,\quad \sqrt{g_{22}} = R + (a+w)\sin\phi\,,\quad \sqrt{g_{33}} = 1$$

Substitution of the g_{ii} into the strain equations yields

$$\epsilon_{11} = \frac{w}{a+w} \cong \frac{w}{a}\;;\quad \epsilon_{22} = \frac{w\sin\phi}{R+(a+w)\sin\phi} \cong \frac{w\sin\phi}{R+a\sin\phi}\;;\quad \epsilon_{33} = 0$$

$$\epsilon_{23} = \epsilon_{32} = \frac{dw/d\theta}{R+(a+w)\sin\phi} \cong \frac{dw/d\theta}{R+a\sin\phi}\;;\quad \epsilon_{12} = \epsilon_{21} = \epsilon_{13} = \epsilon_{31} = 0$$

The stress-strain relations are

$$\sigma_{ii} = \frac{E\nu\Theta}{(1+\nu)(1-2\nu)} + \frac{E}{1+\nu}\epsilon_{ii}$$

$$\sigma_{ij} = \frac{E}{1+\nu}\epsilon_{ij} \qquad \begin{matrix} i = 1,2,3 \\ j = 1,2,3 \end{matrix} \quad i \neq j$$

where: σ_{ij} = stress

E = Young's modulus, ν = Poisson's ratio

$\Theta = \epsilon_{11} + \epsilon_{22} + \epsilon_{33}$

These yield:

$$\Theta = \frac{w}{a} + \frac{w\sin\phi}{R+a\sin\phi} = \frac{w}{a}\,\frac{R+2a\sin\phi}{R+a\sin\phi}$$

$$\sigma_{11} = \frac{E\nu\Theta}{(1+\nu)(1-2\nu)} + \frac{Ew}{a(1+\nu)}$$

$$\sigma_{22} = \frac{E\nu\Theta}{(1+\nu)(1-2\nu)} + \frac{E}{1+\nu}\,\frac{w\sin\phi}{R+a\sin\phi}$$

$$\sigma_{33} = \frac{E\nu\Theta}{(1+\nu)(1-2\nu)}$$

Shear strains and stresses are neglected for a membrane.

The strain-displacement relations can be derived in a somewhat more satisfying way directly from geometry.

Consider the curve on the equilibrium toroid formed by ϕ = const. This curve is a circle about the Z axis at $z = a \cos \phi$ with radius $r = R + a \sin \phi$. One surface containing this curve and the tube axis ($z = 0$, $r = R$) is a cone with its apex on the Z axis:

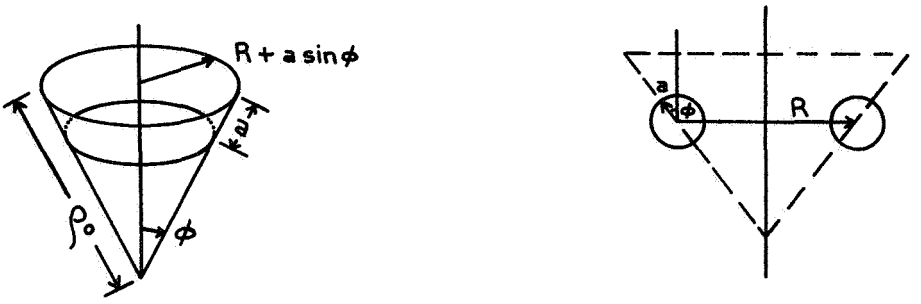

Fig. 2-11. Cone Based on Element of Toroid

The apex half-angle of the cone is ϕ ; the base width is $R + a \sin \phi$. The slant height of the cone is then $\rho_0 = (R + a \sin \phi)/ \sin \phi \; (\phi \neq 0)$.

The advantage of drawing this cone is that the radial displacement w at the angle ϕ is in a direction along one of the elements of the cone. Thus the length of the perturbed surface at the angle ϕ can be computed by inspecting the cone.

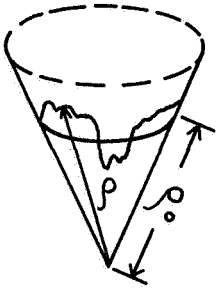

Fig. 2-12
Displacement Shown on Surface of Cone

$$\rho = \rho_0 + w = \frac{R + a \sin \phi}{\sin \phi} + w$$

$$x = \rho \sin \phi \cos \theta = (R + a \sin \phi + w \sin \phi) \cos \theta$$

$$y = \rho \sin \phi \sin \theta = (R + a \sin \phi + w \sin \phi) \sin \theta$$

$$z = \rho \cos \phi = R \cot \phi + (a + w) \cos \phi$$

Since ϕ is considered constant,

$$dx = -(R + a \sin \phi + w \sin \phi) \sin \theta \, d\theta + dw \sin \phi \cos \theta$$

$$dy = (R + a \sin \phi + w \sin \phi) \cos \theta \, d\theta + dw \sin \phi \cos \theta$$

$$dz = dw \cos \phi$$

$$ds^2 = dx^2 + dy^2 + dz^2 = [R + (a + w) \sin \phi]^2 d\theta^2 + dw^2$$

If $w = 0$,

$$ds^2 = (R + a\sin\phi)^2 d\theta^2 \qquad \text{or} \qquad ds = (R + a\sin\phi)\, d\theta = ds_0$$

If w is small, the binomial theorem gives

$$ds \cong \left[R + (a+w)\sin\phi\right] d\theta + \frac{1}{2}\frac{[dw/d\theta]^2 d\theta}{R + (a+w)\sin\phi} \equiv ds_1$$

The strain is, by definition

$$\epsilon_{22} = \frac{ds_1 - ds_0}{ds_0} = \frac{w\sin\phi}{R + a\sin\phi} + \frac{1}{2}\frac{[dw/d\theta]^2}{R + (a+w)\sin\phi}$$

With w and $dw/d\theta$ small,

$$\epsilon_{22} \cong \frac{w\sin\phi}{R + a\sin\phi}$$

ϵ_{11} is easily calculated by comparing the circumferences of circles of radii a and $a+w$. The difference, $2\pi w$, divided by the original value, $2\pi a$, gives $\epsilon_{11} = w/a$. The strains are related to stresses as before. For a complete description, we must add in the equilibrium strains of section 1. Recalling that $T_1 = \sigma_{11} h$ etc.,

$$T_1 = \frac{a\Delta p}{2}\frac{2R + a\sin\phi}{R + a\sin\phi} + \frac{E\nu h\Theta}{(1+\nu)(1-2\nu)} + \frac{E}{1+\nu}\frac{h}{a}w$$

$$T_2 = \frac{a\Delta p}{2} + \frac{E\nu h\Theta}{(1+\nu)(1-2\nu)} + \frac{E}{1+\nu}\frac{wh\sin\phi}{R + a\sin\phi}$$

$$\text{where} \quad \Theta = \frac{w(R + 2a\sin\phi)}{a(R + a\sin\phi)}$$

Again, these can be converted to the nonconcentric form if necessary.

E. Solution of Laplace Equations in Toroidal Coordinates

The fluid velocity potentials appear in at least three places in the system equations (2-1) to (2-8). First, the velocity potential appears explicitly in the Laplace equations $\nabla^2 \Phi = 0$ and $\nabla^2 \Psi = 0$. Second, the pressure difference

Δp is evaluated using the linearized Euler equation

$$p = p_o - \rho \frac{\partial V}{\partial t}$$

where V represents velocity potential and ρ fluid density. Using the subscripts i and e to represent fluid properties inside and outside the membrane respectively, we can evaluate $\Delta p = p_i - p_e$ from

$$p_i = p_{io} - \rho_i \frac{\partial \Phi}{\partial t} \qquad \text{and} \qquad p_e = p_{eo} - \rho_e \frac{\partial \Psi}{\partial t}$$

Then, with $\Delta p_o = p_{io} - p_{eo}$

we have $\Delta p = \Delta p_o - \rho_i \frac{\partial \Phi}{\partial t} + \rho_e \frac{\partial \Psi}{\partial t}$

Third, the boundary conditions to be satisfied by the fluid flow can be given in terms of the velocity potential as:

$$\nabla \Psi \cdot \vec{u}_n \Big|_{\mu = \mu_y} = 0 \; ; \quad \nabla \Phi \cdot \vec{u}_n \Big|_{\mu = \mu_a} = \nabla \Psi \cdot \vec{u}_n \Big|_{\mu = \mu_a} = \frac{\partial w}{\partial t}$$

There is also an implicit boundary condition, that the velocity potential at the tube axis be finite:

$$\Phi \Big|_{r=0} \quad \text{finite}$$

A solution to the Laplace equation exists in the nonconcentric coordinates introduced in section B2. According to Ref. 5, no solution is known in the concentric coordinates defined in section B1.

In the nonconcentric coordinates, solutions to $\nabla^2 \Phi = 0$ are of the form (Ref. 5)

$$\Phi(\mu, \eta, \theta, t) = \sqrt{\cosh \mu - \cos \eta}\, \cos m(\theta - \theta_m) \cos n(\eta - \eta_n)$$

$$\times \left[A_{mn} P^m_{n-\frac{1}{2}} (\cosh \mu) + B_{mn} Q^m_{n-\frac{1}{2}} (\cosh \mu) \right] f(t) \qquad (2\text{-}15)$$

$$m, n = 0, 1, 2, \ldots$$

Here f is an arbitrary function of t; A_{mn}, B_{mn}, θ_m and η_n are arbitrary constants; and $P^m_{n-\frac{1}{2}}$ and $Q^m_{n-\frac{1}{2}}$ are associated Legendre polynomials, of the first and second kind respectively, of half integral order and integral degree.

Any linear combination of the functions Φ of Eq. (2-15) will satisfy the Laplace equation. If possible, we would like to find values of the four free constants such that Φ satisfies the kinematic and dynamic boundary conditions.

The kinematic boundary conditions involve the derivative of Φ in the μ direction. The derivative normal to the membrane, $\nabla\Phi \cdot \vec{u}_n$, is, including the system metric (Ref. 5),

$$\nabla\Phi \cdot \vec{u}_n = \nabla\Phi \cdot \vec{u}_\mu = \frac{\cosh\mu - \cos\eta}{d} \frac{\partial\Phi}{\partial\mu} \tag{2-16}$$

We find $\frac{\partial\Phi}{\partial\mu} = \sinh\mu \cos m(\theta - \theta_m) \cos n(\eta - \eta_n)$

$$\times \left\{ \frac{1}{2\sqrt{\cosh\mu - \cos\eta}} \left[A_{mn} P^m_{n-\frac{1}{2}} + B_{mn} Q^m_{n-\frac{1}{2}}\right] \right.$$

$$\left. + \sqrt{\cosh\mu - \cos\eta} \left[A_{mn} P'^m_{n-\frac{1}{2}} + B_{mn} Q'^m_{n-\frac{1}{2}}\right] \right\} f(t) \tag{2-17}$$

where P' and Q' are the derivatives of the polynomials with respect to their arguments.

It quickly becomes clear that a function of the type in Eq. (2-17) cannot, in general, satisfy a boundary condition such as

$$\nabla\Phi \cdot \vec{u}_n \Big|_{\mu=\mu_\gamma} = 0$$

For instance, we might try to set Eq. (2-17) equal to zero by requiring the term in each square bracket to be zero:

$$A_{mn} P^m_{n-\frac{1}{2}} + B_{mn} Q^m_{n-\frac{1}{2}} = 0$$

and, simultaneously,

$$A_{mn} P'^m_{n-\frac{1}{2}} + B_{mn} Q'^m_{n-\frac{1}{2}} = 0$$

However, unless the determinant

$$\begin{vmatrix} P & Q \\ P' & Q' \end{vmatrix} = 0,$$

which in general is not true, there is no solution except $A_{mn} = B_{mn} = 0$.

If we try to make the entire term in curly brackets equal zero, we find that the dependence on η, in the square roots, does not permit the selection of A_{mn} and B_{mn} as constants. We then conclude that there is no non-trivial solution to $\nabla \bar{\Phi} \cdot \vec{a}_n \big|_{\mu = \mu_r} = 0$ if $\bar{\Phi}$ is constituted as in Eq. (2-15).

This situation is not unprecedented (Ref. 2). We must express each eigenfunction as an infinite sum of the fundamental solutions defined by Eq. (2-15). The coefficients of the terms of the sum are selected to satisfy the kinematic and dynamic boundary conditions. The amount of numerical work needed to carry through an approximate solution, and to develop the specific mode shapes, is enormous.

Before attempting a solution of this type, we should remind ourselves that the validity of the results obtained depends directly on the justifiability of the assumptions made in the analysis. These assumptions have yet to be verified experimentally.

An alternative to this extensive numerical effort would be to introduce simplifying assumptions which would allow us to obtain results without an excessive amount of computation. These results could then be checked against experiments, and the assumptions verified or modified as necessary. In this way we could gain some mathematical insight into the problem—natural frequencies, mode shapes, important parameters, etc.—without undue effort.

This second approach was chosen. In the two succeeding chapters, approximate equations of motion are derived and their solutions developed and compared with experiments.

III. MOENS-KORTEWEG TYPE APPROXIMATION

A. Fluid-Filled Cylinder Model of Membranous Canal

The first attempt at simplifying the problem was to adapt the Moens-Korteweg equation for straight cylinders to toroids. The derivation of the classical Moens-Korteweg equation follows.

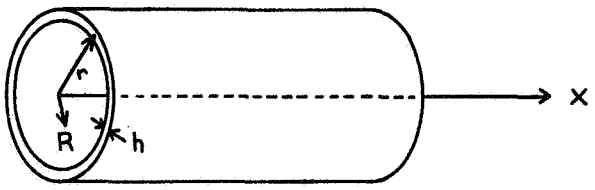

Fig. 3-1. Straight Circular Cylinder

Let the fluid's density be ρ and its pressure p; the wall is isotropic with elastic properties E and ν, thickness h, and equilibrium radius a. The fluid displacement in the x direction is u; the wall displacement in the R direction is w. ($r \equiv a + w$).

These assumptions are made:

(1) The velocity $\partial u/\partial t$ and pressure depend only on the axial coordinate x, i.e. are constant across a cross-section.

(2) Motion is axisymmetric, i.e. the wall moves in the radial direction only, its displacement is a function only of x, and there is no torsional motion of the wall or fluid.

(3) Wall density is zero.

(4) The shell has no bending rigidity; shear is neglected.

(5) Pressure fluctuations are much greater than radius fluctuations, so $rdp >> pdr$; and wavelengths are large, so $\partial w/\partial x << 1$.

(6) The contained fluid is incompressible and inviscid and, in equilibrium, at rest.

(7) All perturbations are small, so that the equations can be linearized.

(8) The cylinder is initially unstressed in the x-direction.

The derivation proceeds by utilizing Newton's Law, Hooke's Law, and the continuity equation for the system.

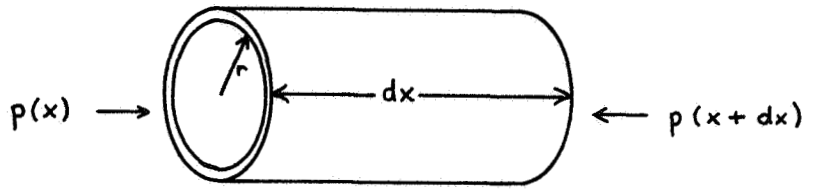

Fig. 3-2. Momentum Equation

Force in x direction = $\pi r^2(x)\,p(x) - \pi r^2(x+dx)\,p(x+dx)$

$$= \pi r^2 p - \pi\left(r + \frac{\partial r}{\partial x}dx\right)^2\left(p + \frac{\partial p}{\partial x}dx\right) \cong -\pi\left[2pr\frac{\partial r}{\partial x}dx + r^2\frac{\partial p}{\partial x}dx\right]$$

By assumption (5), this becomes

$$-\pi r^2 \frac{\partial p}{\partial x}\,dx$$

The mass of the element of fluid is $\pi r^2 \rho\,dx$; its acceleration is $\partial^2 u/\partial t^2$; so

$$-\pi r^2 \frac{\partial p}{\partial x}dx = \pi r^2 \rho\,dx \frac{\partial^2 u}{\partial t^2}$$

or

$$\frac{\partial p}{\partial x} = -\rho \frac{\partial^2 u}{\partial t^2} \qquad (3\text{-}1)$$

Equilibrium for a half-cylindrical section requires

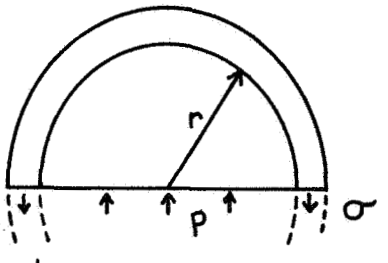

Fig. 3-3
Equilibrium of a Half Section

$2r \cdot p = 2 \cdot \sigma h$ (σ = stress in shell wall)

Hooke's Law gives $\sigma = \epsilon E$ so

$$rp = h\epsilon E \qquad \epsilon = \frac{2\pi r - 2\pi a}{2\pi a} = \frac{r-a}{a} = \frac{w}{a}$$

$$d(rp) = r\,dp + p\,dr \cong r\,dp = hE\,d\epsilon = hE\frac{dr}{a}$$

Then, differentiating with respect to time,

$$\frac{\partial p}{\partial t} = \frac{hE}{a^2}\frac{\partial r}{\partial t} = \frac{hE}{a^2}\frac{\partial w}{\partial t}$$

The continuity equation relates the inflow of mass to the change in volume. Since the fluid is incompressible, the volume inflow of fluid between x and (x + dx) must equal the change in contained volume of that section of the cylinder.

$$\text{Inflow at (x)} = \pi r^2 \frac{\partial u}{\partial t}\, dt$$

$$\text{Outflow at (x + dx)} = -\pi\left(r + \frac{\partial r}{\partial x}\, dx\right)^2 \left(\frac{\partial u}{\partial t} + \frac{\partial^2 u}{\partial x\, \partial t}\, dx\right) dt$$

$$\cong -\pi r^2 \frac{\partial u}{\partial t}\, dt - \left[2\pi r \frac{\partial r}{\partial x} \frac{\partial u}{\partial t} + \pi r^2 \frac{\partial^2 u}{\partial x\, \partial t}\right] dx\, dt$$

The term containing $\partial r/\partial x$ is neglected because of assumption (5). The net change in fluid volume is then $-\pi r^2 \left(\partial^2 u/\partial x \partial t\right)$. This must equal the change in contained volume

$$dx\left[\pi\left(r + \frac{\partial r}{\partial t}\, dt\right)^2 - \pi r^2\right] = 2\pi r \frac{\partial r}{\partial t}\, dx\, dt$$

The continuity equation is then

$$2\pi r \frac{\partial r}{\partial t} = -\pi r^2 \frac{\partial^2 u}{\partial x\, \partial t}$$

or

$$\frac{\partial r}{\partial t} = \frac{\partial w}{\partial t} = -\frac{r}{2} \frac{\partial^2 u}{\partial x\, \partial t}$$

to first order,

$$\frac{\partial w}{\partial t} = -\frac{a}{2} \frac{\partial^2 u}{\partial x\, \partial t} \tag{3-3}$$

Eliminating $\partial w/\partial t$ between Eqs. (3-2) and (3-3)

$$\frac{\partial p}{\partial t} = -\frac{hE}{2a} \frac{\partial^2 u}{\partial x\, \partial t} \tag{3-4}$$

Differentiating Eq. (3-4) with respect to t and Eq. (3-1) with respect to x, and substituting Eq. (3-4) into Eq. (3-1):

$$\frac{\partial^2 p}{\partial t^2} = \frac{hE}{2\rho a} \frac{\partial^2 p}{\partial x^2} \tag{3-5}$$

This is a wave equation, $P_{tt} = c^2 P_{xx}$, so pressure fluctuations are propagated with speed

$$c = \sqrt{\frac{hE}{2\rho a}} \tag{3-6}$$

B. Fluid-Filled Torus Model of Membranous Canal

The Moens-Korteweg derivation is now to be extended to a torus. The assumptions are:

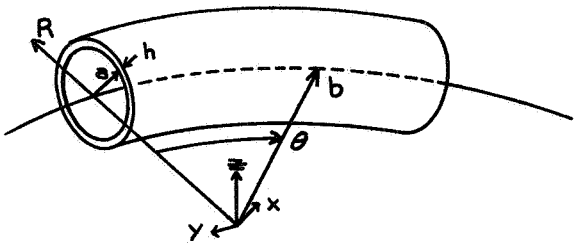

Fig. 3-4
Elastic Toroidal Shell

(1) The tube, of equilibrium radius a and thickness h , is bent so its axis becomes a circle of radius b .

(2) The tube contains incompressible, inviscid fluid; the tube itself is massless and has no shear rigidity.

(3) Fluid pressure and velocity are zero at equilibrium.

(4) The tube wall and the fluid are permitted to move in three directions: radially in the z = 0 plane; radially toward and away from the tube axis in a θ = const plane; and along the tube axis in the θ direction. There is no torsional motion or motion of the tube axis out of plane.

(5) Motions are small so that linearization of the equations is possible.

Notation:

u	Fluid displacement in θ direction
ρ	Fluid density
E, ν	Elastic properties of wall
S	Tension in wall in θ direction
ξ	Wall displacement in θ direction
w	Wall displacement in radial direction (change of tube radius)
ζ	Displacement of tube axis in R direction
M	Bending moment about axis normal to z = 0 plane
I	Area moment of inertia of tube about this axis

The derivation proceeds similarly to the cylindrical case, but is somewhat more complex because of the changed geometry.

Continuity Equation:

Consider a small element of fluid which originally subtends an angle $d\theta$.

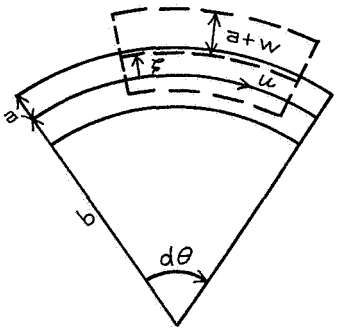

Fig. 3-5
Continuity Equation

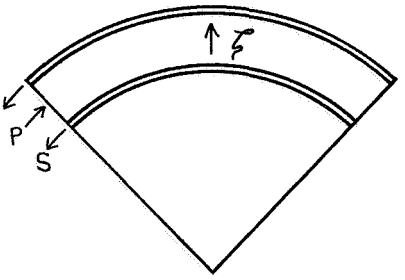

Fig. 3-6
Radial Equilibrium

Original length = $b\,d\theta$

Change in length = $\frac{1}{b}\int (b+\zeta)\frac{\partial u}{\partial \theta}\,d\theta \cong \frac{b+\zeta}{b}\frac{\partial u}{\partial \theta}\,d\theta$

Original volume = $\pi a^2 b\,d\theta$

Final volume = $\pi (a+w)^2\left[\int \frac{b+\zeta}{b}\frac{\partial u}{\partial \theta}\,d\theta + (b+\zeta)\,d\theta\right]$

$$\cong \pi (a^2+2aw)(b+\zeta)\left[1+\frac{1}{b}\frac{\partial u}{\partial \theta}\right]d\theta$$

Change in volume = $\pi a\,d\theta\left[2awb + a^2\zeta + a^2\frac{\partial u}{\partial \theta}\right]$

For continuity of an incompressible fluid, this volume change must be zero:

$$\zeta + \frac{\partial u}{\partial \theta} + \frac{2b}{a}w = 0 \qquad (3\text{-}7)$$

Newton's Laws:

(a) Radial: Fluid and Tube

F = ma requires (in cylindrical coordinates):

$$\pi a^2 b\,d\theta\rho\left[\frac{\partial^2 \zeta}{\partial t^2} - b\left(\frac{1}{b}\frac{\partial u}{\partial t}\right)^2\right] = -S\,d\theta + p\,d\theta\,\pi a^2$$

or, to first order

$$\pi a^2\left[b\rho\frac{\partial^2 \zeta}{\partial t^2} - p\right] = -S \qquad (3\text{-}8)$$

Since S is neglected and p does not appear if the tube is straight, we would then have $\zeta = 0$. Thus the curvature of the tube presents the possibility of a new mode of motion involving flexure.

(b) Axial: Fluid Only

$$\pi a^2 b\,d\theta\rho\left[\frac{\partial^2 u}{\partial t^2} + 2\frac{\partial \zeta}{\partial t}\left(\frac{1}{b}\frac{\partial u}{\partial t}\right)\right] = -\pi a^2\left[\frac{\partial p}{\partial \theta}\,d\theta\right]$$

or, to first order,

$$b\rho\frac{\partial^2 u}{\partial t^2} = -\frac{\partial p}{\partial \theta} \qquad (3\text{-}9)$$

Shear Equation:

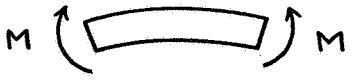

Fig. 3-7
Shear and Moment

Since the fluid is inviscid, and since the shear rigidity of the shell is to be neglected, we require $\partial M/\partial\theta = 0$. This assumes no rotatory inertia of the fluid.

Hooke's Law:

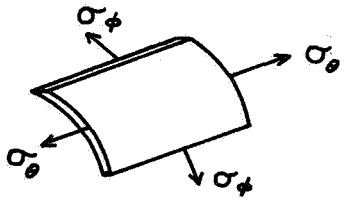

Fig. 3-8. Stress Balance

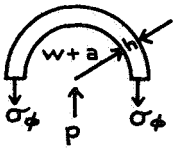

Fig. 3-9. Stress-Strain

We consider the two-dimensional stress-strain equations of an element of the tube:

$$\sigma_\phi = \frac{E}{1-\nu^2}\left[\epsilon_\phi + \nu\epsilon_\theta\right] \; ; \quad \sigma_\theta = \frac{E}{1-\nu^2}\left[\epsilon_\theta + \nu\epsilon_\phi\right]$$

From geometry, $\epsilon_\phi = \frac{w}{a}$; $\epsilon_\theta \cong \frac{1}{b}\left[\frac{\partial \xi}{\partial\theta} + \zeta\right]$ (averaged over ϕ)

$$\equiv \frac{1}{b}\,\partial\hat{\xi}/\partial\theta$$

$$\sigma_\theta = \frac{S}{2\pi a h} \; ; \quad 2(a+w)p = 2\sigma_\phi h \quad \text{or} \quad \sigma_\phi = \frac{(a+w)p}{h} \cong \frac{ap}{h}$$

So

$$\frac{ap}{h} = \frac{E}{1-\nu^2}\left[\frac{w}{a} + \frac{\nu}{b}\frac{\partial\hat{\xi}}{\partial\theta}\right] \tag{3-10a}$$

$$\frac{S}{2\pi a h} = \frac{E}{1-\nu^2}\left[\frac{1}{b}\frac{\partial\hat{\xi}}{\partial\theta} + \frac{\nu w}{a}\right] \tag{3-10b}$$

Beam Equation for Toroidal Tube:

We write the classical equation for the bending of a beam in the form

$$\frac{M}{EI} = K - K_o$$

where K_o is the curvature for zero bending moment and K is the curvature corresponding to M. The "beam" being considered is the tube, and the curve

whose curvature is to be measured is the tube axis. With no displacement, its radius is b , so

$$K_o = \frac{1}{b}$$

Extending the results of Ref. (1), for the wall of a cylinder, to the axis of a torus:

$$K = \frac{1}{b} - \frac{1}{b^2}\left(\zeta + \frac{\partial^2 \zeta}{\partial \theta^2}\right)$$

so

$$\frac{M}{EI} = -\frac{1}{b^2}\left(\zeta + \frac{\partial^2 \zeta}{\partial \theta^2}\right)$$

The area moment of inertia of the tube, about the transverse axis, is one-half the polar moment:

$$I = \frac{1}{2}\int r^2 dA = \frac{1}{2}\int_0^{2\pi} a^2 h \cdot a\, d\phi = \pi a^3 h$$

so

$$\frac{M}{\pi a^3 h E} = -\frac{1}{b^2}\left(\zeta + \frac{\partial^2 \zeta}{\partial \theta^2}\right) \tag{3-11}$$

We now have the seven equations

$$\zeta + \frac{\partial u}{\partial \theta} + \frac{2b}{a} w = 0 \tag{3-12}$$

$$\pi a^2 \left(b\rho \frac{\partial^2 \zeta}{\partial t^2} - p\right) = -S \tag{3-13}$$

$$b\rho \frac{\partial^2 u}{\partial t^2} = -\frac{\partial p}{\partial \theta} \tag{3-14}$$

$$\frac{\partial M}{\partial \theta} = 0 \tag{3-15}$$

$$\frac{E}{1-\nu^2}\left[\frac{w}{a} + \frac{\nu}{b}\frac{\partial \hat{\xi}}{\partial \theta}\right] = \frac{ap}{h} \tag{3-16}$$

$$\frac{E}{1-\nu^2}\left[\frac{1}{b}\frac{\partial \hat{\xi}}{\partial \theta} + \frac{\nu w}{a}\right] = \frac{S}{2\pi a h} \tag{3-17}$$

$$\frac{M}{\pi a^3 h E} = -\frac{1}{b^2}\left(\zeta + \frac{\partial^2 \zeta}{\partial \theta^2}\right) \tag{3-18}$$

in the seven unknowns u , w , ζ , p , S , M , $\hat{\xi}$.

Before proceeding with the solution, let us consider the special case $b \longrightarrow \infty$, which represents a straight tube. As $b \longrightarrow \infty$, $d\theta \longrightarrow 0$ but $b\,d\theta$ remains finite and will be denoted by dx.

We also must decide what to do about the radial force equation (3-13) and the radial motion ζ. For a straight tube the R direction is indeterminate, and we might consider constraining the tube axis so it cannot move at all. This will be done here, by dropping equation (3-13) and setting $\zeta = 0$, but the consequences of allowing such motion will be examined later. We have six equations:

$$\frac{\zeta}{b} + \frac{1}{b}\frac{\partial u}{\partial \theta} + \frac{2}{a}w \doteq \frac{\partial u}{\partial x} + \frac{2w}{a} = 0 \tag{3-19}$$

(3-13) is dropped; (3-14) becomes

$$\rho \frac{\partial^2 u}{\partial t^2} = -\frac{1}{b}\frac{\partial p}{\partial \theta} \doteq -\frac{\partial p}{\partial x} \tag{3-20}$$

(3-15) is unchanged; (3-16) gives

$$\frac{E}{1-\nu^2}\left(\frac{w}{a} + \nu\frac{\partial \xi}{\partial x}\right) = \frac{ap}{h} \tag{3-21}$$

(3-17) becomes

$$\frac{E}{1-\nu^2}\left(\frac{\partial \xi}{\partial x} + \frac{\nu w}{a}\right) = \frac{S}{2\pi a h} \tag{3-22}$$

(3-15) is simply $M = 0$.

For a massless tube, $\partial S/\partial x = 0$; if there is no initial stretch, $S = 0$.
(3-22) is then

$$\frac{\partial \xi}{\partial x} + \frac{\nu w}{a} = 0 \tag{3-23}$$

(3-19), (3-20), (3-21), and (3-23) are four equations in u, ξ, p, w. The equations are easily reduced to:

$$\rho \frac{\partial^2 u}{\partial t^2} = \frac{Eh}{2a}\frac{\partial^2 u}{\partial x^2}$$

a wave equation with $c^2 = Eh/2a\rho$. If Eq. (3-13) and ζ had been retained, the result would have been $c^2 = Eh/[\rho a(2-\nu)]$.

The solution of the set (3-12) to (3-18) proceeds as follows: w is eliminated by substituting (3-12), in the form

$$w = -\frac{a}{2b}\left(\zeta + \frac{\partial u}{\partial \theta}\right)$$

into (3-16) and (3-17).

$$\frac{E}{1-\nu^2}\left[-\frac{1}{2b}\left(\zeta + \frac{\partial u}{\partial \theta}\right) + \frac{\nu}{b}\frac{\partial \hat{\xi}}{\partial \theta}\right] = \frac{ap}{h}$$

$$\frac{E}{1-\nu^2}\left[\frac{1}{b}\frac{\partial \hat{\xi}}{\partial \theta} - \frac{\nu}{2b}\left(\zeta + \frac{\partial u}{\partial \theta}\right)\right] = \frac{S}{2\pi a h}$$

p and S as given by these two are substituted into (3-13) and (3-14):

$$b\rho\frac{\partial^2 u}{\partial t^2} = -\frac{hE}{a(1-\nu^2)}\left[-\frac{1}{2b}\left(\frac{\partial \zeta}{\partial \theta} + \frac{\partial^2 u}{\partial \theta^2}\right) + \frac{\nu}{b}\frac{\partial^2 \hat{\xi}}{\partial \theta^2}\right] \qquad (3\text{-}24)$$

$$\pi a^2\left[b\rho\frac{\partial^2 \zeta}{\partial t^2} - \frac{hE}{a(1-\nu^2)}\left\{-\frac{1}{2b}\left(\zeta + \frac{\partial u}{\partial \theta}\right) + \frac{\nu}{b}\frac{\partial \hat{\xi}}{\partial \theta}\right\}\right]$$

$$= -\frac{2\pi a h E}{1-\nu^2}\left[\frac{1}{b}\frac{\partial \hat{\xi}}{\partial \theta} - \frac{\nu}{2b}\left(\zeta + \frac{\partial u}{\partial \theta}\right)\right]$$

This last becomes

$$ab\rho\frac{\partial^2 \zeta}{\partial t^2} + \frac{hE}{1-\nu^2}\left\{\left(\frac{1}{2b} - \frac{\nu}{b}\right)\left(\zeta + \frac{\partial u}{\partial \theta}\right) + \left(\frac{2}{b} - \frac{\nu}{b}\right)\left(\frac{\partial \hat{\xi}}{\partial \theta}\right)\right\} = 0 \qquad (3\text{-}25)$$

Eqs. (3-15) and (3-18) give:

$$\frac{\partial \zeta}{\partial \theta} + \frac{\partial^3 \zeta}{\partial \theta^3} = 0 \qquad (3\text{-}26)$$

(3-24), (3-25), and (3-26) are the final three equations in u, $\hat{\xi}$, and ζ. We assume solutions of the form

$$u(\theta, t) = A \exp\left[i\frac{\omega}{c}(b\theta - ct)\right]$$

$$\zeta(\theta, t) = B \exp\left[i\frac{\omega}{c}(b\theta - ct)\right]$$

$$\hat{\xi}(\theta, t) = C \exp\left[i\frac{\omega}{c}(b\theta - ct)\right]$$

where frequency ω and wave speed c are parameters. Differentiating and substituting,

$$\begin{bmatrix} b\rho\omega^2 - \frac{h}{a}\frac{E}{1-\nu^2}\frac{\omega^2 b}{2c^2} & \frac{h}{a}\frac{E}{1-\nu^2}\nu\frac{\omega^2 b}{c^2} & \frac{h}{a}\frac{E}{1-\nu^2}\frac{i\omega}{2c} \\ -\frac{hE}{1-\nu^2}\left[\left(\frac{1}{2}-\nu\right)\left(\frac{i\omega}{c}\right)\right] & \frac{hE}{1-\nu^2}(\nu-2)\frac{i\omega}{c} & ab\rho\omega^2 - \frac{hE}{b(1-\nu^2)}\left(\frac{1}{2}-\nu\right) \\ 0 & 0 & 1 - \frac{\omega^2 b^2}{c^2} \end{bmatrix} \begin{bmatrix} u \\ \hat{\xi} \\ \zeta \end{bmatrix} = 0$$

The determinant of the coefficients must be zero for a nontrivial solution to exist. This gives

$$\frac{hE}{1-\nu^2}\frac{\omega^3}{c}\left(1 - \frac{\omega^2 b^2}{c^2}\right)\left[b\rho(\nu-2) + \frac{hEb}{ac^2}\right] = 0$$

Solutions are: $\omega = 0$

$c = b\omega$ (Dispersive)

$$c^2 = \frac{hE}{\rho a(2-\nu)}$$ (Nondispersive)

Precise mode shapes can easily be worked out if needed, but it should suffice to point out that the mode shapes of the dispersive waves resemble a wave on a thin circular rod. The second is a breathing mode resembling the Moens-Korteweg motion in a straight tube, with a wave speed differing by a factor of $(2 - \nu)$ due to the extra degree of freedom.

C. Cylindrical Model of Membranous and Bony Canals

Next we derive the equations for a flexible cylinder of equilibrium radius a inside a rigid cylinder of radius γ. The fluid inside the flexible cylinder has density ρ_i, pressure p_i, and displacement u_i; properties of the fluid between the two cylinders are denoted by subscript e.

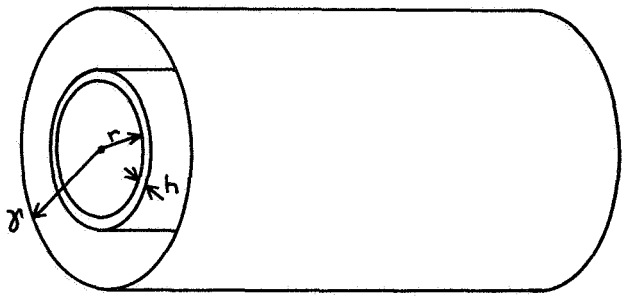

Fig. 3-10. Elastic Cylinder Inside Rigid Cylinder

For the inner fluid, we have, from section A ,

$$\frac{\partial p_i}{\partial x} = -\rho_i \frac{\partial^2 u_i}{\partial t^2}$$

$$\frac{\partial w}{\partial t} = -\frac{a}{2} \frac{\partial^2 u_i}{\partial x^2}$$

and the shell equation (Hooke's Law) is unchanged except that the pressure is replaced by the pressure difference

$$\frac{\partial (p_i - p_e)}{\partial t} = \frac{hE}{a^2} \frac{\partial w}{\partial t}$$

The momentum equation for the outer fluid is easily shown to be analogous to that for the inner fluid:

$$\frac{\partial p_e}{\partial x} = -\rho_e \frac{\partial^2 u_e}{\partial t^2}$$

Finally we need the continuity equation for the outer fluid.

The volume inflow at x in time dt is

$$dV_I = \pi [\gamma^2 - r^2(x)] \frac{\partial u}{\partial t}_e \, dt$$

$$= \pi [\gamma^2 - (a+w)^2] \frac{\partial u}{\partial t}_e \, dt$$

and the outflow at x + dx is

$$dV_o = \pi [\gamma^2 - r^2(x+dx)] \left(\frac{\partial u}{\partial t}_e + \frac{\partial^2 u}{\partial x \partial t}_e dx \right) dt$$

$$r(x+dx) = r(x) + \frac{\partial r}{\partial x} dx = a + w + \frac{\partial w}{\partial x} dx$$

so $$dV_o = \pi [\gamma^2 - (a+w+\frac{\partial w}{\partial x} dx)^2] \left[\frac{\partial u}{\partial t}_e + \frac{\partial^2 u}{\partial x \partial t}_e dx \right] dt$$

To first order, the net inflow $dV_I - dV_o$ is

$$dV = -\pi(\gamma^2 - a^2)\frac{\partial^2 u_e}{\partial x \partial t}\,dx\,dt$$

The change in the volume enclosed between the two cylinders is

$$dV = dx\left[\pi\left(\gamma^2 - \left(r + \frac{\partial r}{\partial t}\,dt\right)^2\right) - \pi(\gamma^2 - r^2)\right]$$

$$= dx\left[\pi\left(\gamma^2 - \left(a + w + \frac{\partial w}{\partial t}\,dt\right)^2\right) - \pi(\gamma^2 - (a+w)^2\right]$$

$$\cong \pi\,dx\left(2a\frac{\partial w}{\partial t}\,dt\right)$$

Continuity requires the two expressions for dV to be equal:

$$\frac{\partial w}{\partial t} = \frac{\gamma^2 - a^2}{2a}\frac{\partial^2 u_e}{\partial x \partial t}$$

We now have five equations in the five unknowns u_i, u_e, p_i, p_e, w. Using simple algebra, we can reduce the system to the single equation

$$\frac{\partial^2(p_i - p_e)}{\partial t^2} = \frac{hE}{a^2}\frac{\gamma^2 - a^2}{2a}\left[\rho_e + \rho_i\frac{\gamma^2 - a^2}{a^2}\right]^{-1}\frac{\partial^2(p_i - p_e)}{\partial x^2}$$

This has the form of a wave equation $p_{tt} = c^2 p_{xx}$, with

$$c^2 = \frac{\frac{hE}{a^2}\frac{\gamma^2 - a^2}{2a}}{\rho_e + \rho_i\frac{\gamma^2 - a^2}{a^2}} = \frac{hE}{2a}\frac{\gamma^2 - a^2}{\rho_e a^2 + \rho_i(\gamma^2 - a^2)}$$

The effects of γ/a and ρ_e/ρ_i on c^2 are easily shown (Fig. 3-11). For $\gamma/a \longrightarrow \infty$, c^2 is the same as if the rigid wall did not exist; as $\gamma/a \rightarrow 1$, $c \longrightarrow 0$. If $\rho_e = 0$, the rigid wall obviously has no effect; as $\rho_e \rightarrow \infty$, $c \rightarrow 0$:

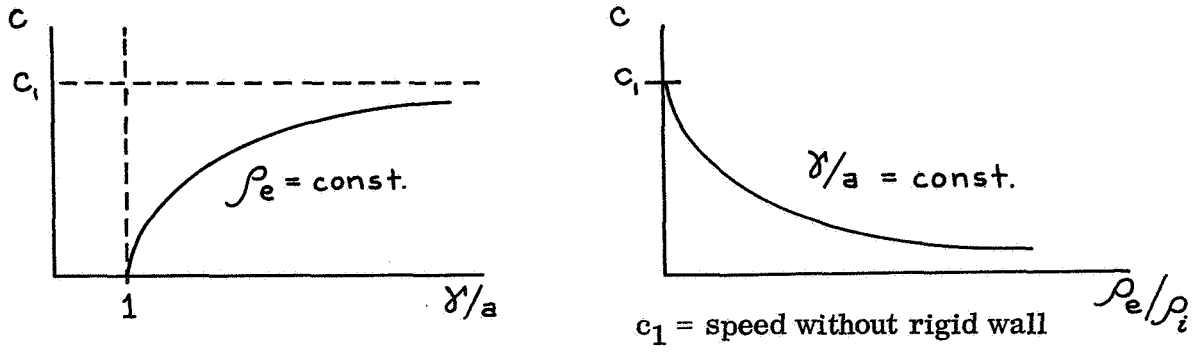

Fig. 3-11. Behavior of Wave Speed With γ/a and ρ_e

To study the simultaneous variation of γ'/a and ρ_e, we rewrite

$$c^2 = \frac{hE}{2a} \frac{1}{\frac{\rho_e}{(\frac{\gamma'}{a})^2 - 1} + \rho_i}$$

If $\frac{\rho_e}{(\frac{\gamma'}{a})^2 - 1} = k$, we have

$$c^2 = \frac{hE}{2a(\rho_i + k)}$$

compared with

$$c^2 = \frac{hE}{2a\rho_i}$$

for no rigid wall.

D. Toroidal Model of Membranous and Bony Canals

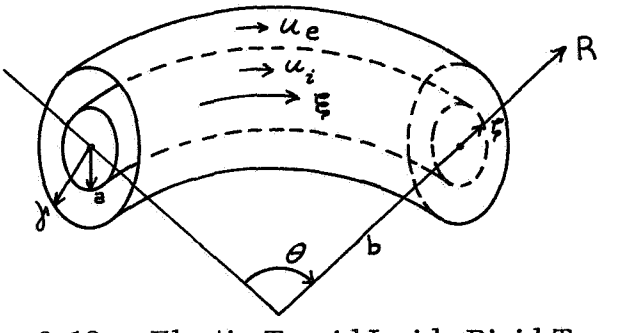

Fig. 3-12. Elastic Toroid Inside Rigid Toroid

Finally we derive a Moens-Korteweg type equation for a toroidal shell inside a rigid toroidal wall. In equilibrium the axes of the two tubes coincide; the elastic tube has radius a, the rigid tube γ'. The subscripts i and e are now used to indicate internal and external quantities, such as u, ρ, and p. Other notation is unchanged.

The first major modification to the equations of motion is the continuity of the external fluid. As in deriving the equation of continuity of the internal fluid, let $d\theta$ represent the angle originally subtended by an element of external fluid, and $d\theta^*$ the angle after displacement. The original volume is $\pi(\gamma'^2 - a^2)\, b\, d\theta$; the final volume is $\pi\gamma'^2 b\, d\theta^* - \pi(a+w)^2(b+\zeta)\, d\theta^*$.

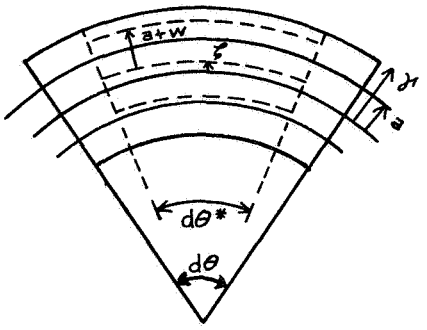

Fig. 3-13
Continuity Equation

To first order the final volume is

$$[\pi a^2 b + \pi \gamma^2 \frac{\partial u_e}{\partial \theta} - \pi (a^2 b + a^2 \frac{\partial u_e}{\partial \theta} + a^2 \zeta + 2abw)]\, d\theta$$

Setting the initial and final volumes equal,

$$\zeta + \frac{2b}{a} w - \frac{\gamma^2 - a^2}{a^2} \frac{\partial u_e}{\partial \theta} = 0$$

The second major change involves the radial force equation. In addition to the force required to accelerate the mass of internal fluid, force must be applied to displace the external fluid. This "apparent mass" effect is estimated using two-dimensional ideal fluid mechanics.

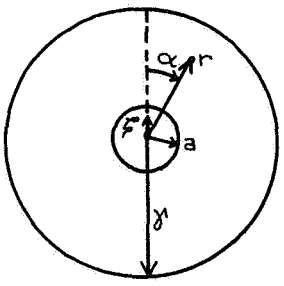

Fig. 3-14
Derivation of
Potential Equation

Let ϕ be the velocity potential of the external fluid. Consider the inner tube and fluid to be a solid body of radius a (a + w can be used but the results will be the same to first order). The inner tube is to be displaced by an amount ζ in the R direction. Angles from this direction are given by α .

We wish to solve the Laplace equation

$$\nabla^2 \phi = \frac{1}{r^2} \frac{\partial^2 \phi}{\partial \alpha^2} + \frac{1}{r} \frac{\partial}{\partial r}\left(r \frac{\partial \phi}{\partial r}\right) = 0$$

Subject to the boundary conditions

$$\nabla \phi \cdot \vec{u}_r \Big|_\gamma = \frac{\partial \phi}{\partial r}\Big|_\gamma = 0 \qquad \text{and} \qquad \nabla \phi \cdot \vec{u}_r \Big|_a = \frac{\partial \phi}{\partial r}\Big|_a = \frac{\partial \zeta}{\partial t} \cos \alpha$$

Assume $\phi(R, \alpha) = R(r)\, A(\alpha)$. The solution of the Laplace equation is then known to be

$$R = C_{11} r^p + C_{12} r^{-p} \qquad p = \text{integer}$$

$$A = C_{21} \sin p\alpha + C_{22} \cos p\alpha = C_2 \sin p(\alpha - \alpha_0)$$

Then

$$\frac{\partial \phi}{\partial r} = AR' = A\left(C_{11}\, p r^{p-1} - C_{12}\, p r^{-p-1}\right)$$

$$\phi = C_2 \sin p(\alpha - \alpha_0)\left(r^p + \gamma^{2p} r^{-p}\right)$$

$$\frac{\partial \phi}{\partial r} = C_2 \sin p(\alpha - \alpha_0)\; p\left(r^{p-1} - \gamma^{2p} r^{-p-1}\right)$$

$$\left.\frac{\partial \phi}{\partial r}\right|_a = C_2 \sin p(\alpha - \alpha_0)\; p\left(a^{p-1} - \gamma^{2p} a^{-p-1}\right) = \frac{\partial \zeta}{\partial t} \cos\alpha$$

which requires $\alpha_0 = -90°$, $p = 1$ (and C_2 such that magnitudes are correct).

Then

$$\phi = \frac{\dfrac{\partial \zeta}{\partial t}}{1 - \dfrac{\gamma^2}{a^2}} \cos\alpha \left(r + \frac{\gamma^2}{r}\right) \qquad a \le r \le \gamma$$

This can be checked by differentiation.

The pressure in the external fluid caused by this motion is calculated from the linearized Euler equation

$$p = p_0 - \rho_e \left.\frac{\partial \phi}{\partial t}\right|_a = -\rho_e \frac{\partial^2 \zeta}{\partial t^2} \frac{1 + \dfrac{\gamma^2}{a^2}}{1 - \dfrac{\gamma^2}{a^2}} \cos\alpha$$

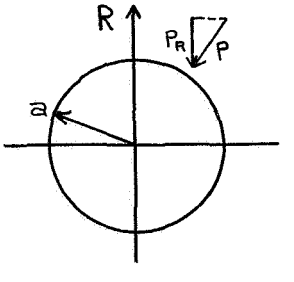

Fig. 3-15. Pressure Integration

The pressure in the R direction on an element of surface is

$$p_R = -p\cos\alpha = \rho_e \frac{\partial^2 \zeta}{\partial t^2} \frac{1 + \frac{\gamma^2}{a^2}}{1 - \frac{\gamma^2}{a^2}} \cos^2\alpha$$

The total force in the R direction on an element $d\theta$ is

$$F_R = \int_{\alpha=0}^{\alpha=2\pi} p_R \, d\ell \cdot b\, d\theta = b\, d\theta \int_0^{2\pi} p_r \, a\, d\alpha$$

$$= \pi a^2 \rho_e \frac{\partial^2 \zeta}{\partial t^2} \frac{a^2 + \gamma^2}{a^2 - \gamma^2} \, b\, d\theta$$

The complete radial force equation adds this term to the previous (true mass) term, with the driving force now due to S and $(p_i - p_e)$:

$$\pi a^2 \left[(p_i - p_e) - b\left(\rho_i + \rho_e \frac{\gamma^2 + a^2}{\gamma^2 - a^2}\right) \frac{\partial^2 \zeta}{\partial t^2} \right] = S$$

Note that if $\rho_i = \rho_e$ and $\gamma \to \infty$, the inertia term has doubled (apparent mass = 1).

Newton's Law in the θ direction now involves two equations:

$$\frac{1}{b} \frac{\partial p_i}{\partial \theta} = -\rho_i \frac{\partial^2 u_i}{\partial t^2}$$

$$\frac{1}{b} \frac{\partial p_e}{\partial \theta} = -\rho_e \frac{\partial^2 u_e}{\partial t^2}$$

Hooke's Law in the ϕ direction now involves $p_i - p_e$:

$$\frac{a(p_i - p_e)}{h} = \frac{E}{1 - \nu^2} \left[\frac{w}{a} + \frac{\nu}{b} \frac{\partial \hat{\xi}}{\partial \theta} \right]$$

The shear and moment equations and the θ component of Hooke's Law are unchanged. We then have two additional equations, continuity and axial force for the external fluid, and two additional variables, u_e and p_e. Listing all nine equations,

$$\zeta + \frac{\partial u_i}{\partial \theta} + \frac{2b}{a} w = 0 \qquad (3\text{-}27)$$

$$\zeta + \frac{2b}{a} w - \frac{\gamma^2 - a^2}{a^2} \frac{\partial u_e}{\partial \theta} = 0 \tag{3-28}$$

$$\frac{1}{b} \frac{\partial p_i}{\partial \theta} = -\rho_i \frac{\partial^2 u_i}{\partial t^2} \tag{3-29}$$

$$\frac{1}{b} \frac{\partial p_e}{\partial \theta} = -\rho_e \frac{\partial^2 u_e}{\partial t^2} \tag{3-30}$$

$$\pi a^2 \left[p_i - p_e - b\left(\rho_i + \rho_e \frac{\gamma^2 + a^2}{\gamma^2 - a^2}\right) \frac{\partial^2 \zeta}{\partial t^2} \right] = S \tag{3-31}$$

$$a \frac{p_i - p_e}{h} = \frac{E}{1 - \nu^2} \left[\frac{w}{a} + \frac{\nu}{b} \frac{\partial \hat{\xi}}{\partial \theta} \right] \tag{3-32}$$

$$\frac{S}{2\pi a h} = \frac{E}{1 - \nu^2} \left[\frac{1}{b} \frac{\partial \hat{\xi}}{\partial \theta} + \nu \frac{w}{a} \right] \tag{3-33}$$

$$\frac{\partial M}{\partial \theta} = 0 \tag{3-34}$$

$$\frac{M}{\pi a^3 h E} = -\frac{1}{b^2} \left(\zeta + \frac{\partial^2 \zeta}{\partial \theta^2} \right) \tag{3-35}$$

We reduce the system algebraically to four equations in the four unknowns p_i, p_e, w, and ζ :

$$-\frac{1}{b^2} \left(\frac{\partial \zeta}{\partial \theta} + \frac{\partial^3 \zeta}{\partial \theta^3} \right) = 0$$

$$a(p_i - p_e)\left(1 - \frac{\nu}{2}\right) = \frac{Ew}{a} - \frac{\nu a b}{2h} \left(\rho_i + \rho_e \frac{\gamma^2 + a^2}{\gamma^2 - a^2}\right) \frac{\partial^2 \zeta}{\partial t^2}$$

$$\frac{\partial^2 \zeta}{\partial t^2} + \frac{2b}{a} \frac{\partial^2 w}{\partial t^2} = \frac{1}{b\rho_i} \frac{\partial^2 p_i}{\partial \theta^2}$$

$$\frac{\partial^2 \zeta}{\partial t^2} + \frac{2b}{a} \frac{\partial^2 w}{\partial t^2} = -\frac{1}{b\rho_e} \frac{\gamma^2 - a^2}{a^2} \frac{\partial^2 p_e}{\partial \theta^2}$$

Next we substitute the exponential form

$$x = x_o \exp\left[i \frac{\omega}{c} (b\theta - ct) \right]$$

where $x = p_i$, p_e, w, or ζ, into these four equations. We find

$$\frac{\partial x}{\partial t} = -i\omega x$$

$$\frac{\partial x}{\partial \theta} = \frac{i\omega b}{c} x$$

Rewriting the four equations in matrix form gives

$$\begin{bmatrix} 0 & 0 & 0 & -\frac{i\omega}{bc} + \frac{i\omega^3 b}{c^3} \\ \frac{a}{h}(1-\frac{\nu}{2}) & -\frac{a}{h}(1-\frac{\nu}{2}) & -\frac{E}{a} & -\frac{\nu ab}{2h}(\rho_i + \rho_e \frac{\gamma^2+a^2}{\gamma^2-a^2})\omega^2 \\ \frac{1}{b\rho_i}\frac{\omega^2 b^2}{c^2} & 0 & -\frac{2b}{a}\omega^2 & -\omega^2 \\ 0 & -\frac{1}{b\rho_e}\frac{\gamma^2-a^2}{a^2}\frac{\omega^2 b^2}{c^2} & -\frac{2b}{a}\omega^2 & -\omega^2 \end{bmatrix} \begin{bmatrix} P_i \\ P_e \\ w \\ \zeta \end{bmatrix} = 0 \qquad (3\text{-}36)$$

The frequency equation, obtained by setting the determinant of the coefficients equal to zero, is

$$\frac{i\omega}{c}\left(\frac{1}{b} - \frac{b\omega^2}{c^2}\right)\frac{\omega^4}{c^2}\left\{\frac{\gamma^2-a^2}{a^2}\frac{b^2}{\rho_e}\frac{E}{ac^2\rho_i} - \frac{2b^2}{h}(1-\frac{\nu}{2})\left[\frac{\gamma^2-a^2}{a^2}\left(\frac{1}{\rho_e}\right) + \frac{1}{\rho_i}\right]\right\} = 0$$

Thus

$$\omega = 0$$

$$\omega = \frac{c}{b}$$

and

$$c^2 = \frac{Eh}{a(2-\nu)}\frac{\gamma^2-a^2}{\rho_e a^2 + \rho_i(\gamma^2-a^2)}$$

are the roots (Fig. 3-16). Surprisingly, as $\gamma \to \infty$, the last becomes

$$c^2 \doteq \frac{Eh}{a(2-\nu)\rho_i}$$

independent of ρ_e, the same results as previously, when there was no exterior fluid. Mathematically, this arises in the following way: the apparent mass term, which might be expected to reduce the wave speed, is in the fourth term of the second row in the matrix above. When the determinant is expanded on the first row, the first three terms being zero, only the minor of the fourth term appears. This minor, of course, involves no terms from the fourth column except that in the first row. Thus the apparent mass term does not appear in the frequency equation. It will, however, affect the mode shapes.

It might also be noted that, as $\gamma/a \to 1$, the apparent mass term approaches infinity, and the wave speed approaches zero; we have an incompressible fluid in a rigid container.

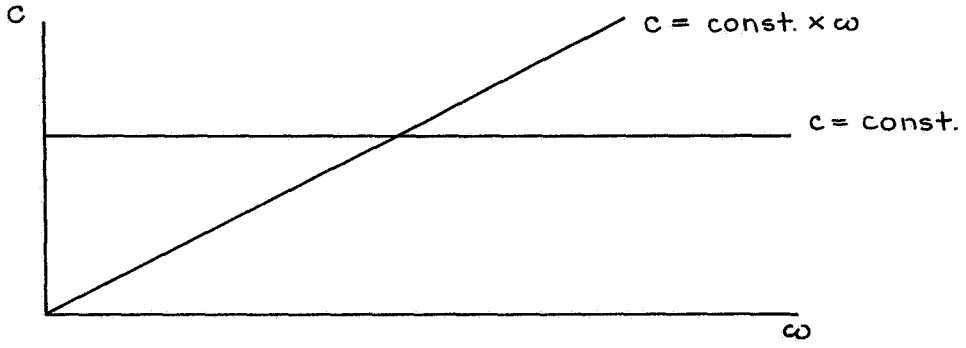

Fig. 3-16
Dispersion Curve for Moens-Korteweg Approximation for a Toroid

Mode shapes are determined from Eq. (3-36). For instance, we can eliminate the second row and transpose the third column:

$$\begin{bmatrix} 0 & 0 & -\frac{\omega}{bc} + \frac{\omega^3 b}{c^3} \\ \frac{1}{b\rho_i}\frac{\omega^2 b^2}{c^2} & 0 & -\omega^2 \\ 0 & -\frac{1}{b\rho_e}\frac{\gamma^2 - a^2}{a^2}\frac{\omega^2 b^2}{c^2} & -\omega^2 \end{bmatrix} \begin{bmatrix} P_i \\ P_e \\ \varphi \end{bmatrix} = \frac{2b}{a}\omega^2 \begin{bmatrix} 0 \\ 1 \\ 1 \end{bmatrix} w$$

The determinant of the 3×3 matrix is

$$\left(\frac{\omega}{bc} - \frac{\omega^3 b}{c^3}\right)\left(\frac{1}{b\rho_i}\,\frac{\omega^2 b^2}{c^2}\right)\left(\frac{1}{b\rho_e}\,\frac{\gamma^2 - a^2}{a^2}\,\frac{\omega^2 b^2}{c^2}\right)$$

which is zero when $\omega = c/b$; so the inversion of this matrix is valid only on the nondispersive curve $c = \text{const}$, away from the intersection of the two modes (see Fig. 3-16). We find

$$\begin{bmatrix} p_i \\ p_e \\ \zeta \end{bmatrix} = \begin{bmatrix} \dfrac{-\omega^2}{\left(\frac{\omega}{bc} - \frac{\omega^3 b}{c^3}\right)\left(\frac{1}{b\rho_i}\,\frac{\omega^2 b^2}{c^2}\right)} & b\rho_i \dfrac{c^2}{\omega^2 b^2} & 0 \\ \dfrac{\omega^2}{\left(\frac{\omega}{bc} - \frac{\omega^3 b}{c^3}\right)\left(\frac{1}{b\rho_i}\,\frac{\omega^2 b^2}{c^2}\right)} & 0 & -b\rho_e \dfrac{a^2}{\gamma^2 - a^2}\,\dfrac{c^2}{\omega^2 b^2} \\ \dfrac{-1}{\left(\frac{\omega}{bc} - \frac{\omega^3 b}{c^3}\right)} & 0 & 0 \end{bmatrix} \begin{bmatrix} 0 \\ 1 \\ 1 \end{bmatrix} \frac{2b}{a}\,\omega^2 w$$

$$= \begin{bmatrix} b\rho_i \dfrac{c^2}{\omega^2 b^2} \\ -b\rho_e \dfrac{a^2}{\gamma^2 - a^2}\,\dfrac{c^2}{\omega^2 b^2} \\ 0 \end{bmatrix} \frac{2b}{a}\,\omega^2 w$$

or: $\zeta = 0, \quad p_i = \dfrac{2\rho_i}{a^2}\,c^2 w, \quad p_e = -\dfrac{2\rho_e}{a}\,\dfrac{a^2}{\gamma^2 - a^2}\,c^2 w$

From $\dfrac{i\omega b}{c}\,u_i + \dfrac{2b}{a}\,w = 0$ we find $i u_i = -\dfrac{2c}{a\omega}\,w$

and similarly $\dfrac{2b}{a}\,w - \dfrac{\gamma^2 - a^2}{a^2}\,\dfrac{i\omega b}{c}\,u_e = 0$ gives $i u_e = \dfrac{2}{a}\,\dfrac{a^2}{\gamma^2 - a^2}\,\dfrac{c}{\omega}\,w$

An analogous method can be used to find the mode shapes for the linearly dispersive mode.

We eliminate the first row from Eq. (3-36) and transpose the last column:

$$\begin{bmatrix} \frac{a}{h}(1-\frac{\nu}{2}) & -\frac{a}{h}(1-\frac{\nu}{2}) & -\frac{E}{a} \\ \frac{1}{b\rho_i}\frac{\omega^2 b^2}{c^2} & 0 & -\frac{2b}{a}\omega^2 \\ 0 & -\frac{1}{b\rho_e}\frac{\gamma^2-a^2}{a^2}\frac{\omega^2 b^2}{c^2} & -\frac{2b}{a}\omega^2 \end{bmatrix} \begin{bmatrix} P_i \\ P_e \\ w \end{bmatrix} = \begin{bmatrix} \frac{\nu ab}{2h}\left(\rho_i + \rho_e \frac{\gamma^2+a^2}{\gamma^2-a^2}\right) \\ 1 \\ 1 \end{bmatrix} \omega^2 \zeta$$

The determinant of the 3×3 matrix is zero at

$$c^2 = \frac{Eh}{(2-\nu)a}\frac{\gamma^2-a^2}{\rho_e a^2 + \rho_i(\gamma^2-a^2)} \equiv c_o^2$$

as well as at $\omega = 0$ and $c \doteq \infty$. At other values, substituting $c = b\omega$,

$$\begin{bmatrix} P_i \\ P_e \\ w \end{bmatrix} = \omega^2 \zeta \begin{bmatrix} \frac{2b}{a}\frac{\omega^2}{b\rho_e}\frac{\gamma^2-a^2}{a^2} & \frac{2b}{h}(1-\frac{\nu}{2}) - \frac{E}{b\rho_e}\frac{\gamma^2-a^2}{a^3} & -\frac{2b}{h}\omega^2(1-\frac{\nu}{2}) \\ -\frac{2\omega^2}{a\rho_i} & \frac{2b}{h}\omega^2(1-\frac{\nu}{2}) & -\frac{2b}{h}(1-\frac{\nu}{2})\omega^2 + \frac{E}{ab\rho_i} \\ \frac{1}{b^2\rho_e\rho_i}\frac{\gamma^2-a^2}{a^2} & \frac{1}{hb\rho_e}(1-\frac{\nu}{2})\frac{\gamma^2-a^2}{a^2} & -\frac{a^2}{hb\rho_i}(1-\frac{\nu}{2}) \end{bmatrix} \begin{bmatrix} \frac{\nu ab}{2h}\left(\rho_i + \rho_e\frac{\gamma^2+a^2}{\gamma^2-a^2}\right) \\ 1 \\ 1 \end{bmatrix}$$

$$\frac{}{\frac{2}{h\rho_e}\frac{\omega^2}{}(1-\frac{\nu}{2})\frac{\gamma^2-a^2}{a^2} + \frac{2\omega^2}{h\rho}(1-\frac{\nu}{2}) - \frac{E}{b^2\rho_e\rho_i}\frac{\gamma^2-a^2}{a^3}}$$

and

$$iu_i = -\frac{2}{a} bw$$

$$iu_e = \frac{2}{a}\frac{a^2 b}{\gamma^2-a^2} w$$

E. Cylindrical Model of Membranous and Elastic Bony Canals

To give some idea of the effects of a bony canal which is not perfectly rigid, the analysis of section C is repeated with the outer wall being elastic.

E_1 and E_2 are the moduli of elasticity of the inner and outer walls respectively; h_1 and h_2 are their thicknesses; v is the displacement of the outer wall in the radial direction. Otherwise the notation is unchanged from section C. We can retain the equations

$$\frac{\partial p_i}{\partial x} = -\rho_i \frac{\partial^2 u_i}{\partial t^2}$$

$$\frac{\partial w}{\partial t} = -\frac{a}{2} \frac{\partial^2 u_i}{\partial x \partial t}$$

$$\frac{\partial (p_i - p_e)}{\partial t} = \frac{h_1 E_1}{a^2} \frac{\partial w}{\partial t}$$

$$\frac{\partial p_e}{\partial x} = -\rho_e \frac{\partial^2 u_e}{\partial t^2}$$

and the stress-strain equation for the outer wall is clearly

$$\frac{\partial p_e}{\partial t} = \frac{h_2 E_2}{\gamma^2} \frac{\partial v}{\partial t}$$

The continuity equation for the outer fluid is derived by setting the difference between inflow and outflow equal to the change in contained volume:

$$\text{Inflow} = \pi \left[(\gamma + v)^2 - (a + w)^2 \right] \frac{\partial u_e}{\partial t} \, dt$$

$$\text{Outflow} = \pi \left[(\gamma + v + \frac{\partial v}{\partial x} dx)^2 - (a + w + \frac{\partial w}{\partial x} dx)^2 \right] \times \left[\frac{\partial u_e}{\partial t} + \frac{\partial^2 u_e}{\partial x \partial t} dx \right] dt$$

Linearizing and subtracting,

$$dV = -\pi (\gamma^2 - a^2) \frac{\partial^2 u_e}{\partial x \partial t} \, dx \, dt$$

The change in contained volume is

$$dV = dx\left[\pi\left(\gamma + v + \frac{\partial v}{\partial t}\,dt\right)^2 - \pi\left(a + w + \frac{\partial w}{\partial t}\,dt\right)^2\right] - dx\left[\pi(\gamma+v)^2 - \pi(a+w)^2\right]$$

$$\cong 2\pi\left(\gamma\frac{\partial v}{\partial t} - a\frac{\partial w}{\partial t}\right)dx\,dt$$

so our sixth equation is

$$2\left(\gamma\frac{\partial v}{\partial t} - a\frac{\partial w}{\partial t}\right) = -(\gamma^2 - a^2)\frac{\partial^2 u_e}{\partial x\,\partial t}$$

Elimination of p_i, p_e, v, and w leaves

$$-\frac{2\rho_e\gamma^3}{h_2 E_2}\frac{\partial^2 u_e}{\partial t^2} + a^2\frac{\partial^2 u_i}{\partial x^2} = -(\gamma^2 - a^2)\frac{\partial^2 u_e}{\partial x^2}$$

$$-\frac{h_1 E_1}{2a}\frac{\partial^2 u_i}{\partial x^2} = -\rho_i\frac{\partial^2 u_i}{\partial t^2} + \rho_e\frac{\partial^2 u_e}{\partial t^2}$$

Substituting the exponential forms,

$$-\frac{2\rho_e\gamma^3}{h_2 E_2}(-\omega^2 u_e) + a^2(-\omega^2 c^2 u_i) = -(\gamma^2 - a^2)(-\omega^2 c^2 u_e)$$

$$-\frac{h_1 E_1}{2a}(-\omega^2 c^2 u_i) = -\rho_i(-\omega^2 u_i) + \rho_e(-\omega^2 u_e)$$

which can be written as a single equation in u_i :

$$\left[-\frac{2\rho_e\gamma^3}{h_2 E_2} + (\gamma^2 - a^2)c^{-2}\right]\left[-\frac{h_1 E_1}{2a}c^{-2} + \rho_i\right]\frac{1}{\rho_e}u_i + \frac{a^2}{c^2}u_i = 0 \qquad (3\text{-}37)$$

or

$$2\frac{\rho_i\rho_e\gamma^3}{h_2 E_2}c^4 - \left[\frac{2\rho_e\gamma^3}{h_2 E_2}\frac{h_1 E_1}{2a} + \rho_i(\gamma^2 - a^2) + \rho_e a^2\right]c^2 + \frac{h_1 E_1}{2a}(\gamma^2 - a^2) = 0$$

then

$$c^2 = \frac{h_2 E_2}{4\rho_e \rho_i \gamma^3}\left[\rho_e\left\{\frac{h_1 E_1}{h_2 E_2}\frac{\gamma^3}{a} + a^2\right\} + \rho_i(\gamma^2 - a^2)\right.$$

$$\pm\left\{\rho_e^2\left(\frac{h_1 E_1}{h_2 E_2}\frac{\gamma^3}{a} + a^2\right)^2 + \rho_i^2(\gamma^2 - a^2)^2 - \frac{4 h_1 E_1}{h_2 E_2}\frac{\rho_e \rho_i (\gamma^2 - a^2)\gamma^3}{2a}\right.$$

$$\left.\left. + 2\rho_e \rho_i (\gamma^2 - a^2)\left(\frac{h_1 E_1}{h_2 E_2}\frac{\gamma^3}{a} + a^2\right)\right\}^{1/2}\right] \qquad (3\text{-}38)$$

Thus there are two modes, corresponding very roughly, if $h_2E_2 >> h_1E_1$, to the wave speeds in the inner and outer shells separately.

F. Conclusions From Moens-Korteweg Type Analysis

The Moens-Korteweg analysis of toroidal tubes results in two modes of motion, one linearly dispersive and one nondispersive.

Some simple experiments were run, using a water-filled bicycle inner tube, either resting on a table, resting on a foam-rubber pad, or immersed in water. Pressure transducers were placed inside the tube and pressure waves were generated by various means. It was shown that Fig. 3-16 does not fully describe the dispersion of waves in a fluid-filled toroidal shell.

Thus the full Laplace equation treatment is too complicated to be conveniently solved, and the Moens-Korteweg method is too simple to provide useful results. It was hoped that a third approach would satisfy both requirements.

IV. REFINED ENGINEERING ANALYSIS

The third approach is similar to that leading to the Moens-Korteweg equation. However, it is based on less restrictive assumptions regarding the behavior of the shell. The effects of shell mass are included, but the constraints on the motion are as before (Fig. 4-1). Shear stresses in the tube are considered in the analysis, although the rotatory inertia is still neglected. These changes result in a third mode of the motion appearing, and in significant changes in the dispersion curves (c vs. ω) for the first two modes.

A. Toroidal Model of Membranous Canal

1. Derivation of Basic Equations

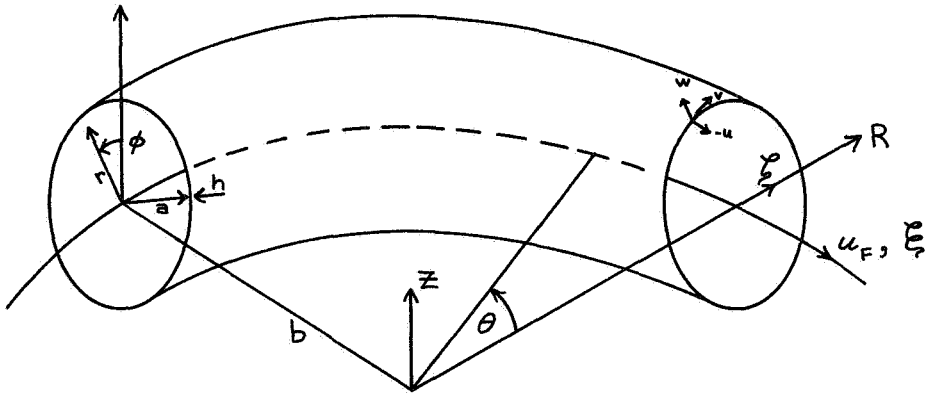

Fig. 4-1. Elastic Toroidal Shell

An elastic shell in the shape of a torus has ring radius b , tube radius a , and thickness h . The tube axis is a circle in the $z = 0$ plane with its center at the origin. The shell material has density ρ_s , modulus of elasticity E , and Poisson's ratio ν . It is filled with incompressible, inviscid fluid of density ρ_f . In a cross-section of the tube at any angle θ , a point is located by its distance r from the tube axis and angle ϕ (see Fig. 4-1). We assume $b >> a >> h$.

The displacement of the centroid of the cross-section is given by ξ in the θ direction and ζ in the R direction. Displacement in the z direction is considered to be zero. Fluid displacement in the ξ direction is u_F; this is considered to be constant across the cross-section. The fluid is assumed to move with the shell in the R direction.

Distortion of the cross-section from a circle of radius a is indicated by displacements u, v, and w of a point on the surface. u is in the θ direction, v in the ϕ direction, w in the r direction. For this analysis we assume axisymmetry: u and w are considered to vary with θ only (thus $u = \xi$ at any point) and v is assumed to be zero.

The stresses in the shell are σ_{11} in the ϕ direction and σ_{21} in the θ direction. These are composed of the stresses which exist at the equilibrium configuration (σ_{10} and σ_{20}) and the stresses due to the perturbations (σ_1 and σ_2).

The strains due to perturbations, i.e. strains minus equilibrium values, are

$$\epsilon_\theta = \frac{1}{b}\frac{\partial \xi}{\partial \theta} + \frac{\zeta + w \sin\phi + \frac{\partial(u-\xi)}{\partial\theta}}{b + a\sin\phi} \tag{4-1}$$

$$\epsilon_\phi = \frac{w}{a} \tag{4-2}$$

These values are then averaged at a cross-section by integrating over ϕ :

$$\bar{\epsilon}_\theta \cong \frac{1}{b}\left(\frac{\partial \xi}{\partial \theta} + \zeta\right) \tag{4-3}$$

$$\bar{\epsilon}_\phi = \frac{w}{a} \tag{4-4}$$

The stresses in the shell are also averaged over ϕ , and the averaged values of stress and strain are related by

$$\sigma_1 = \frac{E}{1-\nu^2}\left(\bar{\epsilon}_\phi + \nu\bar{\epsilon}_\theta\right) \tag{4-5}$$

$$\sigma_2 = \frac{E}{1-\nu^2}\left(\bar{\epsilon}_\theta + \nu\bar{\epsilon}_\phi\right) \tag{4-6}$$

Using these averaged stresses, we compute equilibrium of half a cross-section of the shell:

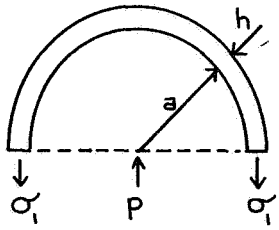

Fig. 4-2
Equilibrium in the ϕ Direction

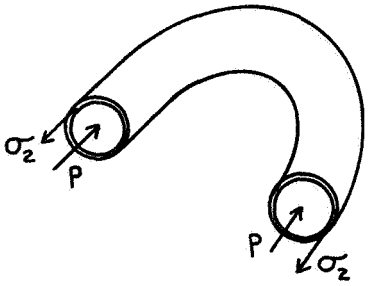

Fig. 4-3
Equilibrium in the θ Direction

$$\sigma_{11} \cdot 2h = p_1 2a \tag{4-7}$$

Here σ_{11} and p_1 represent the total stress and transmural pressure. Subtracting off the equilibrium values ($\sigma_{10} \cdot 2h = p_0 \cdot 2a$), we find

$$2\sigma_1 h = 2pa \qquad \text{or} \qquad \sigma_1 = ap/h \tag{4-8}$$

σ_1 and p represent the deviations from equilibrium due to w, ξ, ζ, u_F, etc.

Similarly, we compute equilibrium in the θ direction for half the torus. With σ_{21} the total stress in the θ direction averaged over ϕ,

$$2\pi a^2 p_1 = 2(2\pi ah)\sigma_{21} \tag{4-9}$$

Subtracting off the equilibrium values,

$$2\pi a^2 p_0 = 2(2\pi ah)\sigma_{20} \tag{4-10}$$

we find

$$2\pi a^2 p = 4\pi ah\,\sigma_2 \qquad \text{or} \qquad \sigma_2 = \frac{ap}{2h} \tag{4-11}$$

The change in curvature of the tube axis due to its deflection ζ is

$$\Delta K = -\frac{1}{b^2}\left(\frac{\partial^2 \zeta}{\partial \theta^2} + \zeta\right) \tag{4-12}$$

Assuming that plane sections remain plane, the bending moment needed to accomplish this is

$$M = EI\Delta K \tag{4-13}$$

The area moment of inertia of a cross-section of shell is

$$I = \frac{\pi}{4}\left(a^4 - (a-h)^4\right) \cong \pi a^3 h \tag{4-14}$$

so

$$M = -\frac{E\pi a^3 h}{b^2}\left(\frac{\partial^2 \zeta}{\partial \theta^2} + \zeta\right) \tag{4-15}$$

Neglecting the effects of rotatory inertia, the shear Q in the z = 0 plane is

$$Q = \frac{1}{b}\frac{\partial M}{\partial \theta} = -\frac{E\pi a^3 h}{b^3}\left(\frac{\partial^3 \zeta}{\partial \theta^3} + \frac{\partial \zeta}{\partial \theta}\right) \tag{4-16}$$

We now write Newton's Law for the shell-fluid system

(1) Fluid and shell in ζ direction:

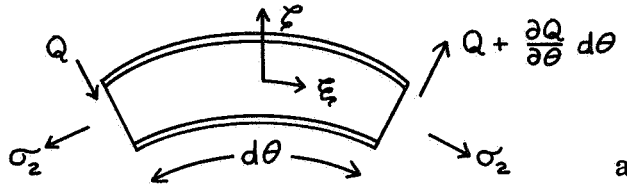

Fig. 4-4
Equilibrium in ζ and ξ Directions

$$b\,d\theta \cdot (2\pi a h \rho_s + \pi a^2 \rho_F)\frac{\partial^2 \zeta}{\partial t^2} = \frac{\partial Q}{\partial \theta}\,d\theta - (2\pi a h \sigma_2 - \pi a^2 p)\,d\theta$$

or

$$(2\pi a h \rho_s + \pi a^2 \rho_F)\, b \frac{\partial^2 \zeta}{\partial t^2} = \frac{\partial Q}{\partial \theta} - 2\pi a h \sigma_2 + \pi a^2 p \tag{4-17}$$

(2) Shell only in ξ direction:

Fig. 4-5
Shell Equilibrium in θ Direction

$$2\pi a h \rho_s b\, d\theta \frac{\partial^2 \xi}{\partial t^2} = 2\pi a h \left(\frac{\partial \sigma_2}{\partial \theta} d\theta\right) + Q\, d\theta$$

or

$$2\pi a h \rho_s b \frac{\partial^2 \xi}{\partial t^2} = 2\pi a h \frac{\partial \sigma_2}{\partial \theta} + Q \tag{4-18}$$

(3) Fluid only in ξ direction:

Fig. 4-6
Fluid Equilibrium
in θ Direction

$$b\rho_F\, d\theta \frac{\partial^2 u_F}{\partial t^2} = -\frac{\partial p}{\partial \theta} d\theta$$

so

$$b\rho_F \frac{\partial^2 u_F}{\partial t^2} = -\frac{\partial p}{\partial \theta} \tag{4-19}$$

Finally we write the continuity equation for the fluid in the tube. In equilibrium, a segment of tube of arc length $d\theta$ has volume

$$V_o = \pi a^2 b\, d\theta$$

After deformations ζ and w its volume becomes (note that ξ motion has no effect on the volume in $d\theta$)

$$V_1 = \pi (a + w)^2 (b + \zeta)\, d\theta \cong \pi (a^2 b + 2awb + a^2 \zeta)\, d\theta$$

This change in volume must be accompanied by a net inflow of fluid of volume $V_1 - V_0$.

$$V_1 - V_o = \pi a^2 u_F(\theta) - \pi a^2 u_F(\theta + d\theta)$$

$$-\pi a^2 \frac{\partial u_F}{\partial \theta} d\theta = \pi (2awb + a^2 \zeta)\, d\theta$$

or

$$\zeta + \frac{2b}{a} w + \frac{\partial u_F}{\partial \theta} = 0 \tag{4-20}*$$

---

* Note that this derivation follows the procedure of observing the volume of fluid which flows into a fixed $d\theta$. The derivation in Chapter III observes the change in subtended angle $d\theta$ of a fixed volume of fluid.

We combine (4-3), (4-4), (4-5), (4-6), (4-8), and (4-11) to get the two equations

$$\sigma_1 = \frac{aP}{h} = \frac{E}{1-\nu^2}\left[\frac{w}{a} + \frac{\nu}{b}\left(\frac{\partial \xi}{\partial \theta} + \zeta\right)\right] \tag{4-21}$$

$$\sigma_2 = \frac{aP}{2h} = \frac{E}{1-\nu^2}\left[\frac{1}{b}\left(\frac{\partial \xi}{\partial \theta} + \zeta\right) + \frac{\nu w}{a}\right] \tag{4-22}$$

We substitute these equations and the shear equation (4-16) into the three equations of motion (4-17, (4-18), and (4-19):

$$\left(2\pi ah\rho_s + \pi a^2\rho_F\right) b \frac{\partial^2 \zeta}{\partial t^2} = -\frac{E\pi a^3 h}{b^3}\left(\frac{\partial^4 \zeta}{\partial \theta^4} + \frac{\partial^2 \zeta}{\partial \theta^2}\right)$$

$$- 2\pi ah \frac{E}{1-\nu^2}\left(\frac{\zeta}{b} + \frac{1}{b}\frac{\partial \xi}{\partial \theta} + \frac{\nu w}{a}\right) + \pi ah \frac{E}{1-\nu^2}\left[\frac{w}{a} + \frac{\nu}{b}\left(\zeta + \frac{\partial \xi}{\partial \theta}\right)\right] \tag{4-23}$$

$$2\pi ah\rho_s b \frac{\partial^2 \xi}{\partial t^2} = 2\pi ah \frac{E}{1-\nu^2}\left(\frac{1}{b}\frac{\partial \zeta}{\partial \theta} + \frac{1}{b}\frac{\partial^2 \xi}{\partial \theta^2} + \frac{\nu}{a}\frac{\partial w}{\partial \theta}\right)$$

$$- \frac{E\pi a^3 h}{b^3}\left(\frac{\partial^3 \zeta}{\partial \theta^3} + \frac{\partial \zeta}{\partial \theta}\right) \tag{4-24}$$

$$b\rho_F \frac{\partial^2 u_F}{\partial t^2} = -\frac{h}{a}\frac{E}{1-\nu^2}\left[\frac{1}{a}\frac{\partial w}{\partial \theta} + \frac{\nu}{b}\left(\frac{\partial \zeta}{\partial \theta} + \frac{\partial^2 \xi}{\partial \theta^2}\right)\right] \tag{4-25}$$

These three, together with the continuity equation

$$\zeta + \frac{2b}{a} w + \frac{\partial u_F}{\partial \theta} = 0 \tag{4-26}$$

are four linear, homogeneous partial differential equations for ζ, ξ, w, and u_F as functions of θ and t. (Note that u does not appear; therefore the subscript on u_F can be dropped without ambiguity.)

As in Chapter III, solutions of exponential form are assumed:

$$\begin{bmatrix} \zeta \\ \xi \\ w \\ u \end{bmatrix} = \begin{bmatrix} A \\ B \\ C \\ D \end{bmatrix} e^{i(L\theta/\lambda - \omega t)}$$

where $L = 2\pi b$, λ is wavelength, and ω is frequency. (Here the equations will be in terms of ω and λ instead of ω and c.) Substituting into (4-23) to (4-26) gives

$$\zeta + \frac{2b}{a} w + \frac{iL}{\lambda} u = 0$$

$$\left[(-2\pi ah\rho_s - \pi a^2\rho_F) b\omega^2 + \frac{E\pi a^3 h}{b^3}\left(\left(\frac{L}{\lambda}\right)^4 - \left(\frac{L}{\lambda}\right)^2\right) + \frac{\pi a^3 hE}{b(1-\nu^2)}(2-\nu)\right]\zeta$$

$$+ \frac{\pi a^3 hE}{b(1-\nu^2)}(2-\nu)\frac{iL}{\lambda} + \pi h \frac{E}{1-\nu^2}(2\nu-1) w = 0$$

$$i\left[\frac{E\pi a^3 h}{b^3}\left(-\left(\frac{L}{\lambda}\right)^3 + \frac{L}{\lambda}\right) - \frac{2\pi ah}{b}\frac{E}{1-\nu^2}\frac{L}{\lambda}\right]\zeta + \left[-2\pi ah\rho_s b\omega^2\right.$$

$$\left. + \frac{2\pi ah}{b}\frac{E}{1-\nu^2}\left(\frac{L}{\lambda}\right)^2\right] \xi - 2\pi h\nu \frac{E}{1-\nu^2}\frac{iL}{\lambda} w = 0$$

$$i\frac{h}{a}\frac{E}{1-\nu^2}\frac{\nu}{b}\frac{L}{\lambda}\zeta - \frac{h}{a}\frac{E}{1-\nu^2}\frac{\nu}{b}\left(\frac{L}{\lambda}\right)^2 \xi + i\frac{h}{a}\frac{E}{1-\nu^2}\frac{L}{\lambda} w - b\rho_F\omega^2 u = 0$$

Introducing $c_p^2 = \frac{E}{\rho_s(1-\nu^2)}$, $\bar{\omega} = \frac{b\omega}{c_p}$, $\bar{\rho} = \rho_F/\rho_s$,

and rewriting the above equations in matrix form we have:

$$\begin{bmatrix} 1 & 0 & 2 & \frac{L}{\lambda} \\ -(2+\bar{\rho}\frac{a}{h})\bar{\omega}^2 + (2-\nu) & (2-\nu)\frac{L}{\lambda} & 2\nu-1 & 0 \\ +(1-\nu^2)(\frac{a}{b})^2\left[\left(\frac{L}{\lambda}\right)^4 - \left(\frac{L}{\lambda}\right)^2\right] & & & \\ (1-\nu^2)(\frac{a}{b})^2\left[\left(\frac{L}{\lambda}\right)^3 - \left(\frac{L}{\lambda}\right)\right] + \frac{2L}{\lambda} & 2\left[-\bar{\omega}^2 + \left(\frac{L}{\lambda}\right)^2\right] & 2\nu\frac{L}{\lambda} & 0 \\ \nu\frac{L}{\lambda} & \nu\left(\frac{L}{\lambda}\right)^2 & -\frac{L}{\lambda} & \bar{\rho}\frac{a}{h}\bar{\omega}^2 \end{bmatrix} \begin{bmatrix} \zeta \\ i\xi \\ \frac{b}{a}w \\ iu \end{bmatrix} = 0$$

(4-27)

These equations can be solved for characteristic frequencies, wavelengths, and wave speeds, as well as for mode shapes. The parameters appearing are $\bar{\rho}$, ν, h/a, and a/b; the variables are $\bar{\omega}$ and L/λ (in addition to ζ, ξ, w, and u). Dimensionless wave speed $\bar{c} = c/c_p$ is easily seen to be $\bar{\omega}/(L/\lambda)$.

To reduce the number of parameters which appear in a numerical solution, we make the biologically realistic and justifiable approximations $\bar{\rho} = 1$ and $\nu = 1/2$. $\bar{\rho} = 1$ means that the density of the fluid and tube material are the same; $\nu = 1/2$ means that the tube material is incompressible.

$$\begin{bmatrix} 1 & 0 & 2 & \frac{L}{\lambda} \\ -(2+\frac{a}{h})\bar{\omega}^2+\frac{3}{2} + \frac{3}{4}(\frac{a}{b})^2\left[(\frac{L}{\lambda})^4-(\frac{L}{\lambda})^2\right] & \frac{3}{2}\frac{L}{\lambda} & 0 & 0 \\ \frac{3}{4}(\frac{a}{b})^2\left[(\frac{L}{\lambda})^3-(\frac{L}{\lambda})\right]+\frac{2L}{\lambda} & 2\left[-\bar{\omega}^2+(\frac{L}{\lambda})^2\right] & \frac{L}{\lambda} & 0 \\ \frac{1}{2}\frac{b}{a}\frac{L}{\lambda} & \frac{1}{2}\frac{b}{a}(\frac{L}{\lambda})^2 & \frac{h}{a}\frac{L}{\lambda} & \bar{\omega}^2 \end{bmatrix} \begin{bmatrix} \zeta \\ i\xi \\ \frac{b}{a}w \\ iu \end{bmatrix} = 0 \qquad (4\text{-}28)$$

The frequency equation is obtained by observing that, for a nontrivial solution to exist, the determinant of the coefficients must be zero. After some manipulation, the determinant is reduced to:

$$\begin{vmatrix} -(2+\frac{a}{h})\bar{\omega}^2+\frac{3}{2} + \frac{3}{4}(\frac{a}{b})^2\left[(\frac{L}{\lambda})^2-1\right](\frac{L}{\lambda})^2 & -\frac{3}{2}\frac{L}{\lambda} & 0 \\ -\frac{3}{4}(\frac{a}{b})^2\frac{L}{\lambda}\left[(\frac{L}{\lambda})^2-1\right]-\frac{3}{2}\frac{L}{\lambda} & -2\bar{\omega}^2+2(\frac{L}{\lambda})^2 & -\frac{1}{2}(\frac{L}{\lambda})^2 \\ 0 & -\frac{1}{2}(\frac{L}{\lambda})^2 & -\frac{a}{h}\bar{\omega}^2+\frac{1}{2}(\frac{L}{\lambda})^2 \end{vmatrix} = 0 \qquad (4\text{-}29)$$

This polynomial is third order in $\bar{\omega}^2$ and fourth order in $(L/\lambda)^2$, so the most convenient method of solution is to assume a value of L/λ, work out the coefficients of the polynomial in $\bar{\omega}^2$, and solve (numerically) for the three roots. $\bar{c}$ is calculated from $\bar{\omega}$ and L/λ.

Mode shapes are found, for each of the three values of $\bar{\omega}^2$ at each (L/λ), by using Eqs. (4-28). We can drop one of the four equations — say the last — and solve for three of the variables ζ, ξ, w, u in terms of the fourth. For example:

$$\begin{bmatrix} 0 & \frac{2b}{a} & \frac{L}{\lambda} \\ \frac{3}{2}\frac{L}{\lambda} & 0 & 0 \\ 2\left[-\bar{\omega}^2+\left(\frac{L}{\lambda}\right)^2\right] & \frac{L}{\lambda}\frac{b}{a} & 0 \end{bmatrix} \begin{bmatrix} i\xi \\ w \\ iu \end{bmatrix} = \begin{bmatrix} -1 \\ (2+\frac{a}{h})\bar{\omega}^2 - \frac{3}{4}\left(\frac{a}{b}\right)^2\left[\left(\frac{L}{\lambda}\right)^4-\left(\frac{L}{\lambda}\right)^2\right]-\frac{3}{2} \\ -\frac{3}{4}\left(\frac{a}{b}\right)^2\left[\left(\frac{L}{\lambda}\right)^3-\left(\frac{L}{\lambda}\right)\right]-\frac{2L}{\lambda} \end{bmatrix} \zeta \tag{4-30}$$

Inverting the 3×3 matrix, we find its determinant is $\frac{3}{2}\left(\frac{L}{\lambda}\right)^3\frac{b}{a}$, which is normally not zero, so the form $\begin{bmatrix} i\xi \\ w \\ iu \end{bmatrix} =$

$$\begin{bmatrix} 0 & \frac{2}{3}\frac{\lambda}{L} & 0 \\ 0 & \frac{4}{3}\frac{a}{b}\left[\bar{\omega}^2\left(\frac{\lambda}{L^2}\right)-1\right] & \frac{a}{b}\frac{\lambda}{L} \\ \frac{\lambda}{L} & \frac{8}{3}\frac{\lambda}{L}\left[-\bar{\omega}^2\left(\frac{\lambda}{L}\right)^2+1\right] & -2\left(\frac{\lambda}{L}\right)^2 \end{bmatrix} \begin{bmatrix} -1 \\ (2+\frac{a}{h})\bar{\omega}^2 - \frac{3}{2} - \frac{3}{4}\left(\frac{a}{b}\right)^2\left[\left(\frac{L}{\lambda}\right)^4-\left(\frac{L}{\lambda}\right)^2\right] \\ -\frac{3}{4}\left(\frac{a}{b}\right)^2\left[\left(\frac{L}{\lambda}\right)^3-\frac{L}{\lambda}\right]-\frac{2L}{\lambda} \end{bmatrix} \zeta \tag{4-31}$$

is generally valid for determining mode shapes. $\bar{\omega}$ and L/λ must, of course, satisfy Eq. (4-29).

Before discussing specific results of the above work, it will be worthwhile to examine some general properties of the equations.

One point of interest would be cutoff frequencies (frequencies at which wave speeds become infinite). From equation (4-28), if $L/\lambda = 0$ (infinite

wavelength), it is easily seen that the frequency equation becomes

$$\left[-\left(2+\frac{a}{h}\right)\bar{\omega}^2+\frac{3}{2}\right]\frac{2a}{h}\bar{\omega}^4=0$$

which has the solutions

$$\bar{\omega}^2=0,\ 0,\ \frac{3/2}{2+a/h}$$

The non-zero solution yields $\bar{c}=\bar{\omega}/(L/\lambda)$ infinite, so this is a cutoff frequency.

Some properties of the mode shapes can be found from Eq. (4-31). We know that the 3×3 matrix is nonsingular — its inverse is in Eq. (4-30) — so the vector $[\,i\xi, w, iu\,]$ can be zero only if the right-hand side is zero. Since the first element of the right-hand side is constant, the vector can be zero only if the multiplier, ζ, is zero. Thus, if ζ remains finite, the other three variables cannot all be zero.

Further, no element of the vector $[\,i\xi, w, iu\,]$ can be infinite unless at least one of the elements on the right-hand side of Eq. (4-31) is infinite. This clearly cannot happen unless L/λ is zero or infinite.

Finally it should be noted that $L/\lambda = 1$ can be seen to be an important transition point in both Eqs. (4-29) and (4-31). Physically, this represents a wavelength equal to the circumference of the tube. If we are considering a closed tube, wavelengths larger than this need not be considered. In fact, only L/λ = integer can exist (see section B3). However, if the tube is less than a full circle, or if it is a helix or spiral so more than a full circle can exist, other values of L/λ are permitted.

2. Dispersion Curves and Mode Shapes

Eq. (4-29) is solved numerically, for fixed values of the parameters a/b and h/a, by assuming successive values for (L/λ) and solving the resulting third-order polynomial in $\bar{\omega}^2$. A plot of $\bar{c}$ vs. $\bar{\omega}$ is more useful than L/λ vs. $\bar{\omega}$, so $\bar{c}=\bar{\omega}/(L/\lambda)$ is computed.

Plots of the dispersion curves ($\bar{c}$ vs. $\bar{\omega}$) (Figs. 4-7 to 4-14) are included for:

a/b	h/a
.02	.02
.02	.1
.1	.02
.1	.1
.05	.06

The three modes are named after the types of motion they represent. The high-speed mode is asymptotic to $\bar{c} = 1$ ($c = c_p$), the speed of a stress wave in the wall material. The mode is referred to as extensional (E).

The two lower-speed modes appear to cross each other; however, very detailed and careful investigation of this region shows that the two curves do not intersect. There is a saddle point in the region of closest approach, but there is no double root of Eq. (4-29). The mode shapes, as will be shown in the next section, change rapidly in this region.

To the left of the saddle point, the higher-speed of the two modes represents a breathing motion; to the right it is a flexural motion of the tube in the $z = 0$ plane. This mode is referred to as breathing-flexure (B-F). The lowest-speed mode has these two types of motion in reverse order and is referred to as flexure-breathing (F-B).

The speed of the breathing portion of these two modes is seen to be almost independent of a/b if, as assumed, $a/b \ll 1$. The classical Moens-Korteweg wave for a straight tube ($a/b = 0$) gives $c^2 = Eh/2\rho a$; normalizing with $c_p^2 = E/\rho(1-\nu^2)$ we find

$$\bar{c}^2 = \frac{h}{2a}(1-\nu^2) \cong 0.375\,\frac{h}{a} \qquad \text{or} \qquad \bar{c} \cong .613\sqrt{\frac{h}{a}}$$

for $h/a = .02$ and $.1$, we find $\bar{c} \cong .0867$ and $.194$ respectively. These are seen to be very close to the breathing modes on the dispersion curves.

The presence of a cutoff frequency in the extensional mode has already been mentioned. The breathing mode appears to increase in speed continuously as $L/\lambda \longrightarrow 0$, but numerical difficulties have prevented precise determination. The flexural mode has the most unexpected behavior. This mode has $\bar{\omega} = \bar{c} = 0$ at $L/\lambda = 1$ (rigid body motion), and assumes the indicated parabolic shape for $L/\lambda > 1$. For $L/\lambda < 1$ (which can exist for a spiral or helical tube), it traces a very small half-open curve and then returns to $\bar{\omega} = 0$ at finite, though small, $\bar{c}$. It has not been possible to ascribe any physical significance to this portion of the curve; it may be that any flexural motion at such wavelengths would be too small to be seen, and the curve is merely a mathematical oddity of the frequency equation (Fig. 4-14).

Mode shapes are obtained for $\zeta \equiv 1$ by assuming given values for

h/a and a/b and substituting a solution of Eq. (4-29), L/λ and $\bar{\omega}$, into Eq. (4-31). For each value of L/λ there are three solutions $\bar{\omega}$; the values ($i\xi$, w, iu) produced by Eq. (4-31) represent the shape of the mode.

If $i\xi > 0$, ξ leads ζ by 90°; if $i\xi < 0$, ξ lags ζ, and similarly for iu. w is in phase or 180° out of phase with ζ depending as $w > 0$ or $w < 0$. ζ, of course, is an arbitrary reference oscillation with frequency $\bar{\omega}$. The relative amplitudes of ξ, w, and u to ζ are given by $|i\xi|$, $|w|$, and $|iu|$.

From the plots of the mode shapes, we can see that, in the flexure region of both low-speed modes, ζ dominates the other quantities (Figs. 4-15 to 4-18). Thus the motion consists primarily of oscillation of the tube axis in the $z = 0$ plane about its equilibrium location.

The breathing motion is different at low and high frequencies. At high frequencies, w and u are dominant, ξ is secondary, and ζ is insignificant. This type of motion would normally be considered a breathing mode (Fig. 4-15). At moderately low frequencies, u is large, w and ξ are smaller, and ζ is smallest but noticeable. At very low frequencies ($L/\lambda < 1$), the analysis predicts peculiar behavior for both breathing and flexure modes. (Figs. 4-15 and 4-17.)

The transition between breathing and flexure near the saddle point along any one mode is quite rapid. This means that, for experimental measurement of mode shapes at frequencies near the saddle point, the input sine wave must be very precise. However, it also means that the range of frequencies which are not clearly either breathing or flexure is very small.

The extensional mode is dominated throughout by ξ, which is orders of magnitude larger than any other component. The mode thus consists mainly of a stress wave in the elastic shell, propagating at its natural velocity, c_p.

The straight-line mode shapes seem to be, approximately,

$$iu = -\left(3.33 + 6\,\frac{h}{a}\right)\bar{\omega}$$

(actually the h/a coefficient varies from 5.2 to 6.8)

$$i\xi = 10\left(\frac{h}{a}\right)^{-0.9}\bar{\omega}$$

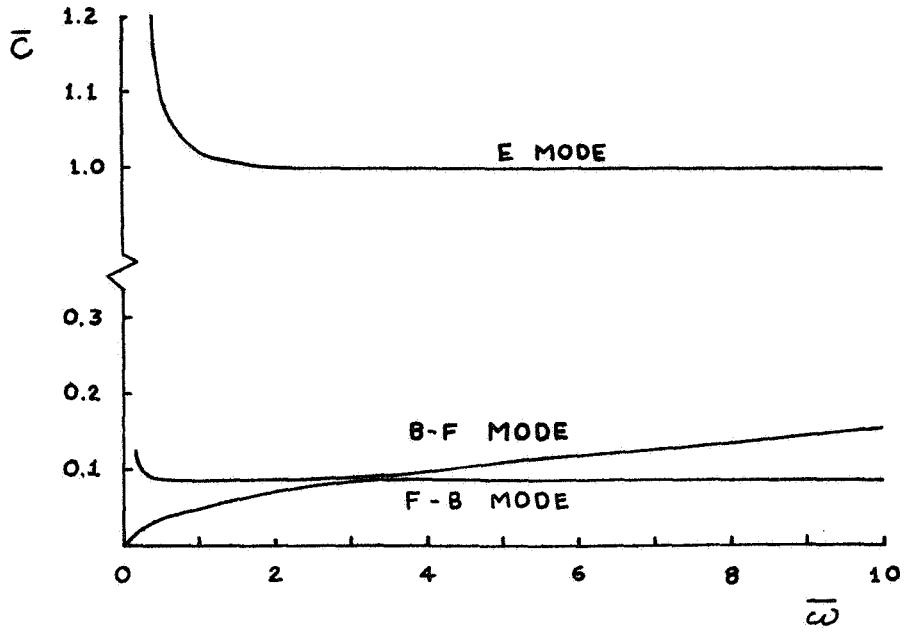

Fig. 4-7

Dispersion Curve for a/b = 0.02, h/a = 0.02
No Rigid Wall

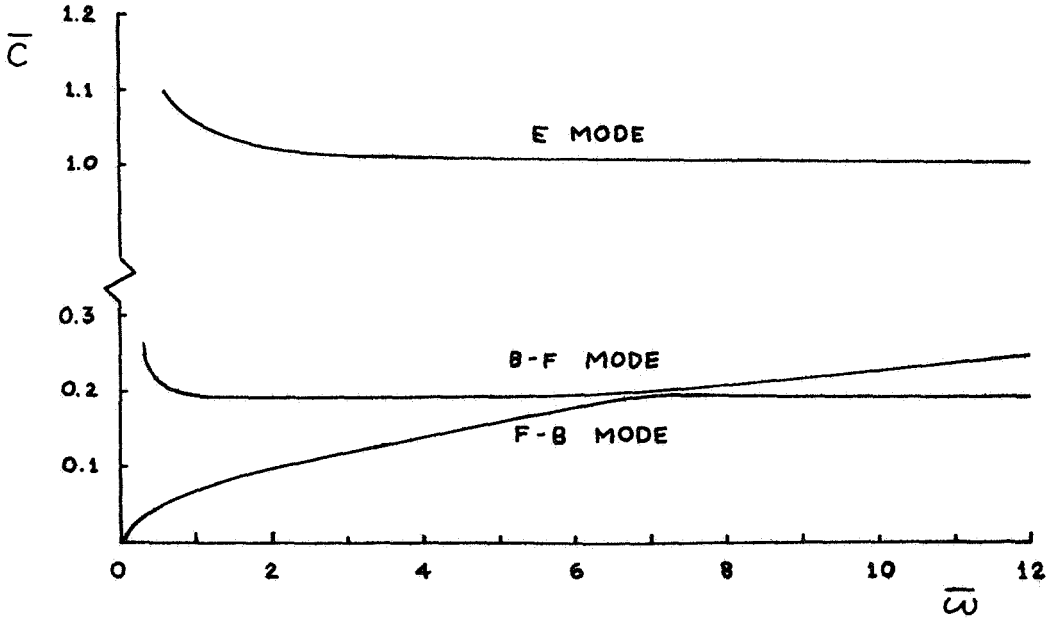

Fig. 4-8

Dispersion Curve for a/b = 0.02, h/a = 0.1
No Rigid Wall

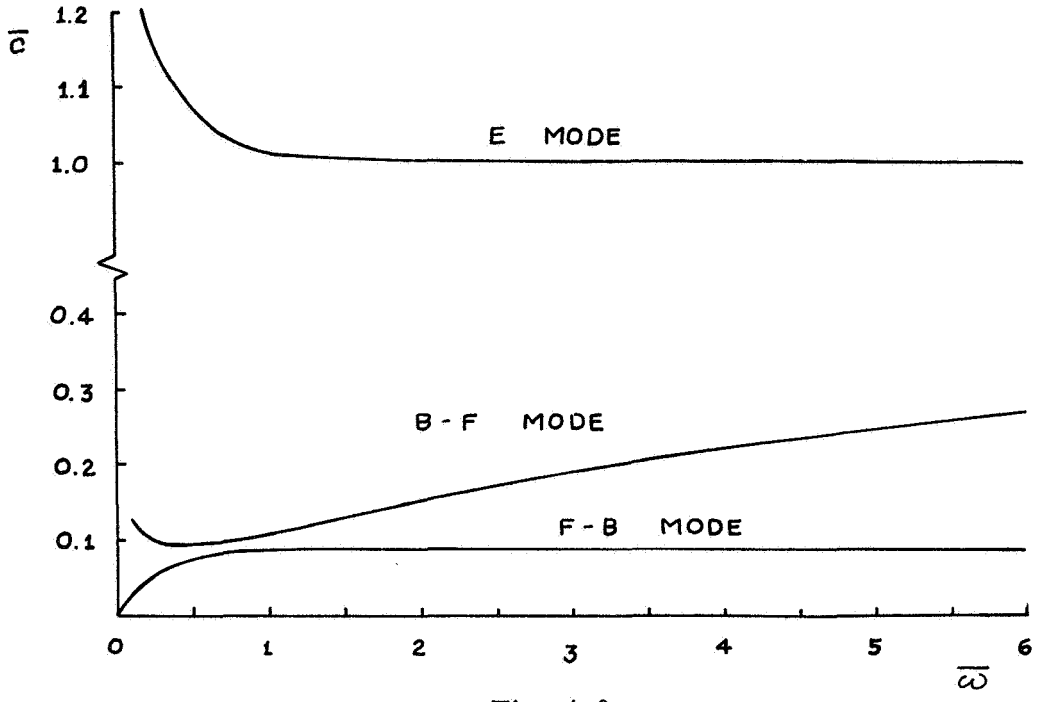

Fig. 4-9

Dispersion Curve for a/b = 0.1, h/a = 0.02
No Rigid Wall

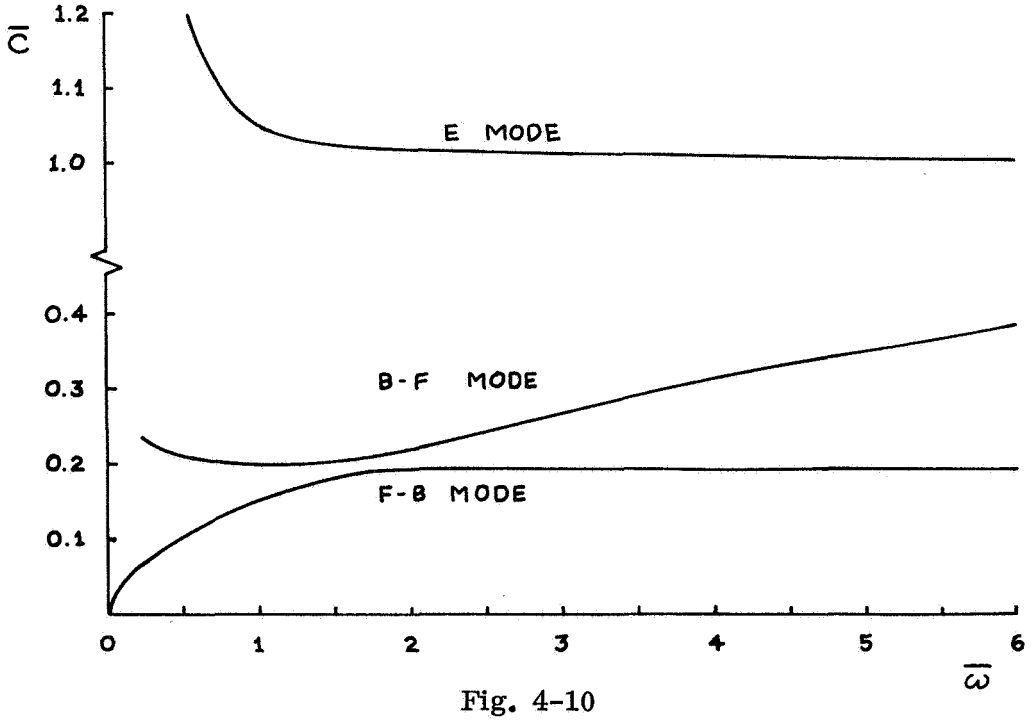

Fig. 4-10

Dispersion Curve for a/b = 0.1, h/a = 0.1
No Rigid Wall

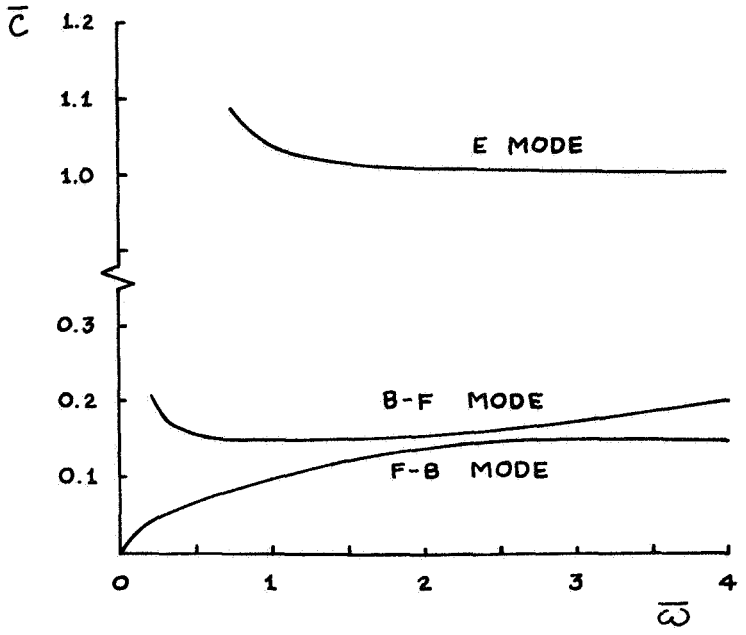

Fig. 4-11

Dispersion Curve for a/b = 0.05, h/a = 0.06
No Rigid Wall

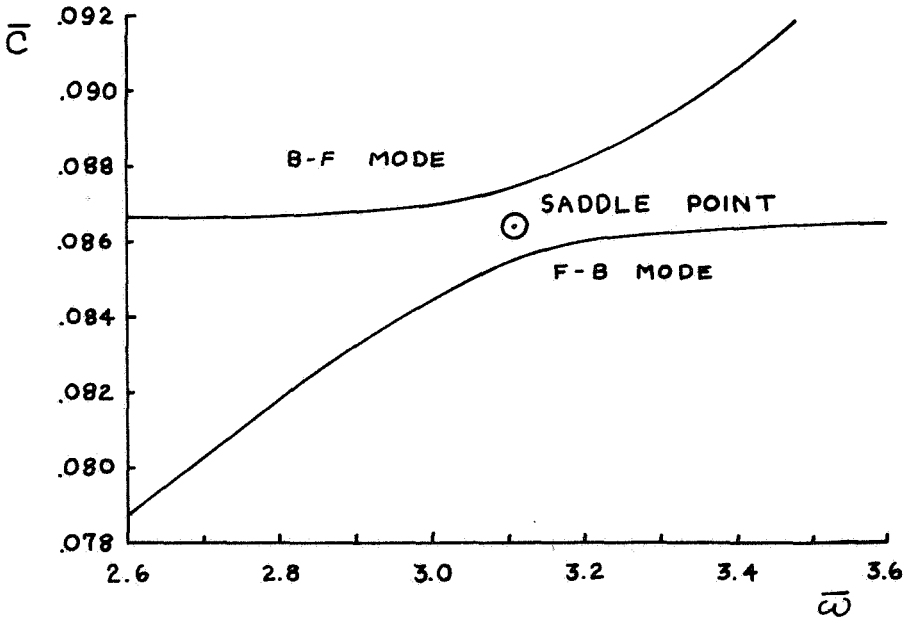

Fig. 4-12

Detail of Fig. 4-7
Near Saddle Point

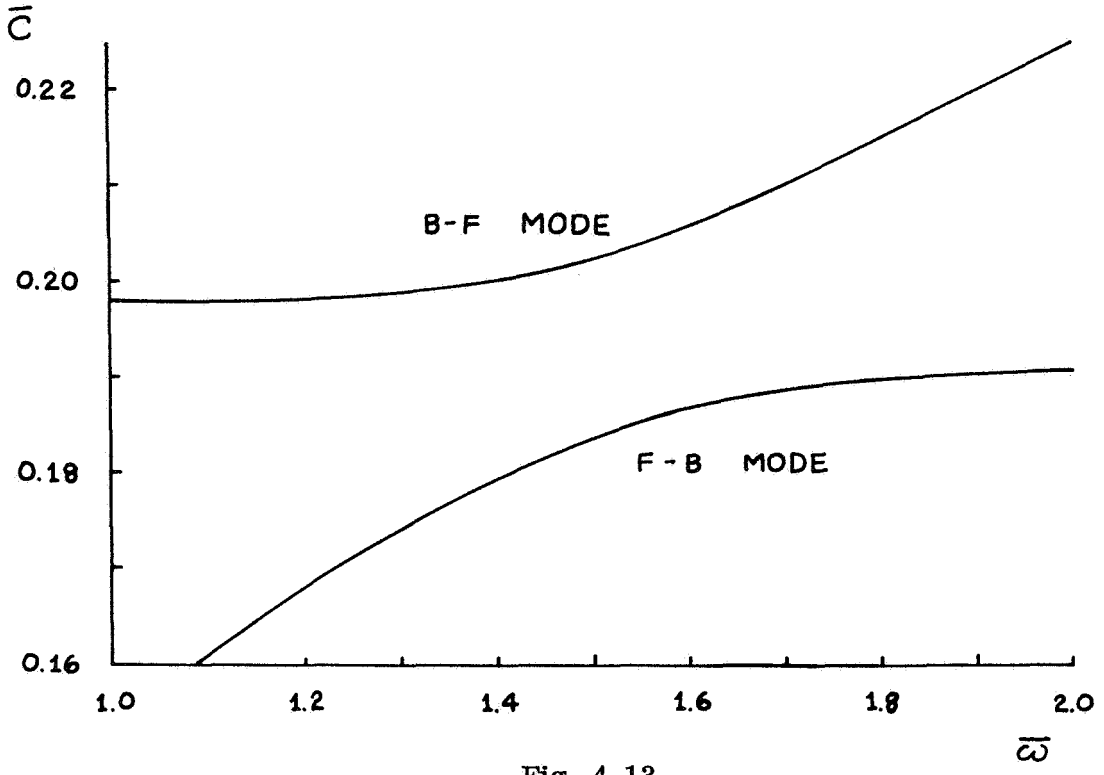

Fig. 4-13

Detail of Fig. 4-10
Near the Saddle Point

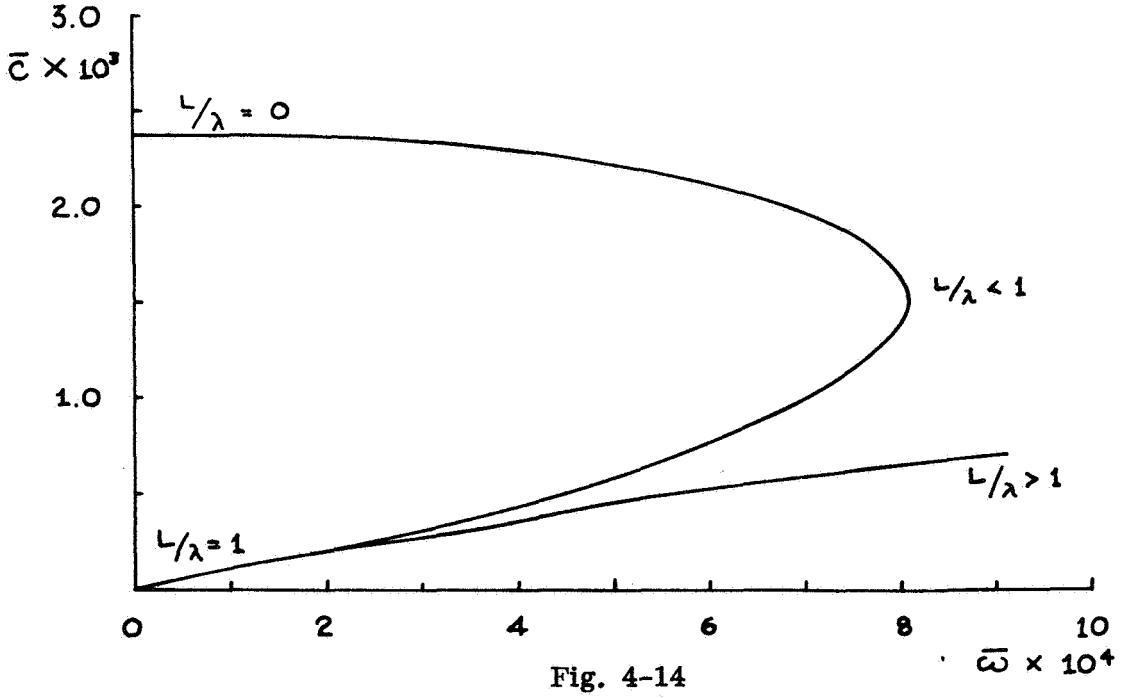

Fig. 4-14

Dispersion Curve for a/b = .02, h/a = .02
No Rigid Wall
$\bar{\omega} \ll 1$

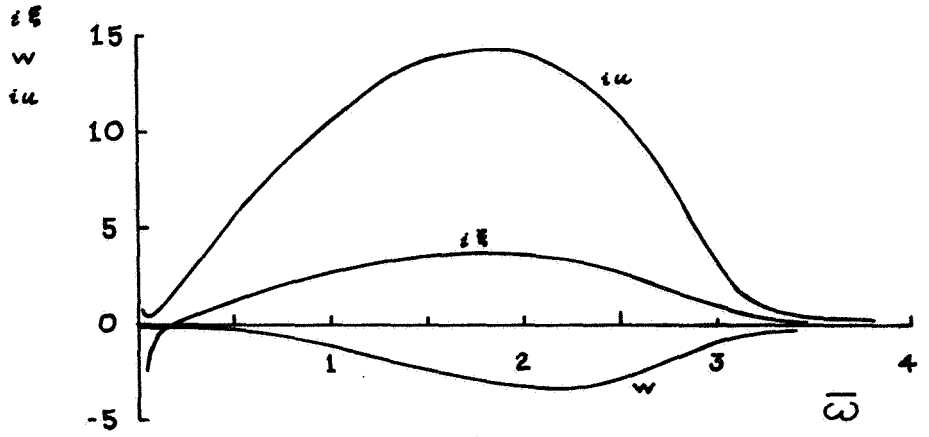

(a) B-F Mode

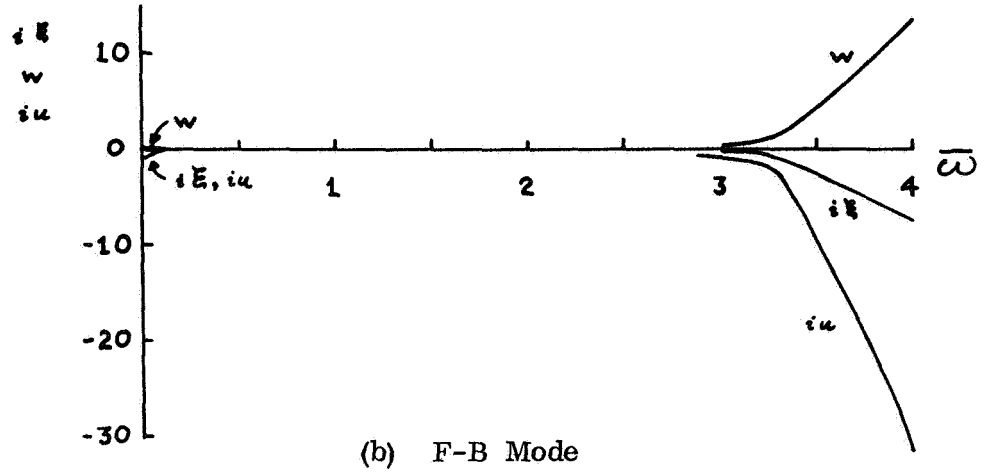

(b) F-B Mode

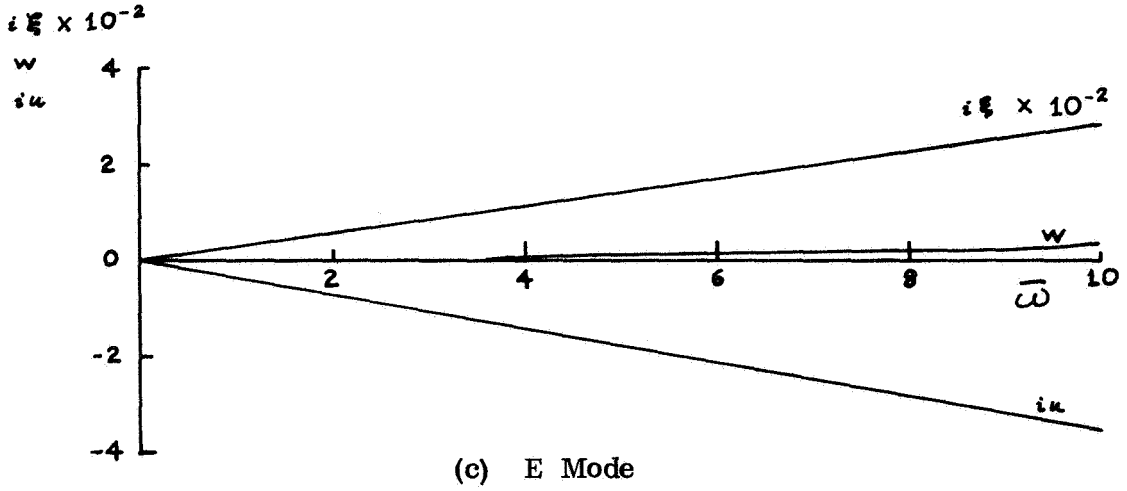

(c) E Mode

Fig. 4-15

Mode Shapes for a/b = 0.02, h/a = 0.02
Based on $\zeta \equiv 1$
No Rigid Wall

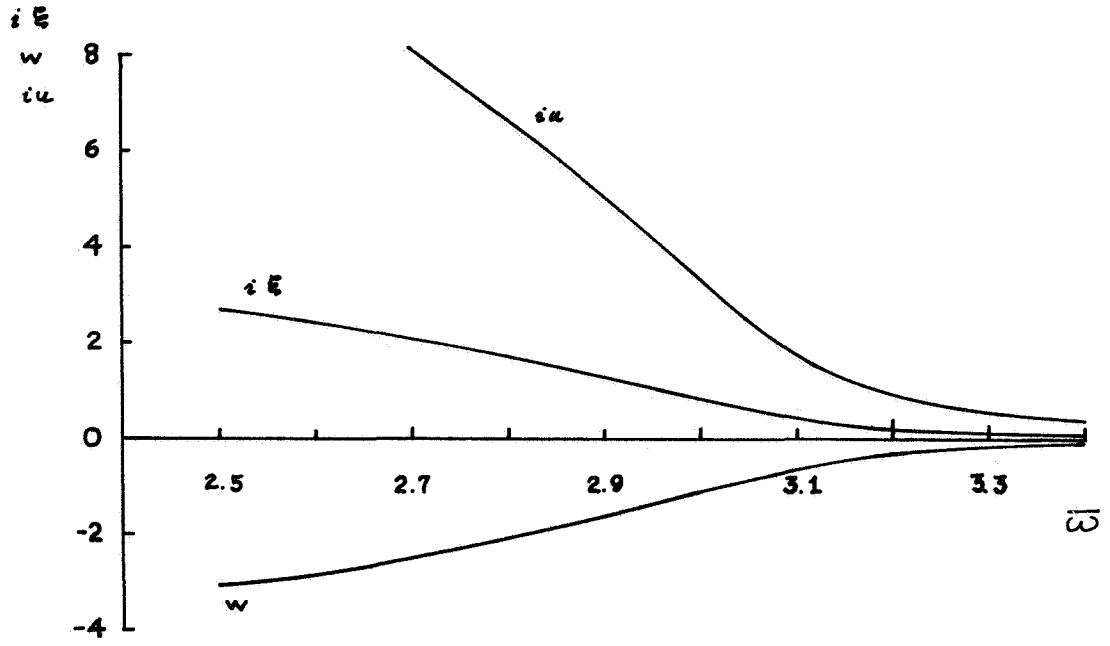

(a) B-F Mode

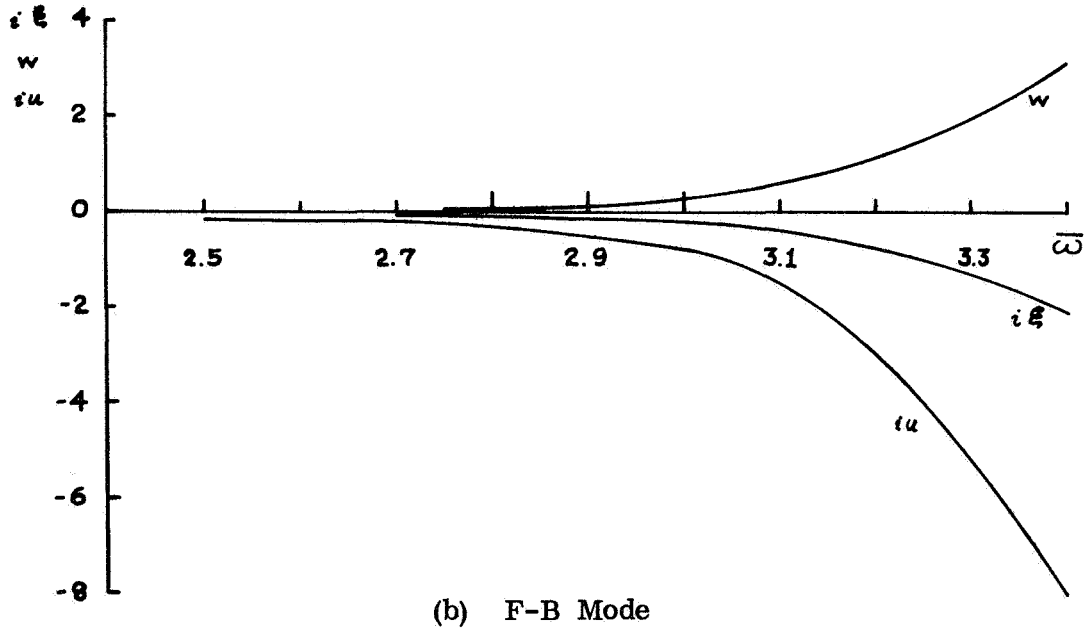

(b) F-B Mode

Fig. 4-16

Detail of Fig. 4-15
Mode Shapes for a/b = h/a = 0.02
Based on $\zeta \equiv 1$
No Rigid Wall

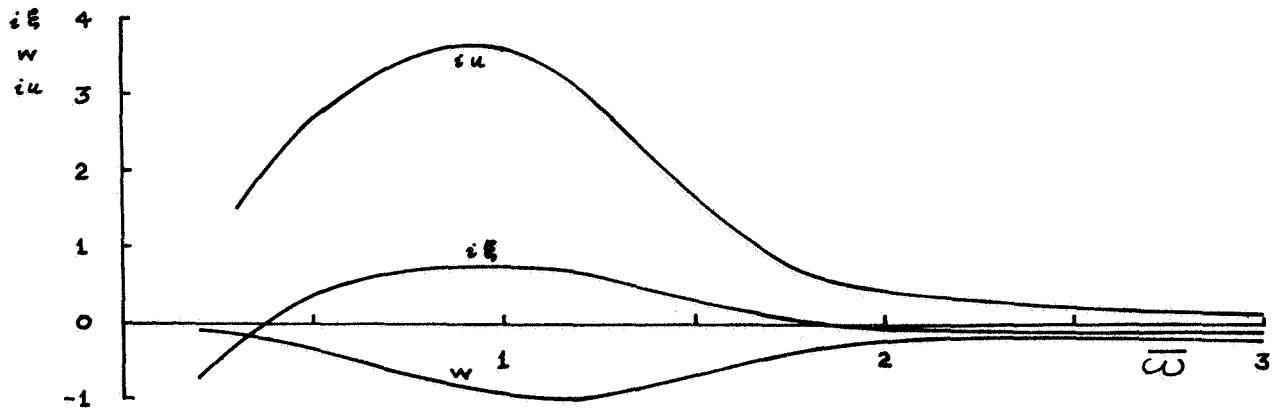

(a) B-F Mode

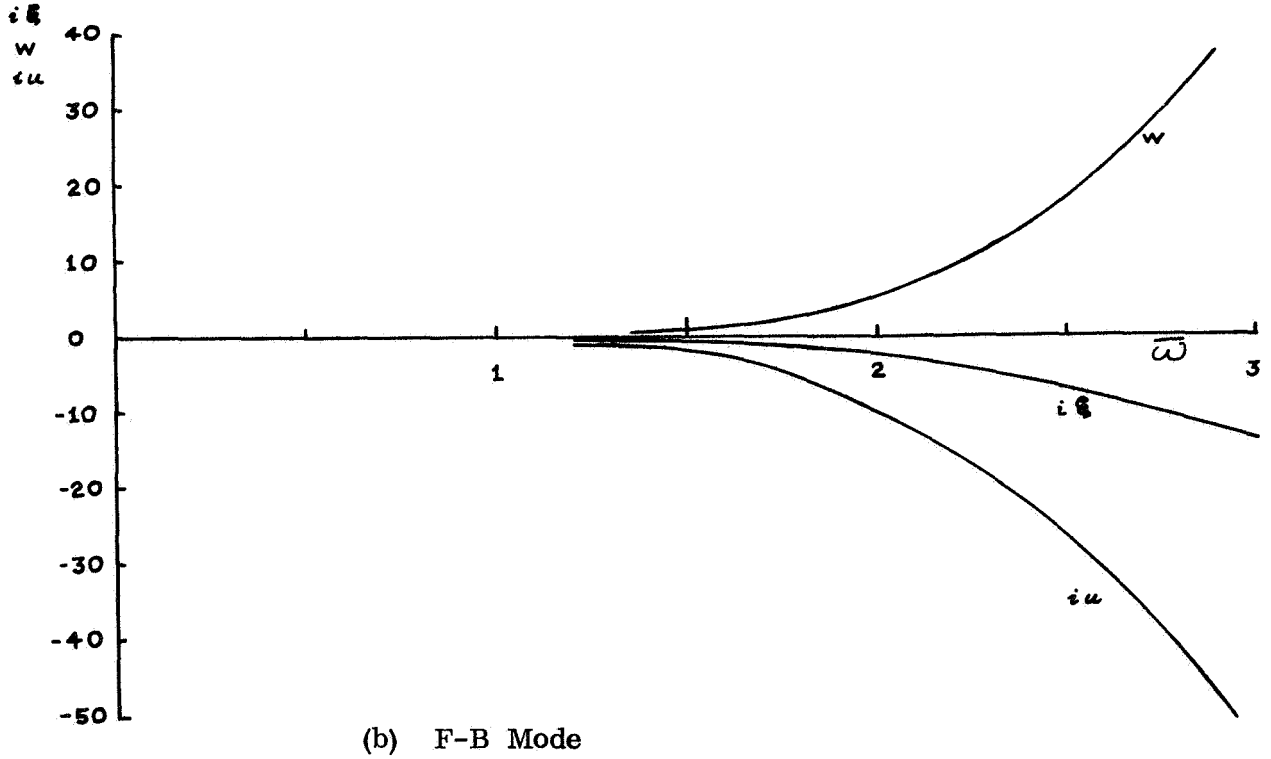

(b) F-B Mode

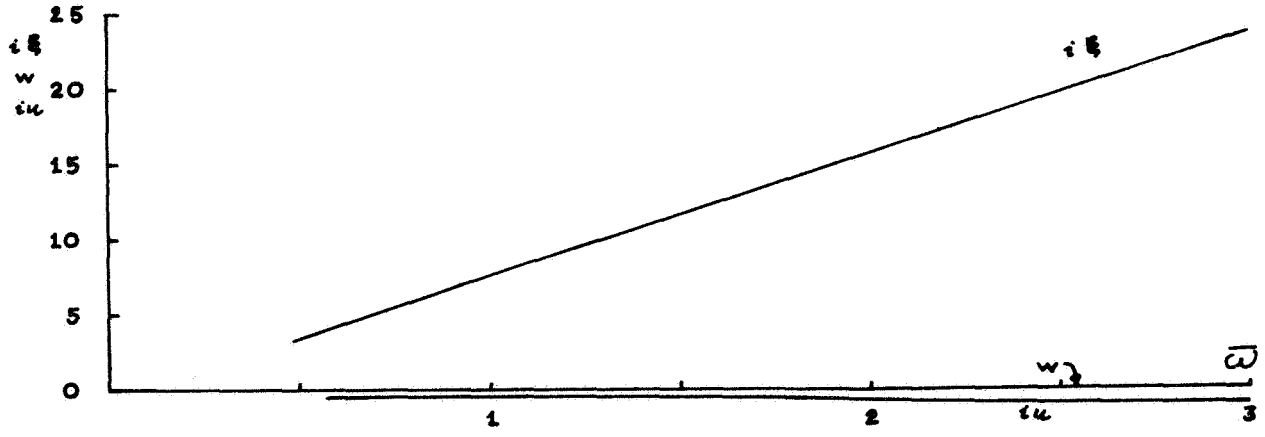

(c) E Mode

Fig. 4-17
Mode Shapes for a/b = 0.1, h/a = 0.1
Based on $\zeta \equiv 1$
No Rigid Wall

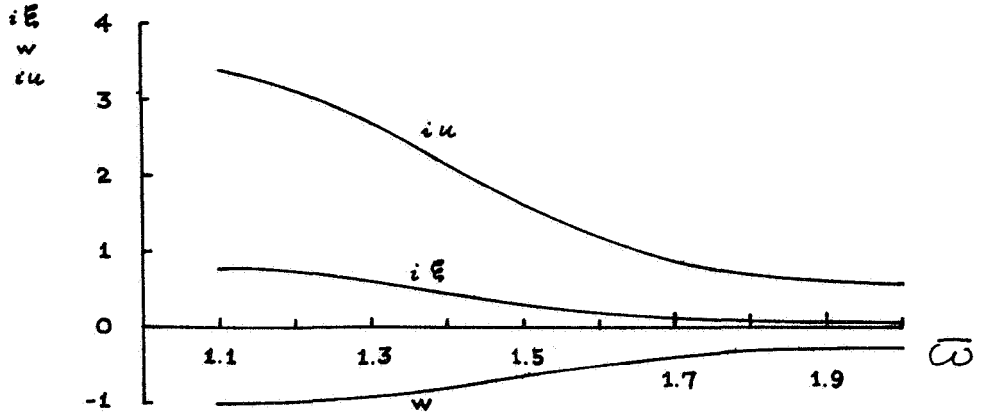

(a) B-F Mode

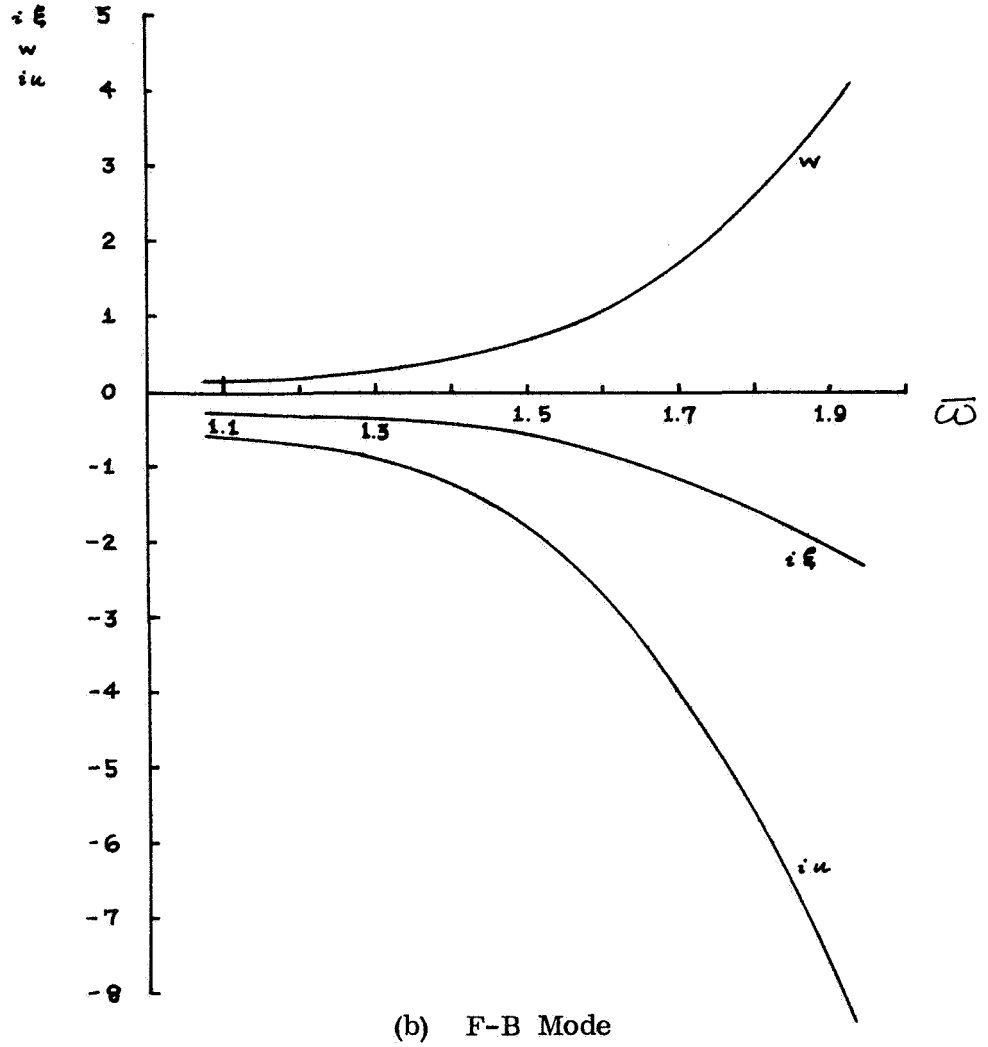

(b) F-B Mode

Fig. 4-18

Detail of Fig. 4-17
Mode Shapes for $a/b = h/a = 0.1$
Based on $\zeta \equiv 1$
No Rigid Wall

B. Toroidal Model of Membranous and Bony Canals

1. Derivation of Basic Equations

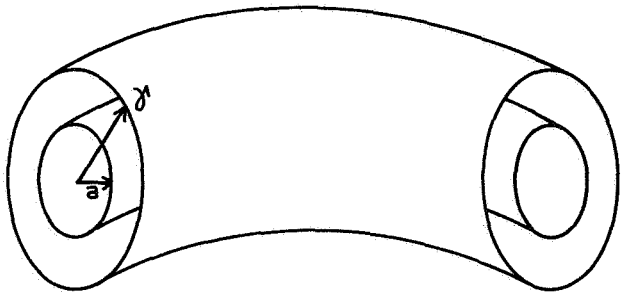

Fig. 4-19. Elastic Toroidal Shell Inside Rigid Wall

We next extend the derivation of section A to the case where the elastic shell is enclosed within a rigid wall of tube radius γ . The pressure, density, and displacement of the fluids are denoted by p, ρ , and u , with subscripts i for inside the shell and e for between the shell and the wall. Most of the equations from section A can be carried over; the changes are:

In the elastic equations (4-7) through (4-11) the pressure p must be replaced by the pressure difference $p_i - p_e$.

In the ζ force equation (4-17) p must be replaced by $p_i - p_e$, and the apparent mass term of Chapter III (D) must be included. The equation becomes

$$b(2\pi ah\rho_s + \pi a^2\rho_i)\frac{\partial^2\zeta}{\partial t^2} + b\pi a^2\rho_e\frac{\partial^2\zeta}{\partial t^2}\frac{\gamma^2+a^2}{\gamma^2-a^2}$$

$$= \frac{\partial Q}{\partial\theta} - 2\pi ah\sigma_2 + \pi a^2(p_i - p_e)$$

Two new equations are needed for the two new unknowns u_e and p_e. They are continuity and momentum equations for the outer fluid. The momentum equation is the same as for the interior fluid:

$$\frac{1}{b}\frac{\partial p_e}{\partial\theta} = -\rho_e\frac{\partial^2 u_e}{\partial t^2}$$

The continuity equation requires the inflow of fluid to be equal to the change in contained volume:

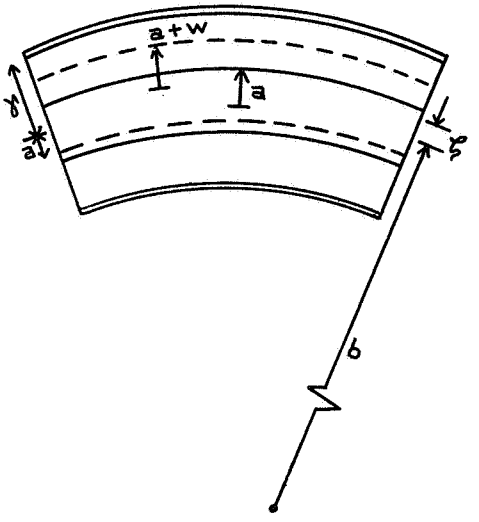

Fig. 4-20. Continuity Equation

$$\text{Fluid volume inflow} = -\pi\left[\gamma^2-(a+w)^2\right]\frac{\partial u_e}{\partial\theta}\,d\theta$$

$$\text{Original contained volume} = \pi\left(\gamma^2-a^2\right)b\,d\theta$$

$$\text{Final contained volume} = \pi\gamma^2 b\,d\theta-\pi(a+w)^2(b+\zeta)\,d\theta$$

$$\cong \pi\gamma^2 b\,d\theta-\pi(a^2b+2awb+a^2\zeta)\,d\theta$$

$$\Delta V = -\pi(2awb+a^2\zeta)\,d\theta$$

Continuity requires

$$2awb+a^2\zeta = (\gamma^2-a^2-2aw)\frac{\partial u_e}{\partial\theta} \cong (\gamma^2-a^2)\frac{\partial u_e}{\partial\theta}$$

or

$$\zeta + 2w\frac{b}{a} - \frac{\gamma^2-a^2}{a^2}\frac{\partial u_e}{\partial\theta} = 0$$

The equations to be considered are then

$$\zeta + \frac{2b}{a} w + \frac{\partial u_i}{\partial \theta} = 0 \tag{4-32}$$

$$\zeta + \frac{2b}{a} w - \frac{\gamma^2 - a^2}{a^2} \frac{\partial u_e}{\partial \theta} = 0 \tag{4-33}$$

$$b \rho_i \frac{\partial^2 u_i}{\partial t^2} = - \frac{\partial p_i}{\partial \theta} \tag{4-34}$$

$$b \rho_e \frac{\partial^2 u_e}{\partial t^2} = - \frac{\partial p_e}{\partial \theta} \tag{4-35}$$

$$b \left(2\pi a h \rho_s + \pi a^2 \rho_i + \pi a^2 \rho_e \frac{\gamma^2 + a^2}{\gamma^2 - a^2} \right) \frac{\partial^2 \zeta}{\partial t^2} = \frac{\partial Q}{\partial \theta} - 2\pi a h \sigma_2 + \pi a^2 (p_i - p_e) \tag{4-36}$$

$$2\pi a h \rho_s b \frac{\partial^2 \xi}{\partial t^2} = 2\pi a h \frac{\partial \sigma_2}{\partial \theta} + Q \tag{4-37}$$

$$p_i - p_e = \frac{h}{a} \frac{E}{1 - \nu^2} \left[\frac{w}{a} + \frac{\nu}{b} \left(\zeta + \frac{\partial \xi}{\partial \theta} \right) \right] \tag{4-38}$$

$$\sigma_2 = \frac{E}{1 - \nu^2} \left(\frac{\zeta}{b} + \frac{1}{b} \frac{\partial \xi}{\partial \theta} + \nu \frac{w}{a} \right) \tag{4-39}$$

$$Q = - \frac{E \pi a^3 h}{b^3} \left(\frac{\partial^3 \zeta}{\partial \theta^3} + \frac{\partial \zeta}{\partial \theta} \right) \tag{4-40}$$

Combining (4-34) and (4-35), and differentiating and substituting (4-38),

$$b \left[\rho_i \frac{\partial^2 u_i}{\partial t^2} - \rho_e \frac{\partial^2 u_e}{\partial t^2} \right] = - \frac{h}{a} \frac{E}{1 - \nu^2} \left[\frac{1}{a} \frac{\partial w}{\partial \theta} + \frac{\nu}{b} \left(\frac{\partial \zeta}{\partial \theta} + \frac{\partial^2 \xi}{\partial \theta^2} \right) \right]$$

Substituting (4-38), (4-39), and (4-40) into (4-36),

$$b \left[2\pi a h \rho_s + \pi a^2 \rho_i + \pi a^2 \rho_e \frac{\gamma^2 + a^2}{\gamma^2 - a^2} \right] \frac{\partial^2 \zeta}{\partial t^2} = - \frac{E \pi a^3 h}{b^3} \left(\frac{\partial^4 \zeta}{\partial \theta^4} + \frac{\partial^2 \zeta}{\partial \theta^2} \right)$$

$$- 2\pi a h \frac{E}{1 - \nu^2} \left(\frac{\zeta}{b} + \frac{1}{b} \frac{\partial \xi}{\partial \theta} + \frac{\nu w}{a} \right) + \frac{\pi a h E}{1 - \nu^2} \left[\frac{w}{a} + \frac{\nu}{b} \left(\zeta + \frac{\partial \xi}{\partial \theta} \right) \right]$$

Substituting (4-39) and (4-40) into (4-37),

$$2\pi ah\rho_s b\frac{\partial^2\xi}{\partial t^2} = 2\pi ah\frac{E}{1-\nu^2}\left(\frac{1}{b}\frac{\partial\zeta}{\partial\theta}+\frac{1}{b}\frac{\partial^2\xi}{\partial\theta^2}+\frac{\nu}{a}\frac{\partial w}{\partial\theta}\right)-\frac{E\pi a^3h}{b^3}\left(\frac{\partial^3\zeta}{\partial\theta^3}+\frac{\partial\zeta}{\partial\theta}\right)$$

The exponential form $x = x_0 \exp(i(L/\lambda)\theta - i\omega t)$ is substituted into the five remaining equations, yielding

$$i\frac{L}{\lambda}u_i + \zeta + \frac{2b}{a}w = 0$$

$$-i\frac{L}{\lambda}\frac{\gamma^2-a^2}{a^2}u_e + \zeta + \frac{2b}{a}w = 0$$

$$-b\omega^2\rho_i u_i + b\omega^2\rho_e u_e + \frac{h}{a}\frac{E}{1-\nu^2}\frac{\nu}{b}\frac{iL}{\lambda}\zeta - \frac{h}{a}\frac{E}{1-\nu^2}\frac{\nu}{b}\left(\frac{L}{\lambda}\right)^2\xi + \frac{h}{a}\frac{E}{1-\nu^2}\frac{1}{a}\frac{iL}{\lambda}w = 0$$

$$\left\{-b\left[2\pi ah\rho_s + \pi a^2\rho_i + \pi a^2\rho_e\frac{\gamma^2+a^2}{\gamma^2-a^2}\right]\omega^2 + \frac{E\pi a^3h}{b^3}\left[\left(\frac{L}{\lambda}\right)^4-\left(\frac{L}{\lambda}\right)^2\right]+\frac{\pi ahE}{1-\nu^2}\frac{2-\nu}{b}\right\}\zeta$$

$$+\pi ah\frac{E}{1-\nu^2}\frac{iL}{\lambda}\frac{1}{b}(2-\nu)\xi + \frac{\pi ahE}{1-\nu^2}\frac{1}{a}(2\nu-1)w = 0$$

$$\left[\frac{E\pi a^3h}{b^3}\left(-i\left(\frac{L}{\lambda}\right)^3+i\frac{L}{\lambda}\right)-2\pi ah\frac{E}{1-\nu^2}\frac{1}{b}\frac{iL}{\lambda}\right]\zeta$$

$$+\left(-2\pi ah\rho_s b\omega^2+2\pi ah\frac{E}{1-\nu^2}\left(\frac{L}{\lambda}\right)^2\frac{1}{b}\right)\xi - 2\pi ah\frac{E}{1-\nu^2}\frac{iL}{\lambda}\frac{\nu}{a}w = 0$$

The parameters $c_p^2 = \frac{E}{\rho_s(1-\nu^2)}$, $\bar{\omega} = b\omega/c_p$, $\bar{\rho} = \rho_i/\rho_s$, and $f = \rho_e/\rho_i$ are substituted.

$$i\frac{L}{\lambda}u_i + \zeta + \frac{2}{a/b}w = 0$$

$$-i\frac{L}{\lambda}\frac{\gamma^2-a^2}{a^2}u_e + \zeta + \frac{2}{a/b}w = 0$$

$$-\bar{\omega}^2\bar{\rho}u_i + \bar{\omega}^2\bar{\rho}f u_e + \frac{h}{a}\frac{iL}{\lambda}\nu\zeta - \frac{h}{a}\left(\frac{L}{\lambda}\right)^2\nu\xi + \frac{h/a}{a/b}\frac{iL}{\lambda}w = 0$$

$$\left\{-\varpi^2\left[2\frac{h}{a}+\bar{\rho}+\bar{\rho}f\frac{\gamma^2+a^2}{\gamma^2-a^2}\right]+(1-\nu^2)\left(\frac{a}{b}\right)^2\left(\frac{h}{a}\right)\left[\left(\frac{L}{\lambda}\right)^4-\left(\frac{L}{\lambda}\right)^2\right]+\frac{h}{a}(2-\nu)\right\}\zeta$$

$$+\frac{h}{a}(2-\nu)\frac{iL}{\lambda}\xi+\frac{h/a}{a/b}(2\nu-1)w=0$$

$$\left[(1-\nu^2)\left(\frac{a}{b}\right)^2\frac{h}{a}\left(-i\left(\frac{L}{\lambda}\right)^3+i\frac{L}{\lambda}\right)-\frac{2h}{a}i\frac{L}{\lambda}\right]\zeta$$

$$+\left[-2\frac{h}{a}\varpi^2+\frac{2h}{a}\left(\frac{L}{\lambda}\right)^2\right]\xi-\frac{2h/a}{a/b}i\frac{L}{\lambda}\nu w=0$$

u_i and u_e are removed by substituting the first two equations into the last three:

$$\left[-\frac{h}{a}\left(\frac{L}{\lambda}\right)^2\nu+\varpi^2\bar{\rho}\left(1+\frac{fa^2}{\gamma^2-a^2}\right)\right]\zeta-i\frac{h}{a}\left(\frac{L}{\lambda}\right)^3\nu\xi$$

$$+\left[-\frac{h/a}{a/b}\left(\frac{L}{\lambda}\right)^2+\frac{2}{a/b}\varpi^2\bar{\rho}\left(1+\frac{fa^2}{\gamma^2-a^2}\right)\right]w=0 \qquad (4\text{-}41)$$

$$\left\{-\varpi^2\left[2\frac{h}{a}+\bar{\rho}\left(1+f\frac{\gamma^2+a^2}{\gamma^2-a^2}\right)\right]+(1-\nu^2)\left(\frac{a}{b}\right)^2\left(\frac{h}{a}\right)\left[\left(\frac{L}{\lambda}\right)^4-\left(\frac{L}{\lambda}\right)^2\right]+\frac{h}{a}(2-\nu)\right\}\zeta$$

$$+\frac{h}{a}(2-\nu)i\frac{L}{\lambda}\xi+\frac{h/a}{a/b}(2\nu-1)w=0 \qquad (4\text{-}42)$$

$$\left\{i(1-\nu^2)\left(\frac{a}{b}\right)^2\frac{h}{a}\left[-\left(\frac{L}{\lambda}\right)^3+\frac{L}{\lambda}\right]-i\frac{2h}{a}\frac{L}{\lambda}\right\}\zeta+\left[\left(\frac{L}{\lambda}\right)^2-\varpi^2\right]\frac{2h}{a}\xi$$

$$-\frac{2h/a}{a/b}i\frac{L}{\lambda}\nu w=0 \qquad (4\text{-}43)$$

To obtain specific results, we consider the case $\nu = 1/2$, $\overline{\rho} = f = 1$. (Note $1 + \frac{a^2}{\gamma^2 - a^2} = \frac{\gamma^2}{\gamma^2 - a^2}$.) Rewriting in matrix form,

$$\begin{bmatrix} -\frac{h}{2a}\left(\frac{L}{\lambda}\right)^2 + \varpi^2\left(\frac{\gamma^2}{\gamma^2 - a^2}\right) & -i\frac{h}{2a}\left(\frac{L}{\lambda}\right)^3 & -\frac{h/a}{a/b}\left(\frac{L}{\lambda}\right)^2 + \frac{2}{a/b}\varpi^2\frac{\gamma^2}{\gamma^2 - a^2} \\ -\varpi^2\left[2\frac{h}{a} + \frac{2\gamma^2}{\gamma^2 - a^2}\right] + \frac{3}{2}\frac{h}{a} & \frac{3}{2}\frac{h}{a} i\frac{L}{\lambda} & 0 \\ +\frac{3}{4}\left(\frac{a}{b}\right)^2\left(\frac{h}{a}\right)\left(\frac{L}{\lambda}\right)^2\left[\left(\frac{L}{\lambda}\right)^2 - 1\right] & & \\ \frac{3}{4}\left(\frac{a}{b}\right)^2\frac{h}{a}\frac{L}{\lambda}\left[\left(\frac{L}{\lambda}\right)^2 - 1\right] + \frac{2h}{a}\frac{L}{\lambda} & i\frac{2h}{a}\left[\left(\frac{L}{\lambda}\right)^2 - \varpi^2\right] & \frac{h/a}{a/b} \end{bmatrix} \begin{bmatrix} \zeta \\ \xi \\ w \end{bmatrix} = 0 \qquad (4\text{-}44)$$

The frequency equation is obtained by setting the determinant of the coefficients equal to zero. After some manipulation,

$$\begin{vmatrix} -\varpi^2\left[2 + \frac{2a}{h}\frac{\gamma^2}{\gamma^2 - a^2}\right] + \frac{3}{2} & & \\ +\frac{3}{4}\left(\frac{a}{b}\right)^2\left(\frac{L}{\lambda}\right)^2\left[\left(\frac{L}{\lambda}\right)^2 - 1\right] & \frac{3}{2}\frac{L}{\lambda} & 0 \\ \frac{3}{4}\left(\frac{a}{b}\right)^2\frac{L}{\lambda}\left[\left(\frac{L}{\lambda}\right)^2 - 1\right] + \frac{3}{2}\frac{L}{\lambda} & 2\left(\frac{L}{\lambda}\right)^2 - 2\varpi^2 & \frac{L}{\lambda} \\ 0 & -\frac{1}{2}\left(\frac{L}{\lambda}\right)^3 & \frac{2a}{h}\varpi^2\frac{\gamma^2}{\gamma^2 - a^2} - \left(\frac{L}{\lambda}\right)^2 \end{vmatrix} = 0 \qquad (4\text{-}45)$$

This equation, as before, is solved numerically. Values of L/λ are assumed and the solutions $\bar{\omega}^2$ are found. $\bar{c} = \bar{\omega} / (L/\lambda)$ is computed.

Again, there are generally three solutions $\bar{c}$ for each L/λ or $\bar{\omega}$. Thus there are three linearly independent modes of motion.

A cutoff frequency exists in this case also; this time it is at

$$\bar{\omega}^2 = \frac{3/2}{2 + \frac{2a}{h}\frac{\gamma^2}{\gamma^2 - a^2}}$$

Mode shapes are calculated as previously:

$$\begin{bmatrix} i\xi \\ w \end{bmatrix} =$$

$$\begin{bmatrix} \frac{2}{3}\frac{a}{h}\frac{\lambda}{L} & 0 \\ -\frac{4}{3}\frac{\left[\left(\frac{L}{\lambda}\right)^2 - \bar{\omega}^2\right]}{\left(\frac{L}{\lambda}\right)^2}\frac{a}{h}\frac{a}{b} & \frac{a}{b}\frac{a}{h}\frac{\lambda}{L} \end{bmatrix} \begin{bmatrix} 2\bar{\omega}^2\left(\frac{h}{a} + \frac{\gamma^2}{\gamma^2 - a^2}\right) - \frac{3}{4}\left(\frac{a}{b}\right)^2\frac{h}{a}\left(\frac{L}{\lambda}\right)^2\left[\left(\frac{L}{\lambda}\right)^2 - 1\right] - \frac{3h}{2a} \\ -\frac{3}{4}\left(\frac{a}{b}\right)^2\frac{h}{a}\left(\frac{L}{\lambda}\right)\left[1 - \left(\frac{L}{\lambda}\right)^2\right] + 2\frac{h}{a}\frac{L}{\lambda} \end{bmatrix} \zeta$$

and, from the original equations,

$$iu_i = -\frac{\zeta + \frac{2}{a/b}w}{L/\lambda}$$

$$iu_e = -\frac{iu_i a^2}{\gamma^2 - a^2}$$

Note that the expressions for mode shapes again remain finite as long as λ is finite.

2. Dispersion Curves and Mode Shapes

The parameter γ/a enters the equations for the case described in section B1. Its effects on wave speed are seen to be small for moderate γ/a. The speed of the breathing wave is lowered slightly (but is drastically lowered

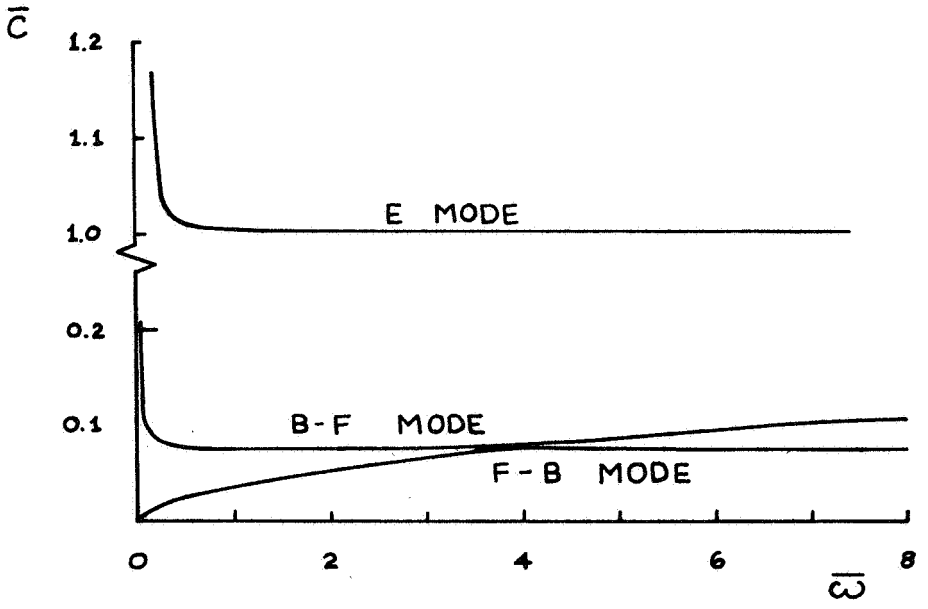

Fig. 4-21

Dispersion Curve for
$a/b = 0.02$, $h/a = 0.02$, $\gamma/a = 2$

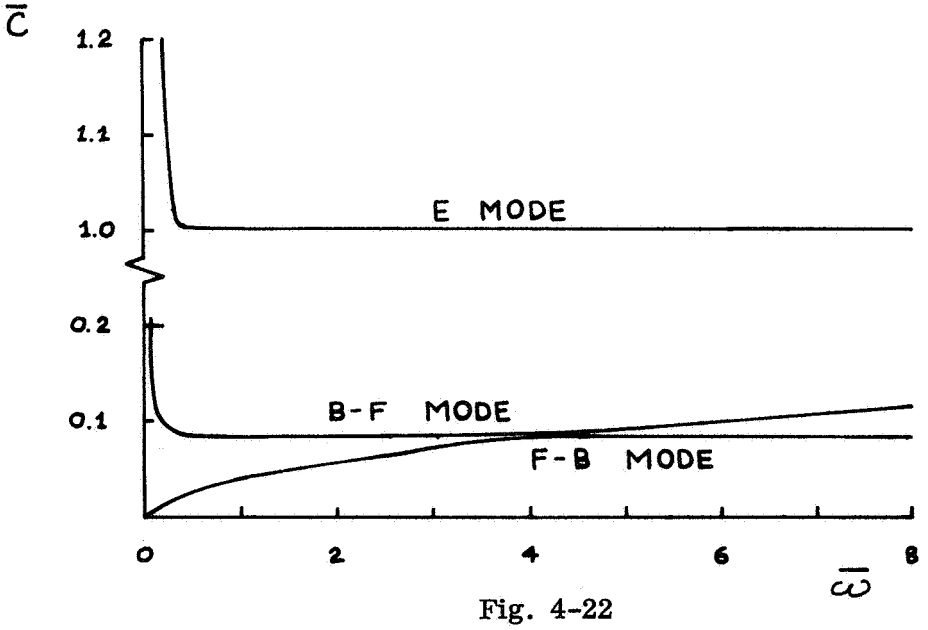

Fig. 4-22

Dispersion Curve for
$a/b = 0.02$, $h/a = 0.02$, $\gamma/a = 5$

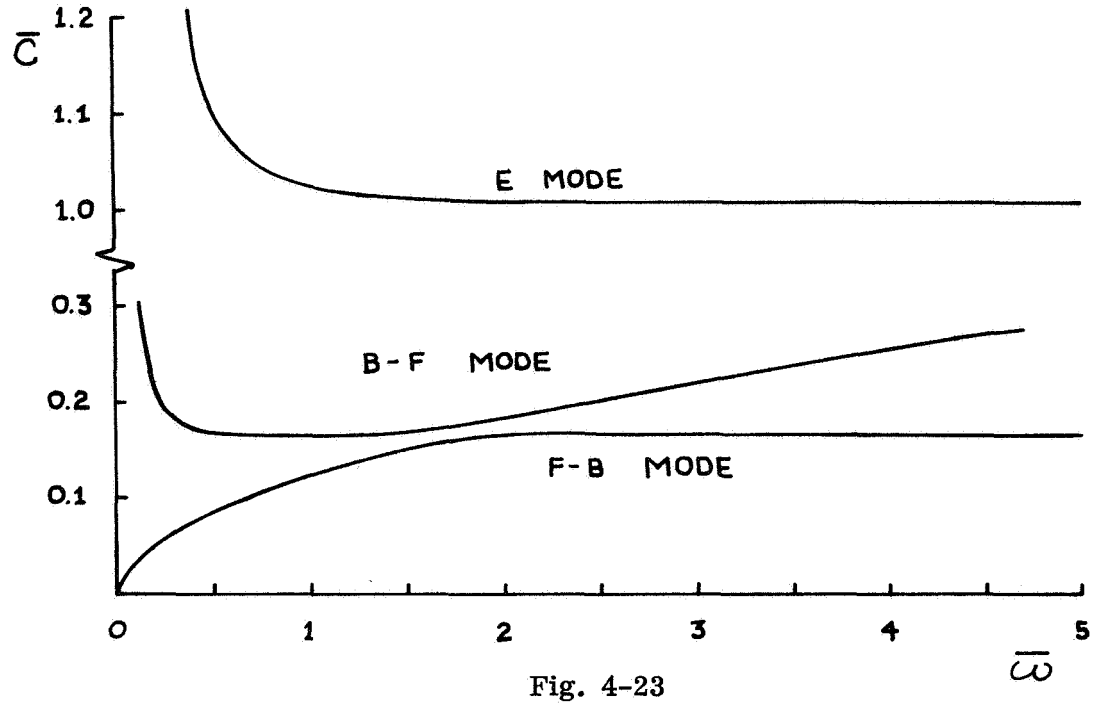

Fig. 4-23

Dispersion Curve for
$a/b = 0.1$, $h/a = 0.1$, $\gamma/a = 2$

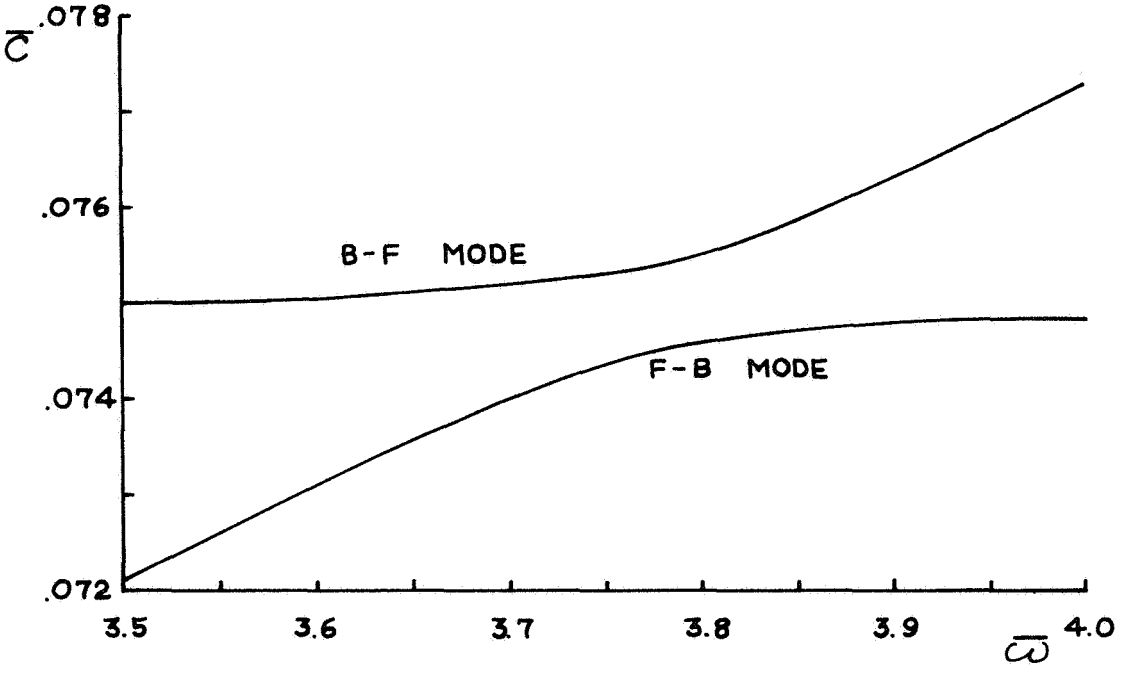

Fig. 4-24

Detail of Fig. 4-21
Near Saddle Point

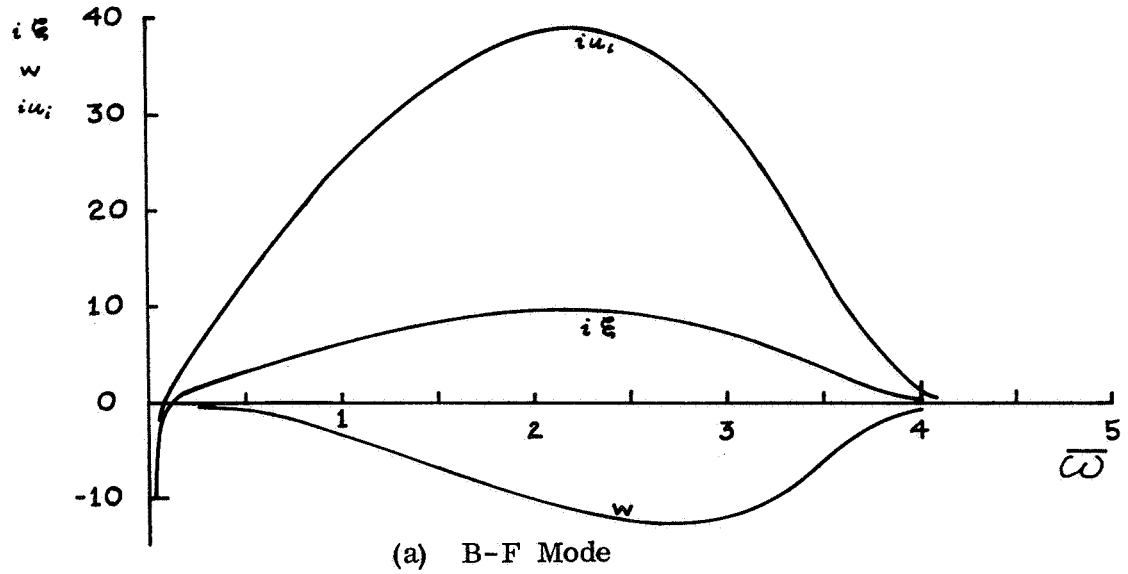

(a) B-F Mode

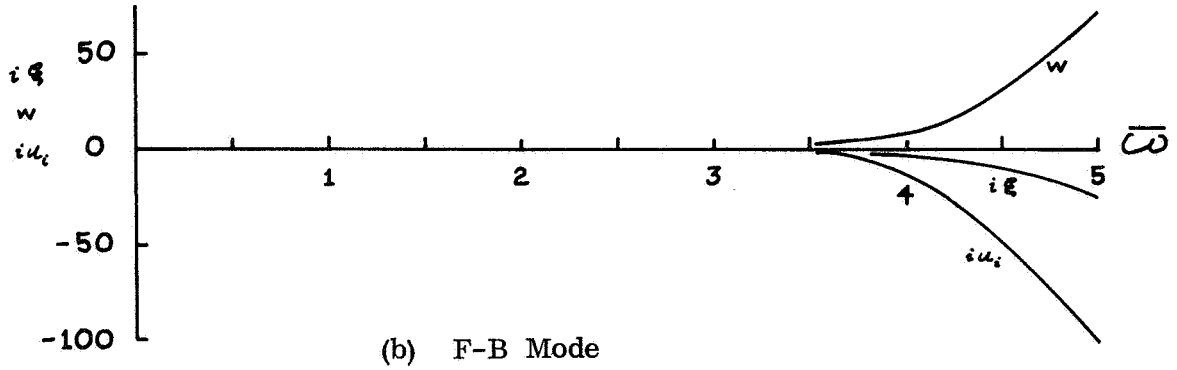

(b) F-B Mode

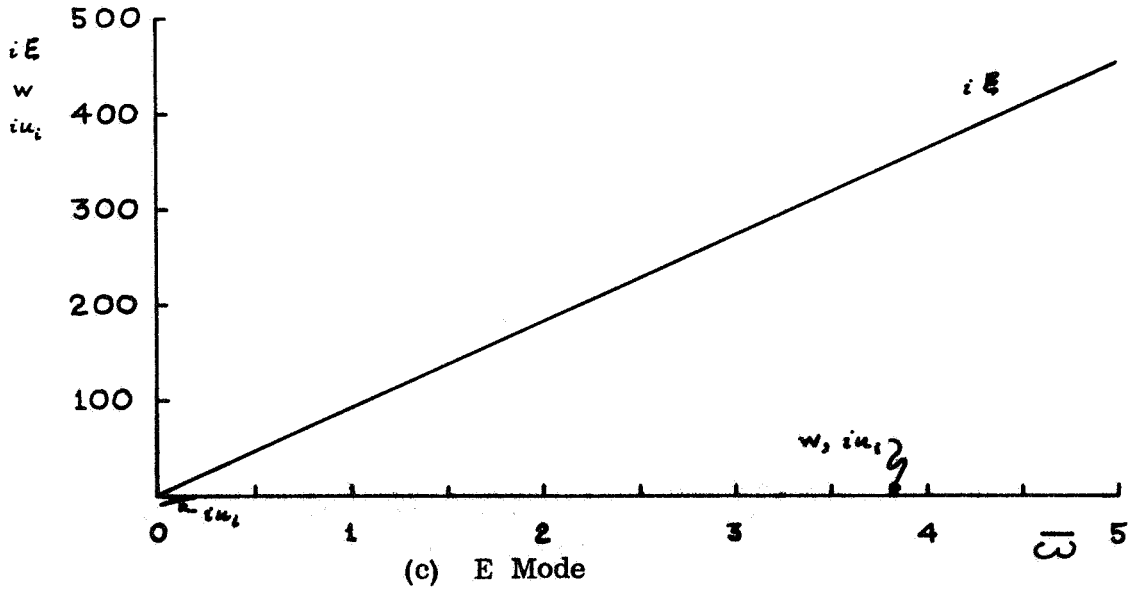

(c) E Mode

Fig. 4-25. Mode Shapes for a/b = 0.02, h/a = 0.02, γ/a = 2
$iu_e = (-1/3)\ iu_i$

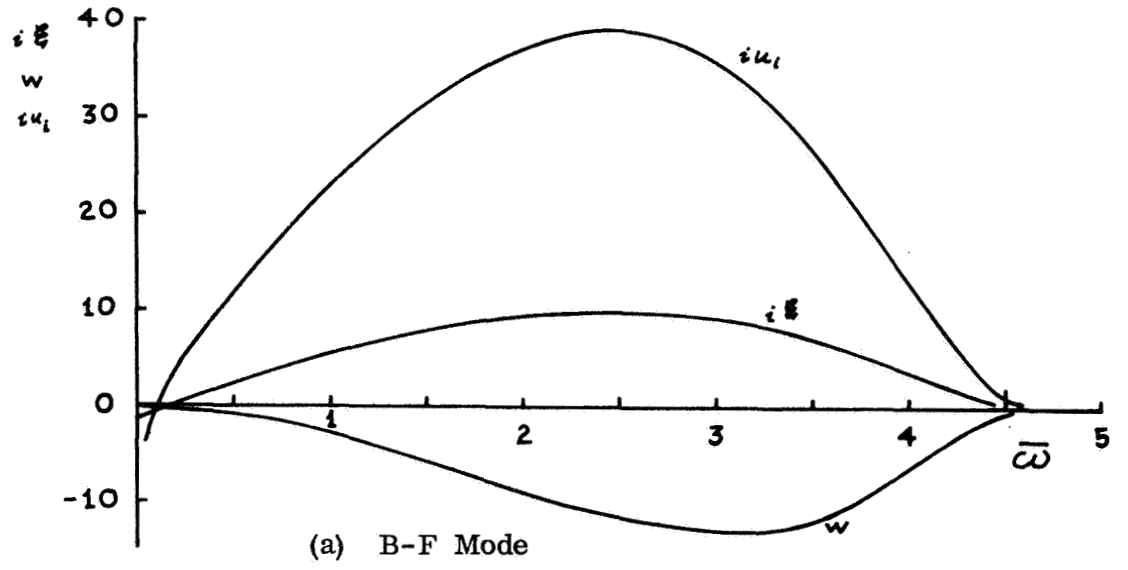

(a) B-F Mode

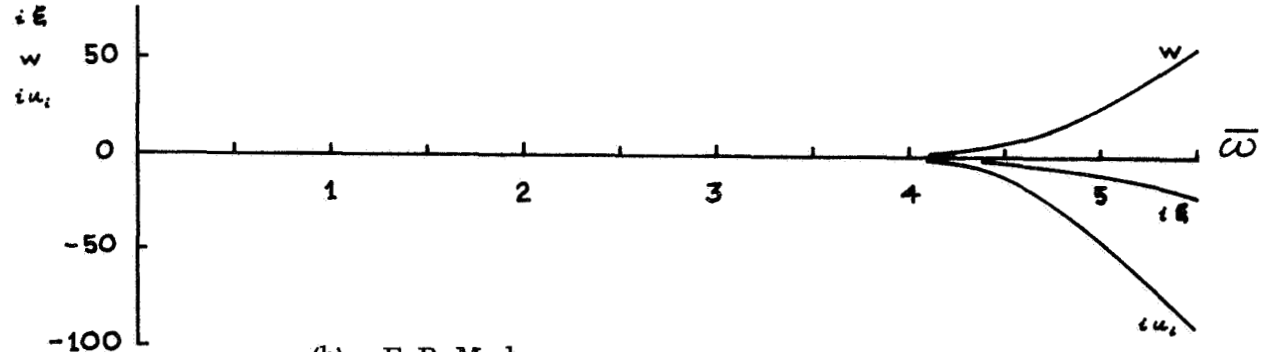

(b) F-B Mode

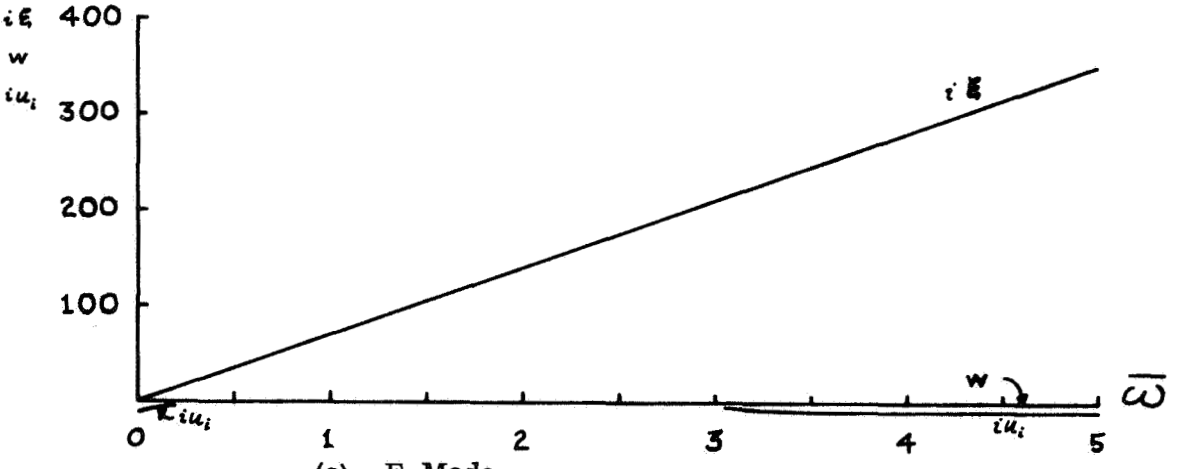

(c) E Mode

Fig. 4-26. Mode Shapes for a/b = 0.02, h/a = 0.02, γ/a = 5
$iu_e = (-1/24)\, iu_i$

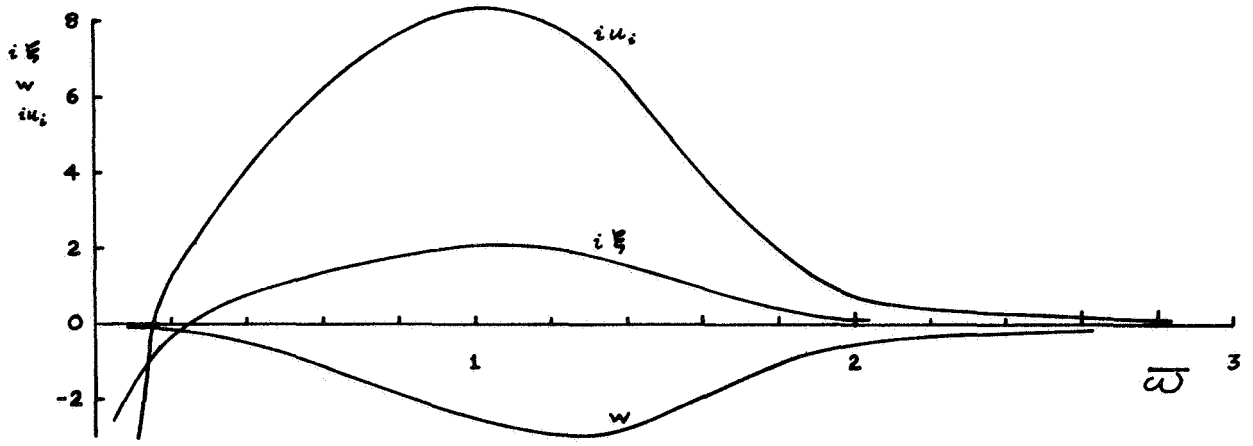

(a) B-F Mode

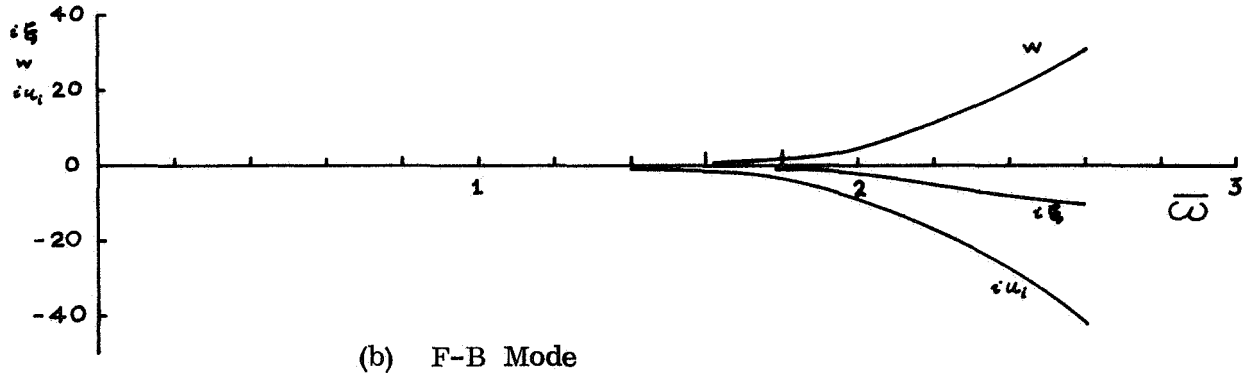

(b) F-B Mode

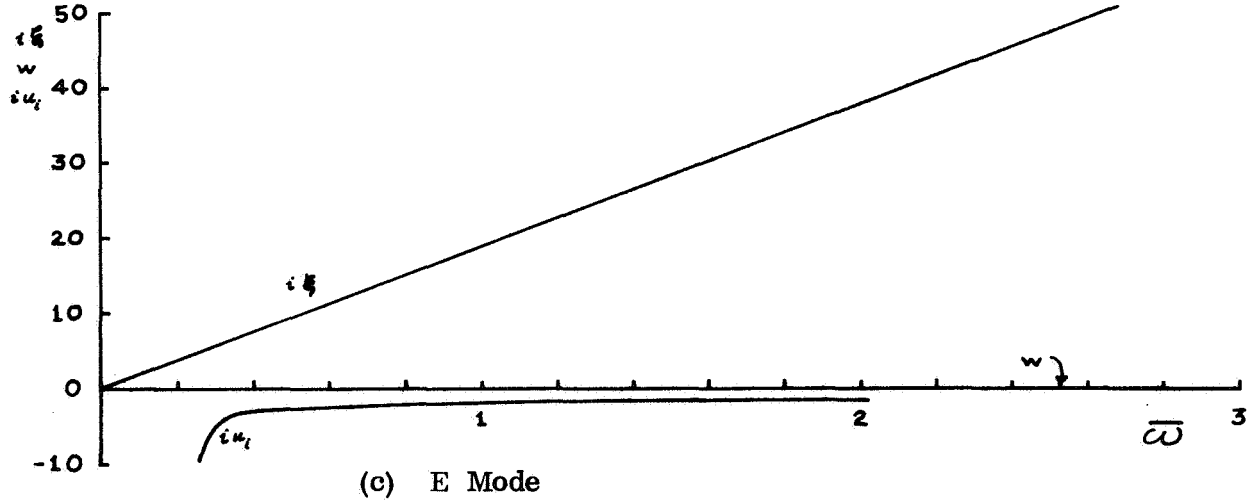

(c) E Mode

Fig. 4-27. Mode Shapes for a/b = 0.1, h/a = 0.1, γ/a = 2
$iu_e = (-1/3)\ iu_i$

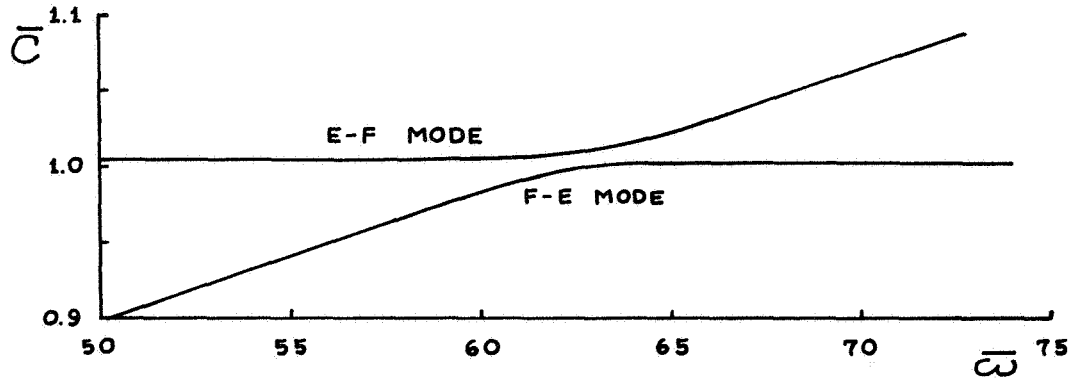

Fig. 4-28. Dispersion Curve for a/b = 0.1, h/a = 0.1, γ/a = 2
Very High Frequencies

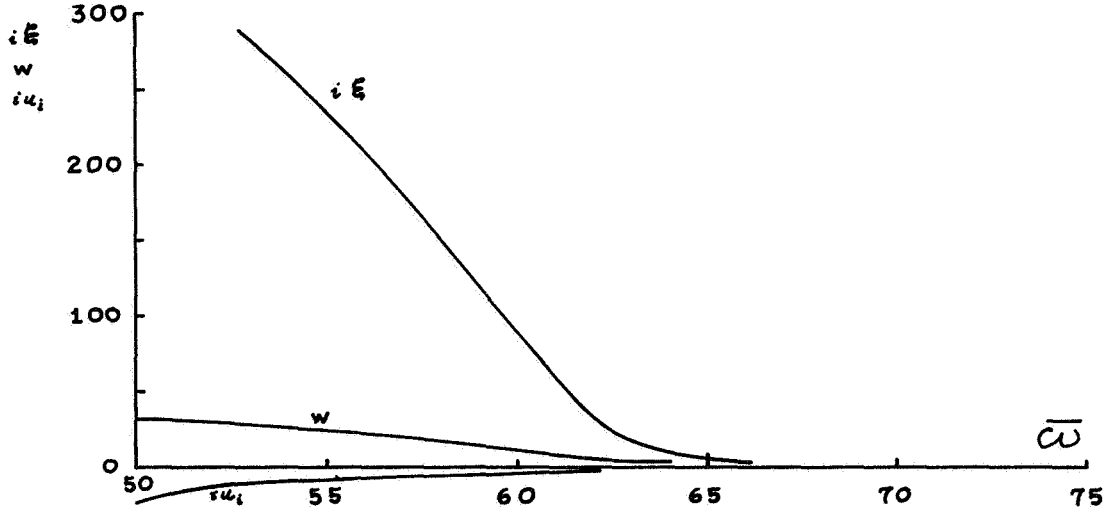

(a) E-F Mode

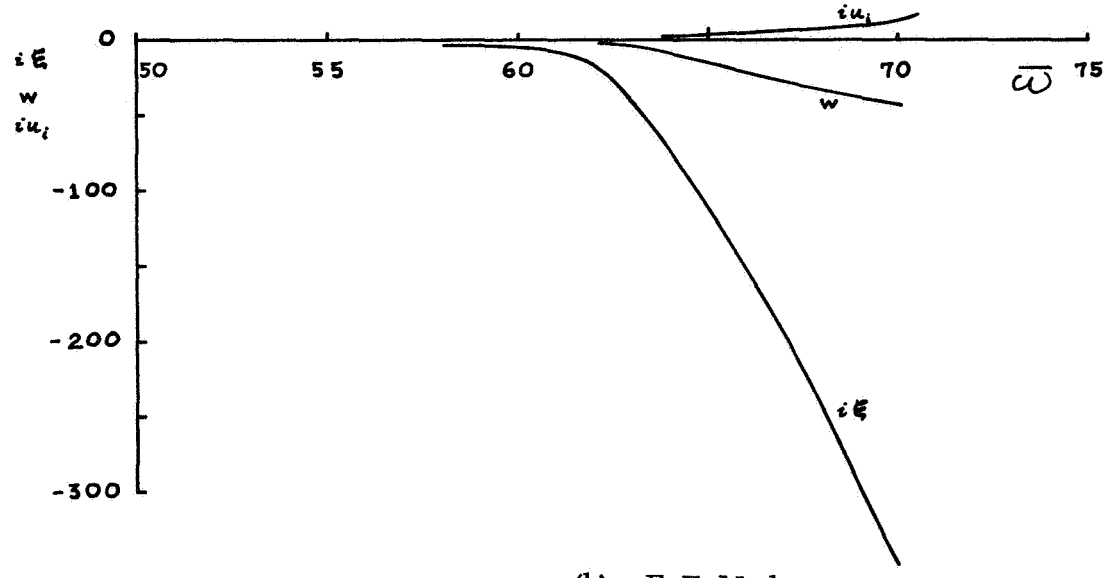

(b) F-E Mode

Fig. 4-29. Mode Shapes for a/b = 0.1, h/a = 0.1, γ/a = 2
Very High Frequencies
$iu_e = (-1/3)\, iu_i$

for $\gamma/a \longrightarrow 1$); the speed of the flexure wave is lowered somewhat more, thus having the effect of moving the saddle point to a higher frequency. The extensional wave speed does not appear to change significantly (Figs. 4-21 to 4-24).

The mode shape curves also retain their general behavior, but small changes in slopes, peak values, and peak frequencies can be observed. It might be noted that, in the breathing part of the F-B mode, while $i\xi$, w, and iu_i all increase rapidly, the ratios $w/i\xi$ and especially $iu_i/i\xi$ remain nearly constant (Figs. 4-25 to 4-27).

This indicates that the high-frequency breathing motion is characterized by nearly-constant amplitudes of ξ, w, and u_i, but rapidly decreasing ζ.

The dispersion curves and mode shapes were run out to very high frequencies to determine whether the speed of the flexural mode continued to increase, and, if so, whether it intersected the extensional mode. It was found (Fig. 4-28) that the flexural and extensional modes "intersect" in exactly the same way as the breathing and flexure modes do at lower frequency: there is no crossover, but there is a saddle point, and near it the mode shapes along the dispersion curves change very rapidly. If we trace the three dispersion curves, one is flexural at low frequencies and breathing elsewhere; the second is breathing at low, flexural at intermediate, and extensional at high frequencies; the third is extensional at low and intermediate, and flexural at high frequencies.

As frequency increases toward the "intersection" of the extensional and flexural modes, the magnitude of ξ in the extensional mode drops off from its straight line increase and reaches the very low value of a breathing mode. The flexural mode includes a rapid increase in the other variables with respect to ζ, notably a tremendous increase in ξ. There are reversals of sign with respect to ζ in the two modes, just as at the lower frequency "intersection" (Fig. 4-29).

3. Free Vibration of the Simple Closed Toroid

The dispersion curves and mode shapes have been considered, up to now, as continuous spectra, valid for all frequencies. While this is the proper interpretation for the general case of a torus of indeterminate or infinite length, the special case of the simple closed torus should be considered.

This situation imposes the condition that all properties must be periodic in θ with a period of 2π. We must then restrict the wavelengths of all motions to be integral fractions of $L \equiv 2\pi b$. That is, we now have a discrete spectrum

of wavelengths

$$\lambda_1 = L$$

$$\lambda_2 = L/2$$

$$\lambda_3 = L/3$$

etc. For each mode, we then have a corresponding sequence of permissible frequencies:

Mode I $\quad \omega_1^{(1)}, \ \omega_2^{(1)}, \ \omega_3^{(1)}, \ \ldots$

Mode II $\quad \omega_1^{(2)}, \ \omega_2^{(2)}, \ \omega_3^{(2)}, \ \ldots$

Mode III $\quad \omega_1^{(3)}, \ \omega_2^{(3)}, \ \omega_3^{(3)}, \ \ldots$

where the superscript represents the mode number and the subscript equals the subscript on the corresponding wavelength.

In the scheme of computation used here, λ is the independent value in the numerical solution, and the required frequencies and mode shapes are determined simply by using $\lambda_n = L/n$ as inputs. If the curves were generated by other methods, we note that constant values of λ correspond to straight lines through the origin on the dispersion curves:

$$\bar{c} = \frac{\bar{\omega}}{L/\lambda}$$

so

$$\lambda = \text{const} \implies \bar{c} = \frac{\text{const}}{L} \cdot \bar{\omega}$$

The constant corresponding to the desired λ_n is inserted and the line is drawn. The intersection of this line with the j^{th} mode's dispersion curve occurs at $\bar{\omega}_n^{(j)}$. From the mode shape curve for the j^{th} mode at this frequency, the quantities $i\bar{\xi}_n^{(j)}$, $w_n^{(j)}$, and $iu_n^{(j)}$ are read.

We then apply the theorems of Fourier series to the system to find the coefficients associated with each wavelength λ_n.

The notation $x = x_0 e^{i(L\theta/\lambda - \omega t)}$ used in Chapters III and IV is

an abbreviation for one term of the full series

$$x = \frac{1}{2}\sum_{j=1}^{\infty}\left[a_j e^{i(L\theta/\lambda_j - \omega_j t)} + \hat{a}_j e^{-i(L\theta/\lambda_j - \omega_j t)}\right.$$

$$\left. + b_j e^{i(L\theta/\lambda_j + \omega_j t)} + \hat{b}_j e^{-i(L\theta/\lambda_j + \omega_j t)}\right]$$

where $\hat{a}_j$ is the complex conjugate of a_j. The form is equivalent to the classical solution of the wave equation

$$x = \sum_{j=1}^{\infty}\left[\bar{a}_j \cos(j\theta - \omega_j t) + \bar{b}_j \sin(j\theta - \omega_j t)\right.$$

$$\left. + \bar{c}_j \cos(j\theta + \omega_j t) + \bar{d}_j \sin(j\theta + \omega_j t)\right]$$

since $L/\lambda_j = L/(L/j) = j$. The notation can be made more compact:

$$x = \frac{1}{2}\sum_{j=-\infty}^{\infty}\left[\alpha_j e^{i(j\theta - \omega_j t)} + \beta_j e^{i(j\theta + \omega_j t)}\right]$$

where $\omega_j = -\omega_{-j}$ and

$$\alpha_j = \begin{cases} \bar{a}_j - i\bar{b}_j, & j > 0 \\ \bar{a}_j + i\bar{b}_j, & j < 0 \\ 0, & j = 0 \end{cases} \quad ; \quad \beta_j = \begin{cases} \bar{c}_j - i\bar{d}_j, & j > 0 \\ \bar{c}_j + i\bar{d}_j, & j < 0 \\ 0, & j = 0 \end{cases}$$

Using this form, we express the variables ζ, ξ, w, and u as

$$\zeta(\theta,t) = \frac{1}{2}\sum_{j=-\infty}^{\infty}\sum_{k=1}^{3}\left[a_{jk} e^{i(j\theta - \omega_j^{(k)} t)} + b_{jk} e^{i(j\theta + \omega_j^{(k)} t)}\right]$$

$$i\xi(\theta,t) = \frac{1}{2}\sum_{j=-\infty}^{\infty}\sum_{k=1}^{3}(i\xi)_j^{(k)}\left[a_{jk} e^{i(j\theta - \omega_j^{(k)} t)} + b_{jk} e^{i(j\theta + \omega_j^{(k)} t)}\right]$$

$$w(\theta,t) = \frac{1}{2}\sum_{j=-\infty}^{\infty}\sum_{k=1}^{3} w_j^{(k)}\left[a_{jk} e^{i(j\theta - \omega_j^{(k)} t)} + b_{jk} e^{i(j\theta + \omega_j^{(k)} t)}\right]$$

$$iu(\theta,t) = \frac{1}{2}\sum_{j=-\infty}^{\infty}\sum_{k=1}^{3}(iu_j^{(k)})\left[a_{jk} e^{i(j\theta - \omega_j^{(k)} t)} + b_{jk} e^{i(j\theta + \omega_j^{(k)} t)}\right]$$

where a_{jk} and b_{jk} are complex, $(i\xi)_j^{(k)}$, $w_j^{(k)}$, and $(iu)_j^{(k)}$ are real, $(i\xi)_{-j}^{(k)} = (i\xi)_j^{(k)}$ etc.

The a_{jk} and b_{jk} are determined by applying appropriate initial conditions to the variables and their rates. The presence of the three modes in the solution indicates that three linearly independent types of motion can exist simultaneously at each permitted wavelength λ_j, each with its own frequency $\omega_j^{(k)}$, $k = 1,2,3$. Thus the initial conditions must specify values for three (independent) variables and their rates at $t = 0$. Let

$$\zeta(\theta,0) = f_1(\theta) \qquad \frac{\partial \zeta(\theta,0)}{\partial t} = g_1(\theta)$$

$$w(\theta,0) = f_2(\theta) \qquad \frac{\partial w(\theta,0)}{\partial t} = g_2(\theta)$$

$$i\xi(\theta,0) = f_3(\theta) \qquad i\,\frac{\partial \xi(\theta,0)}{\partial t} = g_3(\theta)$$

The series expansions for the variables are solved for the coefficients by the conventional method of multiplying by conjugate exponentials, integrating over θ, and using the orthogonality relations. We find:

$$\int_0^{2\pi} f_1(\theta)\, e^{-ni\theta}\, d\theta = \int_0^{2\pi} f_1(\theta)\cos n\theta\, d\theta + i\int_0^{2\pi} f_1(\theta)\sin n\theta\, d\theta$$

$$= \sum_{k=1}^{3} \pi(a_{nk} + b_{nk}) = \pi \sum_{k=1}^{3} [\mathrm{Re}(a_{nk} + b_{nk}) + i\, \mathrm{I_m}(a_{nk} + b_{nk})]$$

$$\int_0^{2\pi} g_1(\theta) e^{-ni\theta}\, d\theta = \int_0^{2\pi} g_1(\theta)\cos n\theta\, d\theta + i\int_0^{2\pi} g_1(\theta)\sin n\theta\, d\theta$$

$$= \sum_{k=1}^{3} [-i\omega_n^{(k)} a_{nk} + i\omega_n^{(k)} b_{nk}] = \pi \sum_{k=1}^{3} \omega_n^{(k)} [i\,\mathrm{Re}(-a_{nk} + b_{nk}) + \mathrm{I_m}(a_{nk} - b_{nk})]$$

Similar equations are found for f_2, g_2, f_3, and g_3. Then, for each value of n, we have six equations involving the real and imaginary parts of a_{n1}, b_{n1}, a_{n2}, b_{n2}, a_{n3}, and b_{n3}, by making use of the relations between a_{nj} and a_{-nj}, $\omega_n^{(k)}$ and $\omega_{-n}^{(k)}$, etc.

C. Related Experimental Work

Experiments conducted by Mr. William C. Van Buskirk, of Stanford's Biomechanics Laboratory, have confirmed the existence of the three modes of motion described above, and have verified the general shape of the dispersion curves (Ref. 9). His work will be reported completely in a subsequent dissertation but it might be appropriate to present some preliminary results at this time.

Fig. 4-30 shows the experimental apparatus used. A water-filled bicycle inner tube is softly suspended within half of a plastic toroidal shell. Additional water-filled tubes are attached to the end of the primary tube to absorb reflections. Pressure within the tube is controlled by varying the level of water in the inlet tubes. Waves are generated by applying the illustrated vibrator to the end or side of the tube, or by oscillating a plastic clamp, which fits around the tube at one cross-section, in the axial or radial direction (θ or R direction in Fig. 2-2). Two measurement systems were used: shown in the figure are pressure transducers which are inserted into the tube; also used were electro-optical trackers which measure the displacement of the tube surface. In both cases, the wave speed was computed from the phase difference between the sinusoids recorded at two points.

Fig. 4-31 compares the experimental dispersion data with the theory of section A (no rigid wall). The relative nondispersiveness of two modes, and the normal dispersiveness of the third, are confirmed. The accuracy of 10 to 20% in the moderately low frequency range of the breathing and flexure modes is all that should be expected in view of the approximations in the analysis.

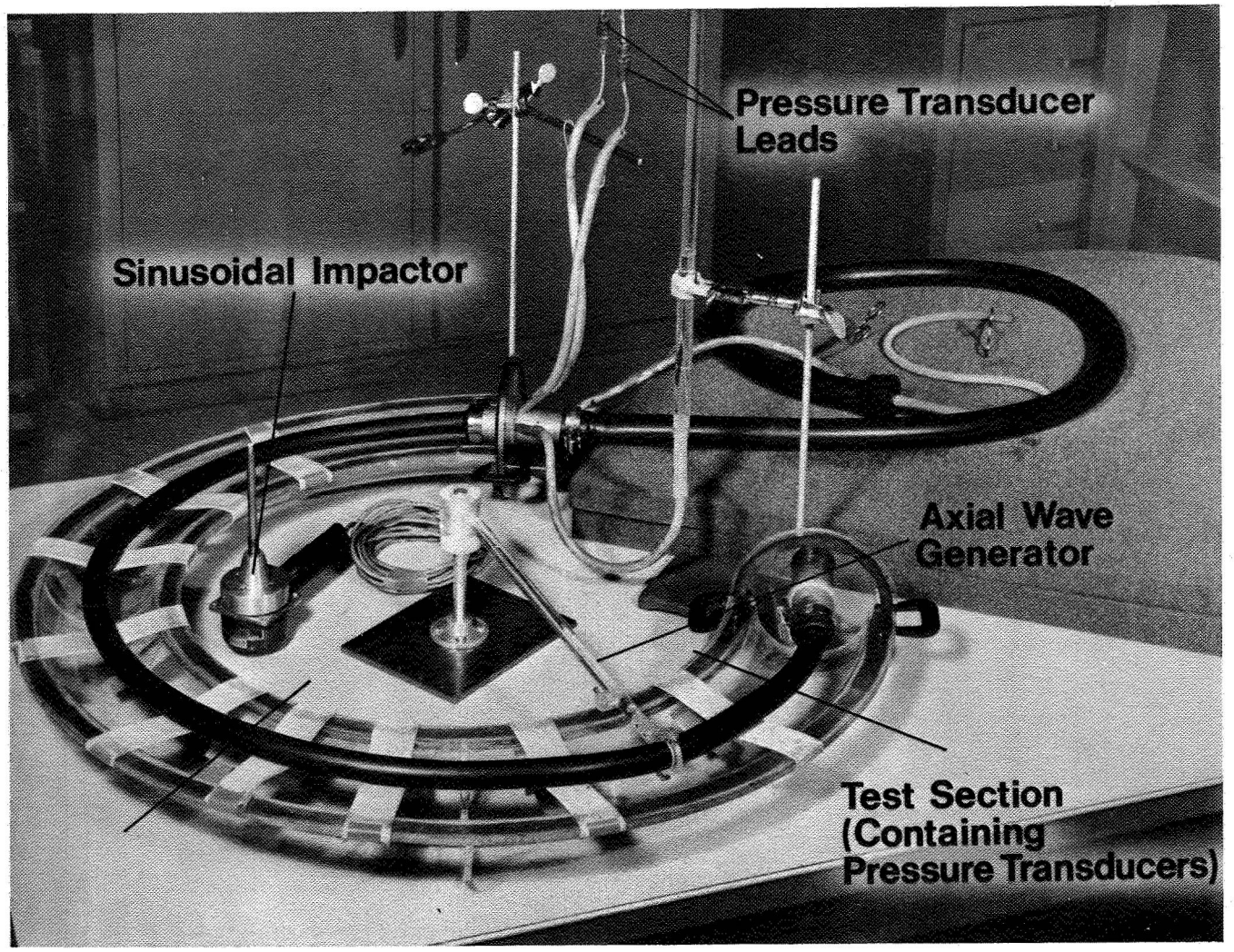

Fig. 4-30. Experimental Apparatus for Measuring Wave Speeds in Water-filled Bicycle Inner Tube

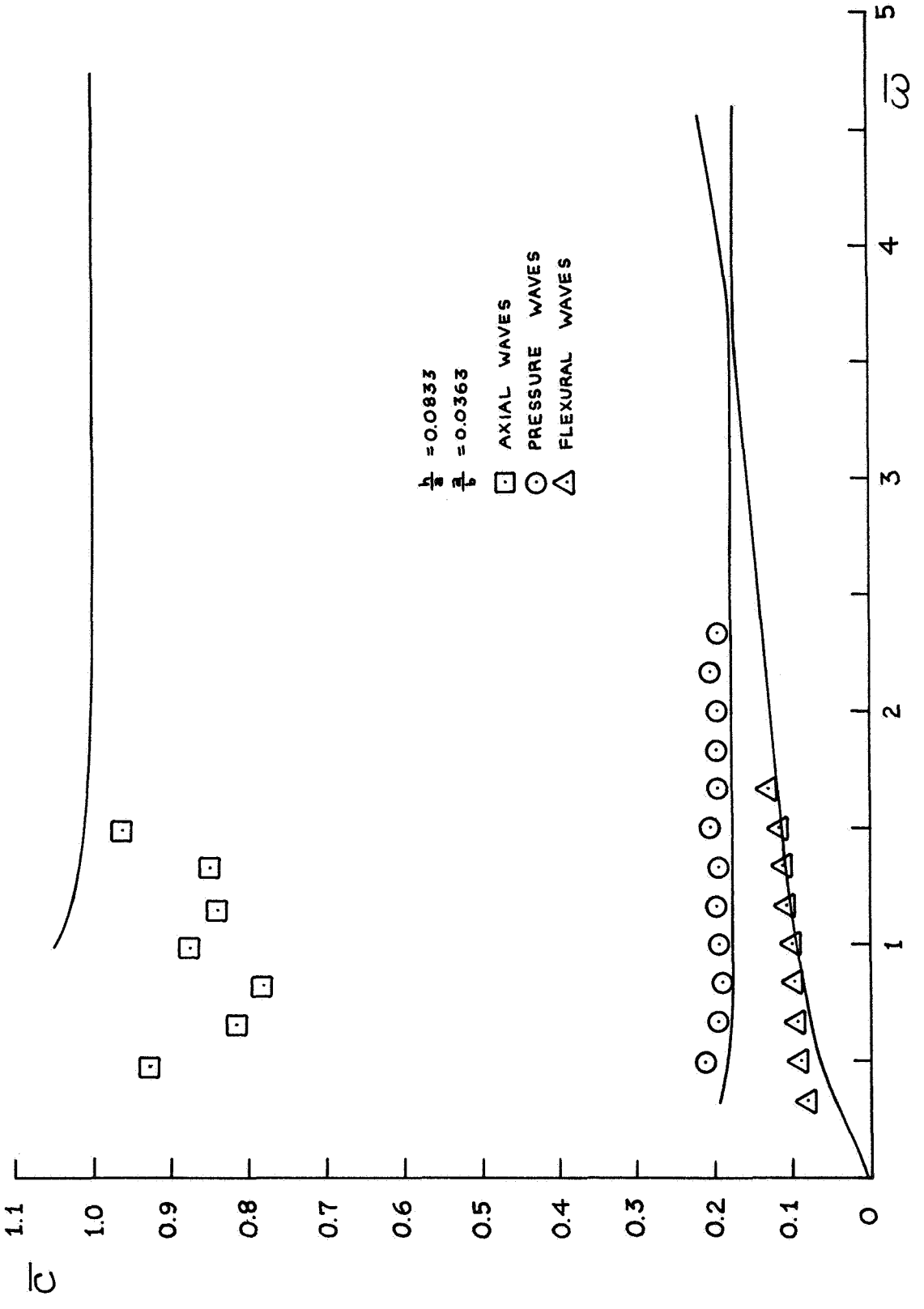

Fig. 4-31. Experimental and Theoretical Dispersion Curves

V. CONCLUSION

As was mentioned in the Introduction, this work represents only a first step in studying the semicircular canals. Before a quantitative understanding of the behavior of the canals can be achieved, we will have to go far beyond this approximate study of free vibrations of a single, isolated elastic toroid inside a rigid channel. It would also be desirable to have experimental confirmation of the increasing accuracy of the successive approximate models, as well as precise measurements of the mechanical behavior of the organ itself.

Of course, the present work may lead to results in other areas besides the one directly intended. For example, a study of the behavior of the aortic arch would proceed by refining the current analysis to consider nonlinear pulse propagation, nonisotropic and pressure-varying elastic properties, and the effects of the surrounding elastic tissues. Here again, experimental models and in vivo measurements are necessary for a complete study.

We can conclude, on the basis of the agreement between the theory of Chapter IV and the relevant experiments, that the decision to use simplified equations of motion, rather than numerical solution of the potential flow equations of Chapter II, has been amply justified. The approximate theory developed here should help to provide an understanding of the mechanical behavior of fluid-filled toroidal shells.

BIBLIOGRAPHY

1. Anliker, Max, and K.R. Raman, Korotkoff Sounds at Diastole - A Phenomenon of Dynamic Instability of Fluid-Filled Shells. International Journal of Solids and Structures, Vol. 2, No. 3, 1966, pp. 467-491.

2. Eversman, Walter, The Transverse Vibrations of a Spinning Annular Elastic Membrane With Free Edges. SUDAER Report No. 184; also Ph. D. Thesis, Stanford University, Department of Aeronautics and Astronautics, June 1964.

3. Jacob, Stanley W., and Clarice A. Francone, Structure and Function in Man. Philadelphia: W.B. Saunders Co., 1965.

4. Kreyszig, Erwin, Differential Geometry. Toronto: University of Toronto Press, 1959.

5. Morse, Philip M., and Herman Feshbach, Methods of Theoretical Physics. New York: McGraw-Hill, 1953.

6. Rainville, Earl D., Elementary Differential Equations, 3rd Edition. New York: Macmillan Co., 1964.

7. Sokolnikoff, I.S., Mathematical Theory of Elasticity. New York: McGraw-Hill, 1956.

8. Steer, Robert W., Jr., The Influence of Angular and Linear Acceleration and Thermal Stimulation on the Human Semicircular Canal. Sc.D. Thesis, Massachusetts Institute of Technology, Department of Aeronautics and Astronautics, August 1967.

9. Van Buskirk, W.C., Ph.D. Thesis, Stanford University, Department of Aeronautics and Astronautics (to be published).

10. Van Egmond, A.A.J., J.J. Groen, and L.B.W. Jongkees, The Mechanics of the Semicircular Canal. Journal of Physiology, Vol. 110, pp. 1-17, 1949.